AN INVESTIGATION INTO THE FEASIBILITY OF CONSTRUCTING WAVE RESISTANCE INFLUENCE DIAGRAMS BY APPLICATION OF LINEAR SUPERPOSITION PRINCIPLES

by

Lcdr. F. J. Moran, Jr. Lt. A. J. Johnson
Lt. C. A. Bartholomew

May 14, 1968

AN INVESTIGATION INTO THE FEASIBILITY OF CONSTRUCTING WAVE RESISTANCE INFLUENCE DIAGRAMS BY APPLICATION OF LINEAR SUPERPOSITION PRINCIPLES

A Thesis

Presented to the Faculty of

Webb Institute of Naval Architecture

in Partial Fulfillment of the

Requirements for the Degree of

Master of Science in Naval Architecture

by

Lcdr. F. Joseph Moran, Jr.

Lt. Charles A. Bartholomew

Lt. Alan J. Johnson

May 14, 1963

ABSTRACT

The main objective of this study has been to determine whether the principles of linear wave superposition could be combined with model tests using wave survey techniques to obtain a practical method of deriving "influence diagrams", which relate the influence of small hull form variations on wave resistance. Tests were run in the Webb towing tank using a 5.5 ft Destroyer-type form with protuberances added at a number of locations over a range of speeds. Results showed attempts to apply linear superposition for this purpose to be largely unsuccessful. This result implies serious limitations of the linearized theory of wave resistance and its application to develop optimum hull forms. However, several of the results point to the conclusion that, with some modification, linear superposition may be successfully applied toward the development of influence diagrams.

ACKNOWLEDGEMENTS

The authors would like to extend their appreciation to the following people whose assistance in this endeavor was invaluable:

Dr. L. W. Ward for suggesting the topic of study and for the guidance and timely assistance he offered when it was most needed.

Capt. R. A. Hinners, USN(Ret) for his interest and encouragement throughout the project.

The personnel of Code 584, NSRDC for the generous donation of their time and effort and for the several suggestions they offered to the authors which have been incorporated into this report.

TABLE OF CONTENTS

LIST OF FIGURES

LIST OF FIGURES (CONT.)

LIST OF TABLES

Three wise men of Gotham
Went to sea in a bowl
If the bowl had been stronger,
My story would have been longer.

.... Mother Goose

INTRODUCTION

William Froude's investigation of ship resistance of nearly one hundred years ago inferred that waves produced by a ship moving through the water are a measure of the energy imparted to the fluid. It is only in the past ten years, however, that this question has received the close attention of hydrodynamicists from an experimental point of view. Much of this attention has been focused on the theoretical aspects of the wave resistance as derived from the wave pattern of a ship, and experimental verification by model tests. Some of the most promising experimental techniques developed to date have been assessed by Eggers, Sharma, and Ward (1)[1] with very favorable results. Therefore, it is the authors' contention that the state of the art has now been advanced to the point where practical applications of wave resistance survey techniques may be made.

An important assumption made in linearized wave theory is the purported ability to superimpose the individual wave patterns of independent hull form variations to obtain a compound wave pattern equivalent to the pattern which would have been obtained had the hull and form variations been towed simultaneously.

---

1. Numbers in brackets indicate references at the end of this paper.

This paper will report the results of an exhaustive investigation into this linear superposition theory, and of attempts to develop it into a practical means of predicting the wave resistance trends of Destroyer-type hulls. To this end the following technique is introduced:

A Destroyer-type model will be tested to determine its bare hull wave slope record by means of the longitudinal cut, wave survey method. A protuberance will then be attached to the model and the tests replicated. From these records the wave resistance of the model may be determined. Also, assuming linear superposition of the wave records, the wave record of the protuberance alone may be determined by: $\zeta_{y_{\text{protuberance}}} = \zeta_{y_{\substack{\text{model with} \\ \text{protuberance}}}} - \zeta_{y_{\substack{\text{model} \\ \text{bare hull}}}}$

That is, the wave record of the protuberance will be assumed to be unaffected by its location on the model and to give the same wave slope record when attached to the model as it would if it were alone in a free stream. This hypothesis is investigated in depth in a later section of this paper.

The protuberance wave record will be shifted along the model length and added back into the bare hull record. The resultant wave record obtained is, by the linear superposition assumption, equivalent to the wave record that would have been obtained had the model been towed with the protuberance at that shifted location on the model. An influence diagram, as suggested by Hogner (2), can be developed by considering the protuberance as an increase of

the sectional area at the point of attachment. An influence diagram indicates the change in wave resistance per unit change of displacement at the different locations on the hull surface, and therefore shows at what points a given form should be modified in order to reduce its wave resistance.

Influence diagrams developed completely from experimental testing require an exorbitant amount of data recording and analysis. However, if linear superposition methods are successful in this paper, diagram construction effort will be greatly reduced, and an extremely useful tool will be made readily available to the designer.

THEORY

Introduction

The particular wave measuring technique to be employed in this paper will be the longitudinal cut, wave slope method (3), which is selected for the following reasons: (a) a longitudinal cut through a wave pattern is readily obtained by towing a model past a stationary probe, (b) the wave slope record terminates much more rapidly than do height records, (c) it is a method recommended by Eggers, Sharma, and Ward (1,3), and (d) all of the necessary equipment was available at Webb Institute of Naval Architecture.

Basic Equations and Definitions

The wave theory which forms the basis for the lateral wave slope method of survey is developed by Sharma (4) via energy flow considerations across a boundary or continuum. The final expression relating the wave resistance to its respective wave pattern is given by:

$$R_w = \frac{\rho g}{2\pi} \int_{-\infty}^{\infty} (S_y^2 + C_y^2) \frac{k_o^4}{w^6} \frac{du}{(2 - \frac{k_o^2}{w_o^2})} \quad (1)$$

where S_y and C_y are Fourier sine and cosine transforms of the free wave slope profile. That is,

$$S_y = \int_{-\infty}^{\infty} \zeta_y \, \mathrm{SIN}(wx)\, dx \quad (2)$$

$$C_y = \int_{-\infty}^{\infty} \zeta_y \, \mathrm{COS}(wx)\, dx \quad (3)$$

where ζ_y is the wave slope corresponding to any given value of x, u and w are the longitudinal and transverse circular wave numbers respectively, and k_o is a velocity parameter equal to g/V_m^2. To fully understand the steps required in arriving at a usable solution of equation (1), simple wave theory will be reviewed.

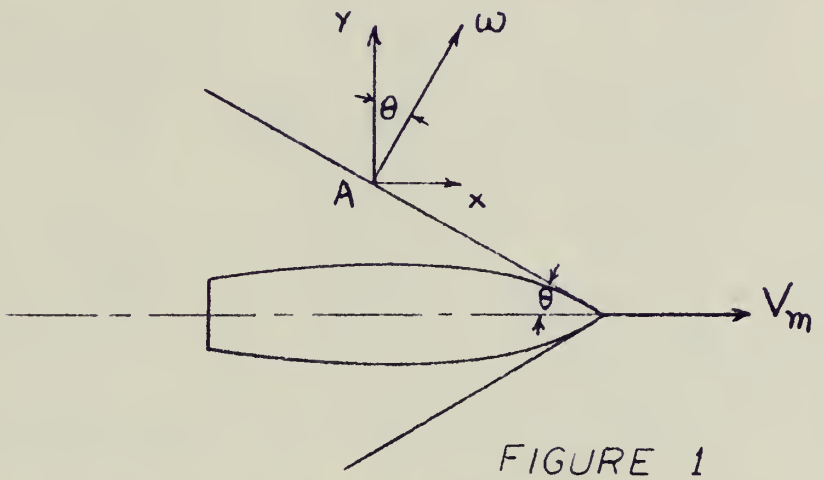

FIGURE 1

A representative wave of wave length λ (at point A) in the wave pattern of a ship advancing with velocity V_m is sketched in Figure 1. From the axes' orientations it can be seen that Θ is the angle between ω, the resultant coordinate of the wave, and the ship velocity. Two conditions must be satisfied: namely, that the wave system remain stationary with respect to the ship, and that the ship be in deep water. Therefore, wave speed is equal to $\sqrt{g\lambda/2\pi}$. With k termed the wave number $= 2\pi/\lambda$ and letting the subscript zero denote conditions at the ship centerline, we have:

$$C = V_m \cos\theta \sqrt{g\lambda/2\pi} = \sqrt{g/k} \quad (4)$$

$$C_o = V_m = \sqrt{g\lambda_o/2\pi} = \sqrt{g/k_o} \quad (5)$$

and $$k = g/V_m^2 \cos^2\theta = k_o \sec^2\theta \quad (6)$$

From Figure 1 it is seen that (7)

$$\omega = X\cos\theta + Y\sin\theta$$

Multiplying equation (6) by equation (7),

$$k\omega = k_o(X\cos\theta\sec^2\theta + Y\sin\theta\sec^2\theta)$$

$$k\omega = k_o X \sec\theta + k_o Y \sec\theta\tan\theta$$

$$k\omega = WX + UY \quad (8)$$

where $W = k_o \sec\theta$; $U = k_o \sec\theta\tan\theta$ (9)

squaring and adding equations (9),

$$U = W\sqrt{W^2 - 1} \quad (10)$$

$$W = \sqrt{1/2 + \sqrt{1/4 + U^2}} \quad (11)$$

The circular wave numbers u and w have thus been expressed in terms of known quantities and each other.

A solution of equation (1) is outlined by Ward (2) as follows. The wave numbers can be non-dimensionalized by dividing each by k_o. $\therefore W' = W/k_o = \sec\theta$

$$U' = U/k_o = \sec\theta\tan\theta$$

Equation (1) then reduces to

$$R_w = \frac{\rho g}{2\pi}\int_{-\infty}^{\infty}(S_y^2 + C_y^2)\,\frac{du'}{w'^6 k_o(2 - 1/w'^2)}$$

Since $k_o = g/V_m^2$, $R_w = \frac{\rho V_m^2}{2\pi}\int_{-\infty}^{\infty}(S_y^2 + C_y^2)\,\frac{du}{w^4(2w^2-1)}$ (12)[2]

---

2. The primes will be omitted throughout the remainder of the text.

S_y is determined in a straightforward manner where x varies from zero at some point ahead of the wave to a point, N, where the ζ_y's die out.

$$\therefore \begin{Bmatrix} S_y \\ C_y \end{Bmatrix} = \int_0^N \zeta_y \begin{Bmatrix} \text{SIN} \\ \text{COS} \end{Bmatrix} (W k_0 x)\, dx \qquad (13)$$

where each ζ_y corresponds to the wave recorded slope tape record. This integration must be carried out for each value of u. A plot of $\sqrt{S_y^2+C_y^2}$ (i.e., the wave amplitude) versus u, w, or θ gives a measure of the generated energy of the wave system. Similar wave patterns will display similar wave amplitude spectra. It can be anticipated that two wave records possessing seemingly large discrepancies may have very similar wave amplitude spectra, because of the smoothing effect of the integration process. A further discussion of these spectra will be conducted in a later section.

Equation (12) can be non-dimensionalized to compute the wave resistance coefficient, Cw, since

$$R_w = \tfrac{1}{2} C_w \rho V_m^2 S \quad . C_w = \frac{1}{\pi S} \int_{-\infty}^{\infty} (S_y^2+C_y^2) \frac{du}{w^4(2w^2-1)} \qquad (14)$$

The basic equation is now in a final form convenient for adaptation of a digital computer program solution. The programming details and assumptions will be described in Appendix B.

EXPERIMENTS

Characteristics of Model and Protuberances

Stevens model number 393 was modified for use in this project by removing the bilge keels and adding turbulence stimulators. Figure 2 is the model body plan and Table I lists the model and ship particulars. The two protuberances used are shown in Figure 3. Both are bodies of revolution and, consequently, all sections are circular.

TABLE I SHIP - MODEL CHARACTERISTICS

SHIP

Length of load waterline	342.5 ft
Length between perpendiculars	341.0 ft
Beam	35.9 ft
Draft	12.7 ft
Displacement - tons salt water	2,296.0
Wetted surface	14,160.0 ft^2
C_b	0.517
Displacement-Length ratio	57.9
Beam-Draft ratio	2.83

TABLE I SHIP-MODEL CHARACTERISTICS (con.)

MODEL

Lambda ratio	62.0
Length load waterline	5.524 ft
Length between perpendiculars	5.500 ft
Displacement-pounds fresh water	21.04
Wetted surface	3.682 ft^2
Measured freeboard aft focsle break	2.17 in
Trim	none
Number of stations	10

Exploratory Testing

In order to proceed with the proposed objectives, it was necessary to determine approximate towing speeds as well as protuberance sizes which would generate significant wave slope difference signals. Practical limitations confined the size of the protuberances between the design water line and the keel. Moreover, selection of a suitable hull location was necessary for comparison of the difference signals and the shifting technique which would be developed. Regarding towing speed, it was felt that the selection should depict the typical operational speeds of a Destroyer, since design techniques (influence diagrams) were of concern. A three wire resistance gage and Brush recording device were used to obtain the wave slope records. Equipment details are described in Appendix A.

BODY LINES
DD 393 - 1

LBP SHIP 341FT
LBP MODEL 66 INS
LENGTH RATIO 62
BEAM SHIP 35.9FT
DRAFT 12.7FT

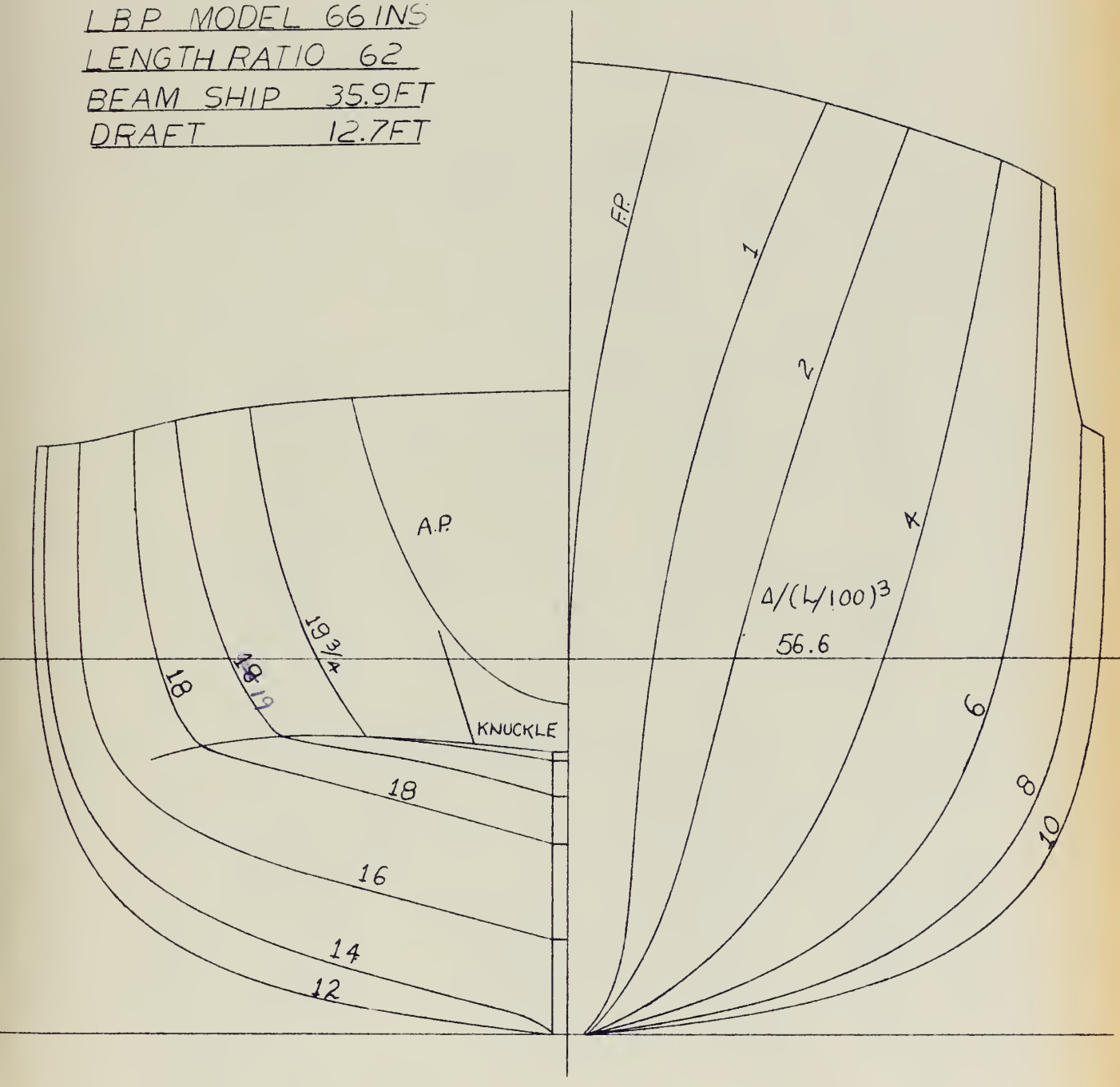

FIGURE 2.

FIG 3.
PROTUBERANCE DIMENSIONS
FULL SCALE

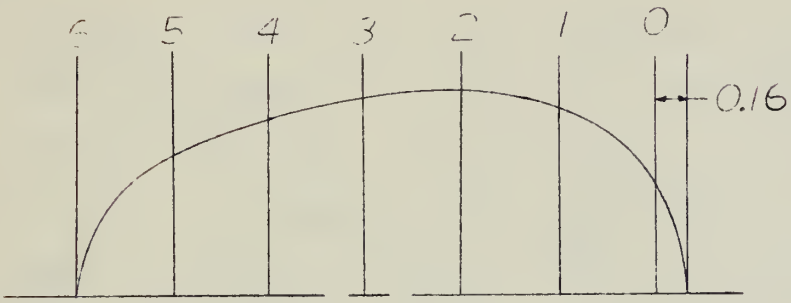

LARGE PROTUBERANCE

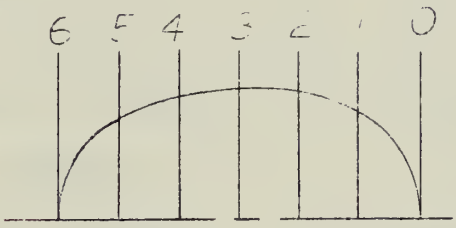

SMALL PROTUBERANCE

TABLE OF DIMENSIONS

SIZE	TAPERING	LOA	SECTION RADII						
—	IN.	IN.	0	1	2	3	4	5	6
LARGE	1/2	3.16	0.56	0.97	1.06	1.03	0.92	0.72	0.00
SMALL	5/16	1.88	0.00	0.55	0.66	0.67	0.63	0.52	0.00

Preliminary model runs were made with two hemispherically shaped protuberances attached at station 1 of a 10-station model. It was assumed that this forward location would give the best representation of a bulb generated wave since it had the least hull separation of the protuberances. The results of these equipment-model familiarization tests tentatively verified that the speeds and the selected protuberance size would give sufficient difference signals necessary for meaningful computer analysis. Consequently, qualitative testing could proceed.

Resistance Tests

A standard model resistance test was made to obtain sufficient data to develop model residuary and total resistance curves. The computed values of C_w could therefore be compared with C_r and C_t to determine the relative magnitude of the wave resistance at various speeds. It could also serve as a check to insure that the computed wave resistance constitutes a reasonable percentage of residuary resistance.[#3]

From the results of the aforementioned investigations, it was decided to tow off-center at Froude numbers of .242, .363, and .484 (corresponding to ship speeds of 15, 22.5, and 30 knots respectively), with the larger of the two protuberances attached successively at stations 1, 3, and 5, and

---

#3 The authors know of no previous wave resistance testing of a Destroyer-type model. Therefore, the expected range of values is uncertain.

the smaller attached only at station 3. To provide additional data for translation analysis techniques, later tests were conducted with the large protuberance at stations 2 and 3. The protuberances would be investigated at a common waterline for comparative purposes. Figure 4 shows the model being towed at Froude numbers of 0.242 and 0.484 with the large protuberance attached at station 2.

Any errors introduced when comparing the records at each configuration, and the sensitivity of the testing equipment must be minimized throughout testing. Additionally, the influence on wave resistance of the transverse distance between the gage and the model must be consistent. A detailed error analysis will be presented in Appendix D. Suffice it to say, the following procedures were employed to reduce areas of possible error:

1. A calibration factor relating the recorded values in mm to a slope in radians is essential for each tape record. Since the equipment gain settings tend to drift during the testing, calibration records were obtained prior to and immediately after each testing configuration. The gage was physically rotated through known angles and the ensuing deflections were recorded on Brush recorder tape. The values were plotted to determine an <u>average</u> calibration factor for each specific configuration. It was noted that these values were a definite function of

FIGURE 4

Large Protuberance Station 4, Fr. No. = .242

Large Protuberance Station 2, Fr. No. = .424

the equipment settings and that they greatly affect the final wave resistance coefficients.

2. The employment of micro-switches established a common wave slope reference point and a rough verification of the model speed. One micro-switch was positioned on the tow rail at the point where the bow at design water line passed the wave slope probe, the other was positioned at a point near the end of the run. The switches produced a set of marks on each Brush recorder tape record, and by aligning these visually, the records at a given Froude number could be quickly compared for consistency.

3. Bare hull model tests were conducted at the middle speed (Fr = .363) with the distance between the model and wave probe being varied between 18 and 24 inches, in order to determine a range of off-set distance where C_w remained essentially constant and near the maximum. The midpoint of this range was utilized throughout all towing configurations. Detailed results are shown in the data analysis section.

Three wave slope records were obtained at each Froude number for each of seven model-protuberance configurations, each speed varying no more than $\pm$ .01 ft/sec over a 35-foot measured run. Figure 5 shows a sample wave record of the bare hull model at Froude number .363 and Figure 6 shows a sample wave record with the large protuberance located at station 3 at Froude number .363. It is worthy of note that all testing (total of 63 acceptable records) required

FIGURE 5

SAMPLE WAVE SLOPE RECORD

FOR BARE HULL MODEL

FR. NO. 0.363

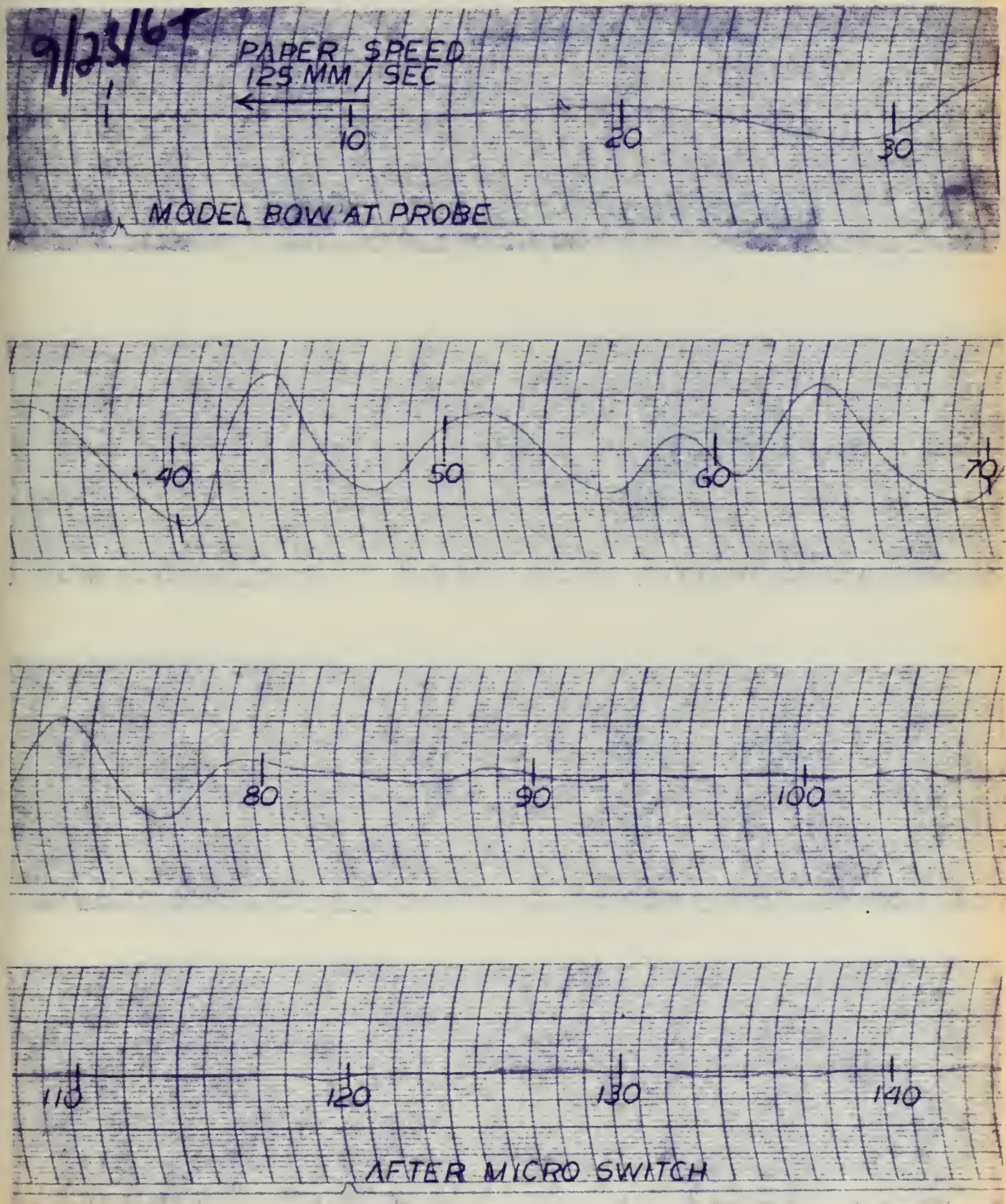

FIGURE 6

SAMPLE WAVE SLOPE RECORD

PROTUBERANCE AT STATION NO. 1

FR. NO. 0.363

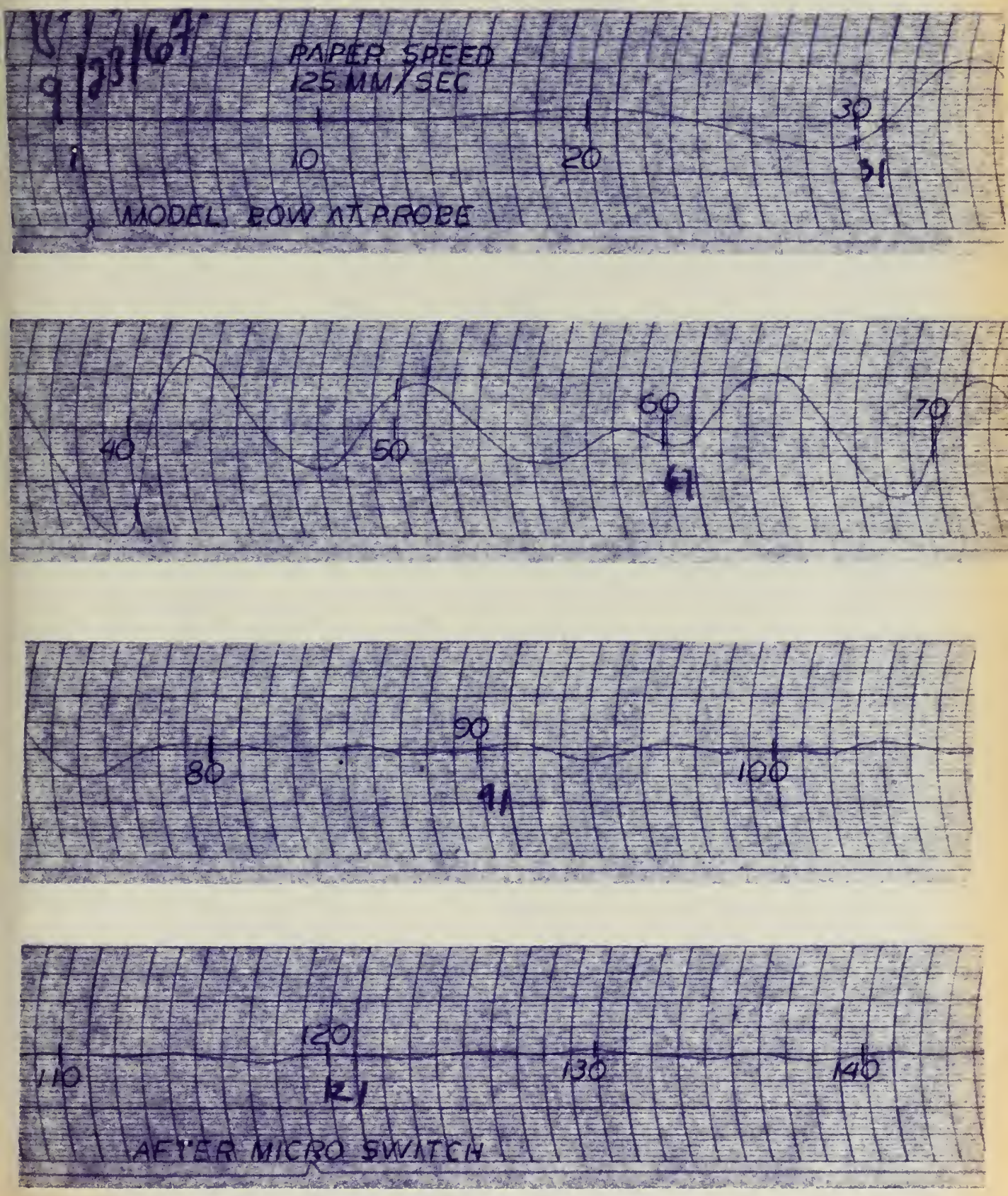

only an eleven-hour period. This time included preparing the model for each configuration, reballasting, trimming, and calibration of the wave slope measuring probe, as well as conducting the series of off-center runs.

METHOD OF DATA ANALYSIS

Since there have been no known previous wave resistance tests on Destroyer-type models, a method of reading and processing the data had to be developed before any detailed analyses, comparisons, or protuberance shifting could be initiated. Three representative sets of data were used to standardize the data reading and processing procedures. Data used were for the bare hull configuration with the large bulb attached at station 1 at a Froude number of 0.242. The following discussion pertains to these three sets of data, unless otherwise specified.

The records obtained from the model tests had to be magnified before they could be accurately read. Several methods were tried. It was found that the easiest and most reliable method was to project the wave slope records on the wall next to the computer console and to read the data directly onto computer tape. The accuracy of the readings thus obtained is estimated to be $\pm$ 0.2 mm.

Two alternatives were available for making use of the three data tapes obtained for each speed and protuberance location. Data tapes could be averaged and a wave resistance coefficient calculated from the resulting data, or a resistance coefficient could be obtained for each data tape, and the coefficients averaged for a final wave resistance coefficient. Both methods were applied and

the difference between wave resistance coefficients obtained was sufficiently small as to be attributable to the rounding-off error introduced in averaging the individual data points. However, there was sufficient difference between the wave resistance coefficients obtained from the individual tapes to preclude use of a single tape as representative of the given configuration.

It was decided to analyze the wave records on the basis of an averaged data tape since this method adapts itself more easily to shifting the protuberance and requires less computer core time.

Two reading intervals were considered, 2.5 mm and 5.0 mm. Data tapes for each configuration were read at 2.5 mm. intervals. In each case the tape length read was 600 mm. Wave resistance coefficients were then obtained by using (a) all data points obtained (240 points, 2.5 mm. interval), and (b) every other point (120 points, 5.0 mm. interval). Comparison of the wave resistance coefficients for a given configuration and speed showed less than 3% deviation, as shown in Table II. It was therefore decided to use the 5.0 mm. interval in further analyses to simplify the tape reading procedures. This will have no effect on the results since they are comparative in nature.

TABLE II

Wave Resistance Coefficients at 2.5 and 5.0 mm. Reading Intervals

Fr.	Protub. Size	Protub. Loca.	Length of Data Tape Read	No. of Inter-vals of u	C_w at 2.5 mm. Inter-vals	C_w at 5.0 mm. Inter-vals	% Diff. from 5.0 mm. value
		(Sta.)	(mm.)		($x10^3$)	($x10^3$)	
0.242	Large	1	240	100	0.317	0.323	- 1.9
0.363	Bare Hull	-	240	100	0.648	0.666	- 2.7
0.484	Bare Hull	-	240	100	2.359	2.344	+ 0.6

Theory states that the integration of wave slope data with respect to the transverse circular wave number cover the range $-\infty$ to $+\infty$. The basic interval between wave numbers used was 0.1 (See Appendix C) and resistance coefficients were obtained for lengths of 0 through 125 intervals of u. The results showed that beyond 100 intervals the increase obtained in the resistance coefficient was less than 1%.

To determine the maximum number of data points required to obtain reliable wave resistance coefficients, two procedures were used. First, the data tapes were analyzed for lengths varying between 400 and 600 mm. The results did not appear to be approaching a limiting value for any of the three Froude numbers. Therefore, the tank geometry, Figure 7, was developed, assuming the bow wave angle to be equal to the Kelvin angle ($19\frac{1}{2}^{o}$), and a maximum tape length

MODEL TEST GEOMETRY
SCALE ¼" = 1'0"

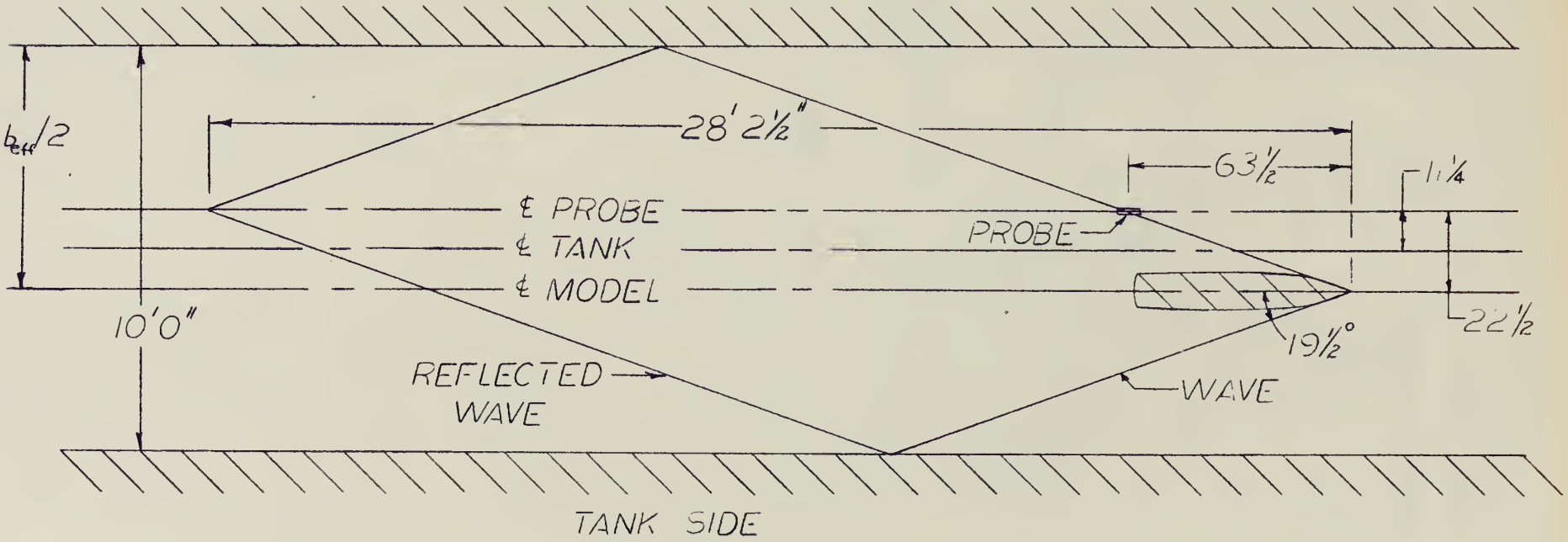

to avoid reflection was determined. The data tapes were then re-analyzed. Figure 8 is a graphical representation of the final analysis. The final data tape reading lengths selected were 800 mm. for a Froude number of 0.242, since the wave records die out beyond this tape length, and 700 mm. and 550 mm. for Froude numbers of 0.363 and 0.484 respectively, since reflection occurs beyond these lengths.

The data obtained for model tests with varying offset was analyzed for a data tape length of 600 mm. and a reading interval of 5.0 mm. The results, shown as Figure 8, are considered to verify that the offset used in the main resistance tests (22½ inches) was well within the range which gives little or no change of wave resistance coefficient with change in offset.

Fig 8.

DATA ANALYSIS CURVES

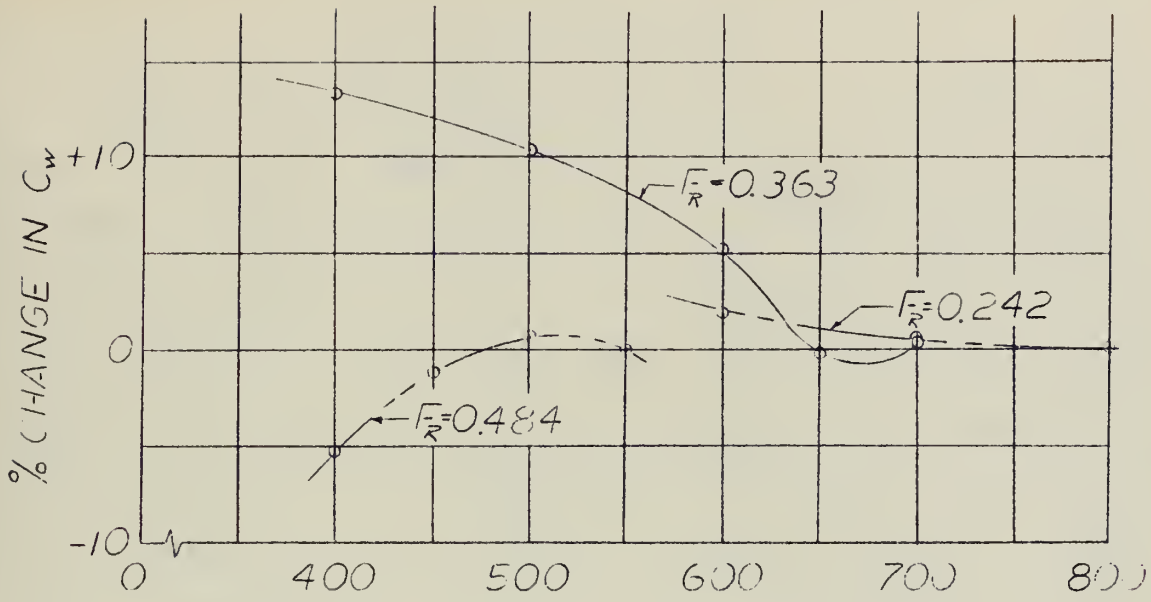

MODEL-PROBE OFFSET=22½" U=100

READING INTERVAL=5.0 MM

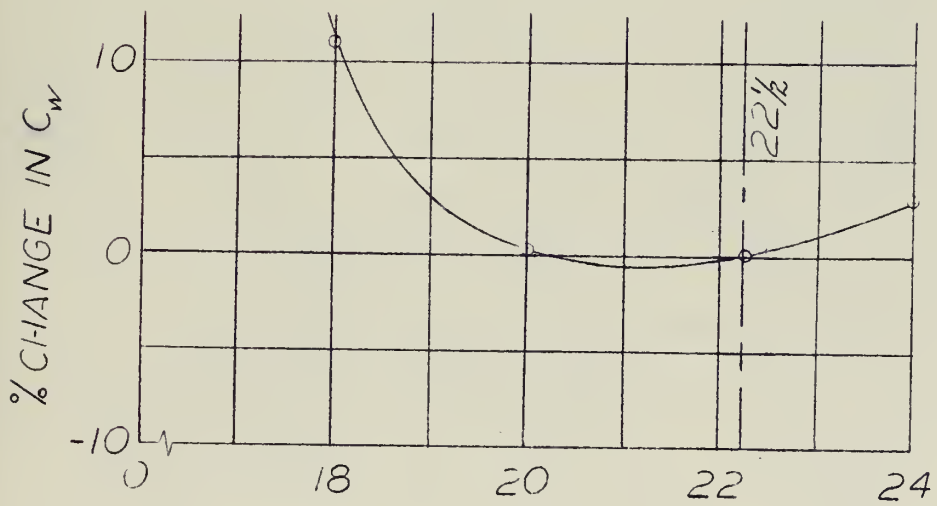

LENGTH OF DATA TAPE READ = 660 MM

READING INTERVAL=5.0 MM

F_R=0.242 U=100

DISCUSSION OF RESULTS

The results were compared in a number of different ways. These were: comparison of residuary and total resistance to wave resistance, linear shifts of the difference signals, translation of the influence diagrams, small interval shifts of the difference signals, wave spectra analysis, comparison of difference signals, and a comparison of the effects of protuberance size. Each of these and representative curves will be discussed in the following section.

Comparison of Residuary and Total Resistance with Wave Resistance

In order to obtain a quantitative comparison of the wave resistance component with the total and residual components, and thus evaluate the predicted savings in resistance in later discussions, Figure 9 has been prepared. Table III is also presented to give a percentage comparison between the various resistances. These ratios are for the most part in keeping with the results of wave resistance tests on merchant type hull forms and are thus considered as an indication of the validity of the tests performed for this report.

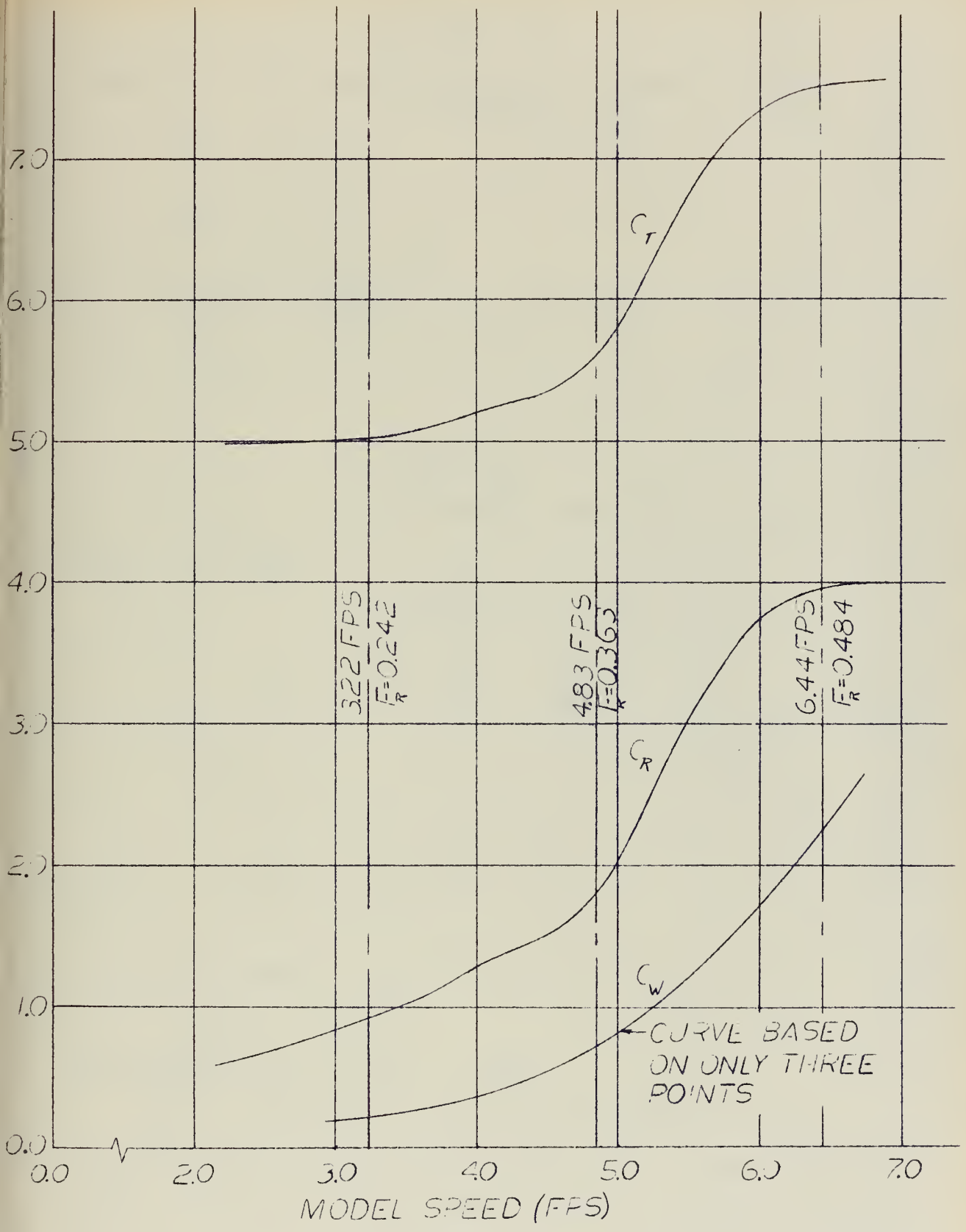

FIG 9

BARE HULL MODEL RESISTANCE COEFFICIENTS

TABLE III

Resistance Coefficients versus Froude Number for Bare Hull Model

Fr	Ship Speed Kts	C_w x10^3	C_r x10^3	C_t x10^3	C_w/C_r %	C_w/C_t %
0.242	15.0	0.204	0.92	5.00	22.2	4.1
0.363	22.5	0.703	1.78	5.58	39.5	12.6
0.484	30.0	2.445	3.97	7.53	61.6	32.5

TABLE IV

Wave Resistance Coefficient x10^3 versus Configuration

Bulb Location (Sta)	Bulb Size	Froude Numbers 0.242	0.363	0.484
Bare Hull	-	0.204	0.703	2.244
1	Large	0.329	0.781	1.956
2	"	0.218	0.741	2.228
3	"	0.183	0.744	2.683
4	"	0.261	0.715	2.473
5	"	0.255	0.641	2.151
3	Small	0.220	0.549	2.510

Construction of Influence Diagrams

Table IV gives the computed wave resistance coefficients versus Froude number for each of the seven configurations. Disregarding the small protuberance valves at this

time, and dividing each large protuberance coefficient by its corresponding bare hull coefficient, influence diagrams showing the effect of the increased sectional area at various points along the hull may be constructed for each speed. Figure 10 represents the influence diagrams for the model, based completely on experimental values. The remainder of this section discusses attempts to replicate Figure 10 utilizing the linear superposition hypothesis. If the techniques applied are successful, the amount of model testing and wave record analysis required to obtain an influence diagram will be greatly reduced.

In order to apply the linear superposition hypothesis, the PROTUB computer program was modified and adapted to the NSRDC 7090 computer. The difference signals were shifted one data point at a time with respect to the bare hull wave record and the wave resistance coefficient was computed for each altered configuration. This is equivalent to a series of discreet shifts of the protuberance along the model hull. Figures 11 and 12 are the non-dimensionalized influence diagrams derived in this manner for the model with large protuberances attached. The experimentally-obtained wave resistance coefficients at each station are also noted. These curves show that the predicted wave resistance coefficients at a shifted position are highly dependent upon the initial position of the

FIG 10.

INFLUENCE DIAGRAMS BASED ON EXPERIMENTAL WAVE RESISTANCE COEFFICIENTS

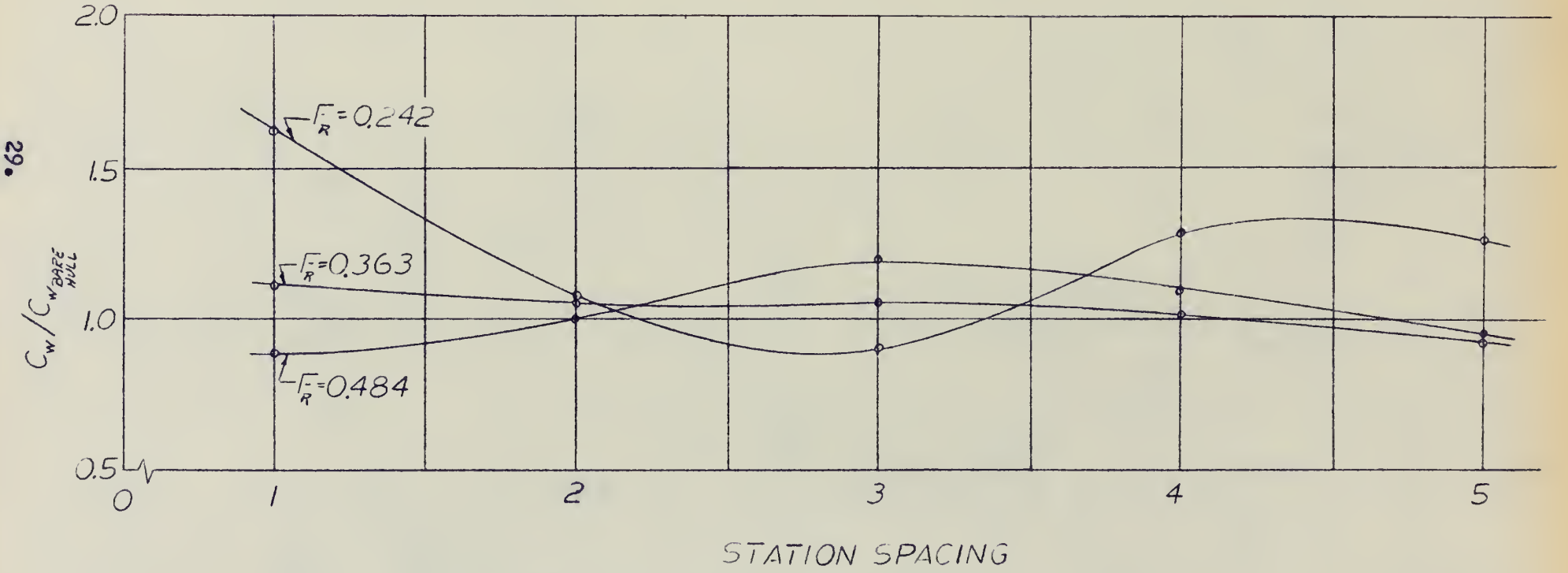

INFLUENCE DIAGRAMS BASED ON LINEAR SHIFT OF THE DIFFERENCE SIGNALS

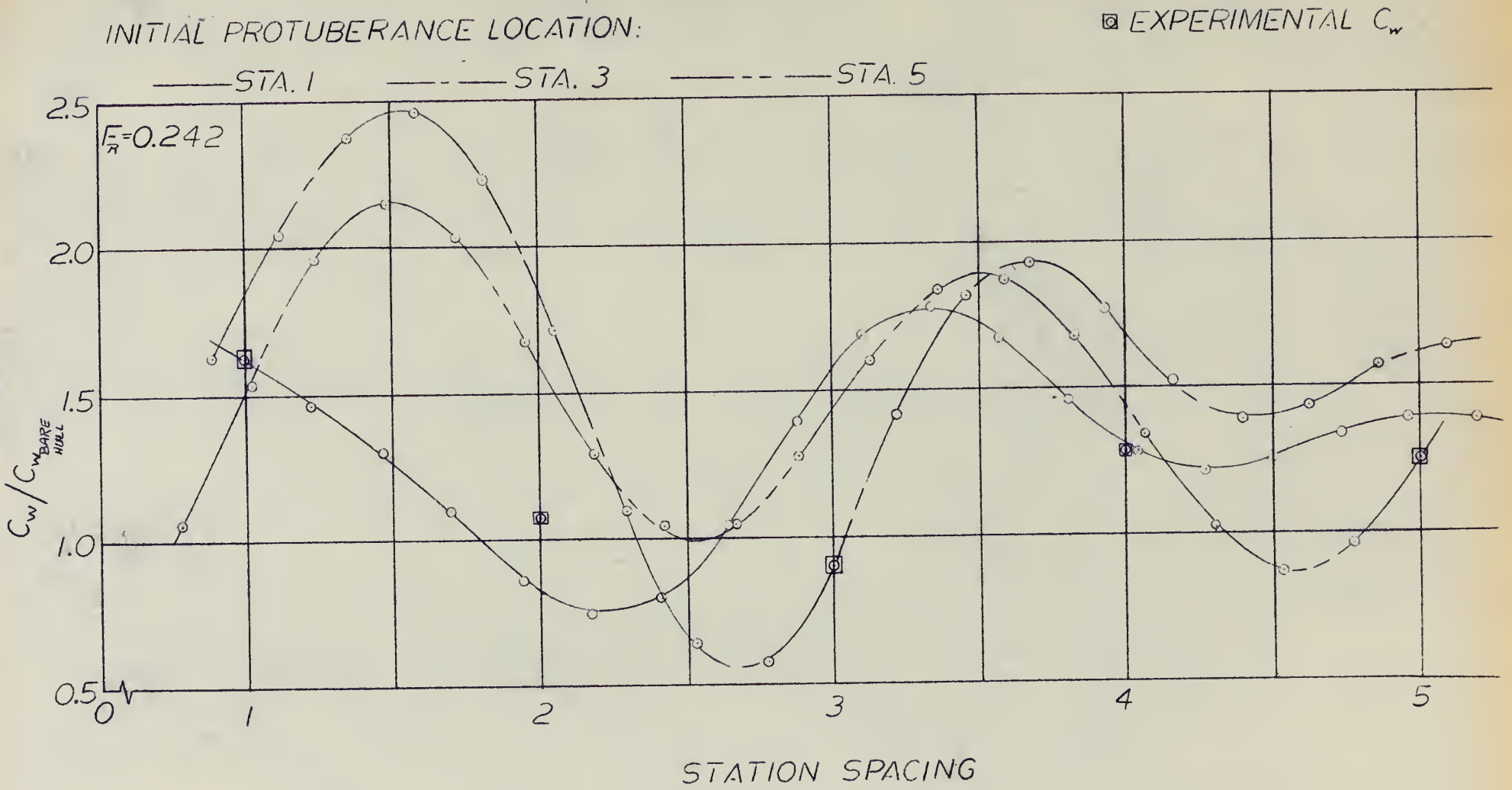

INFLUENCE DIAGRAMS BASED ON LINEAR SHIFT OF THE DIFFERENCE SIGNALS

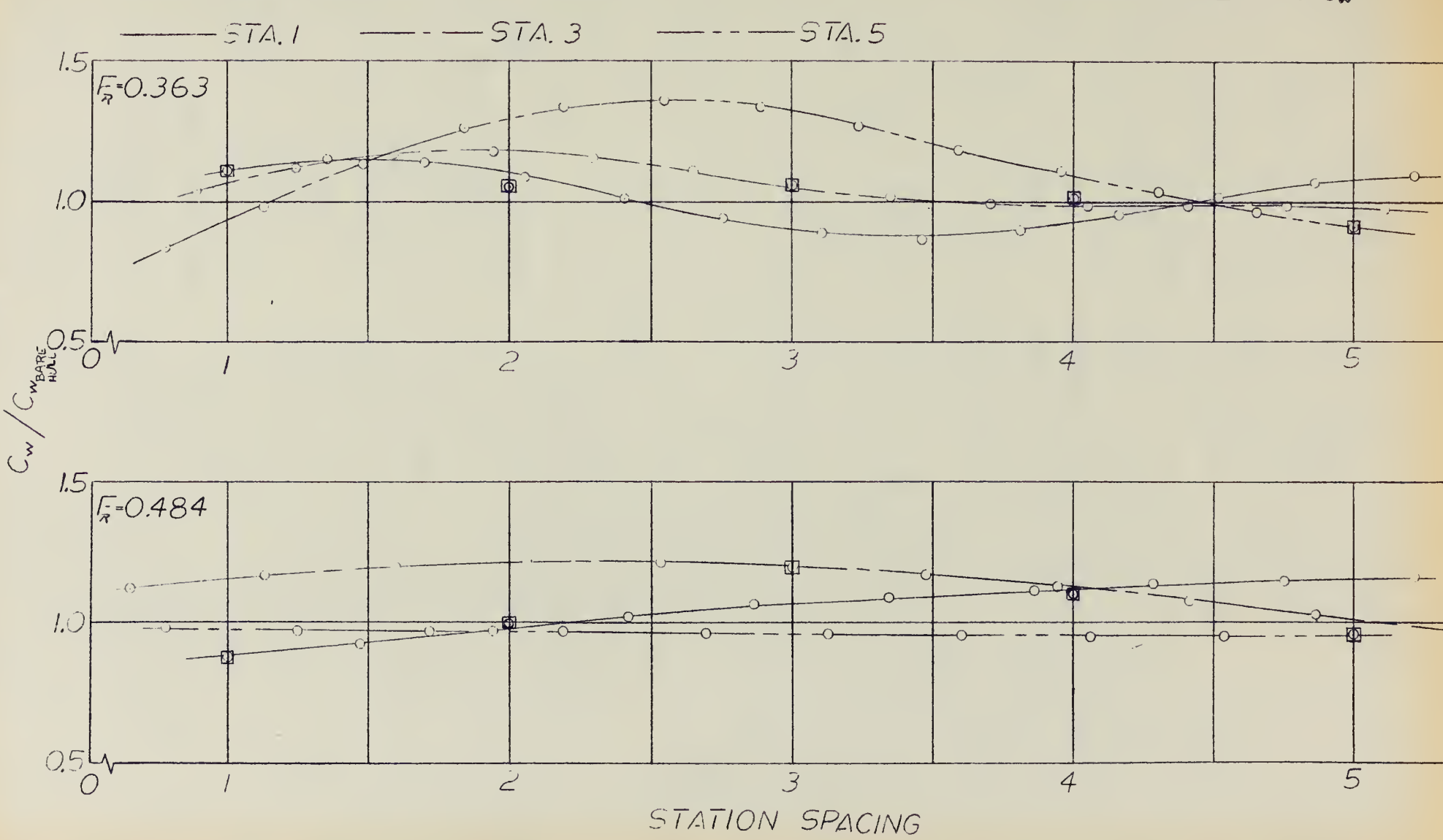

protuberance and that the predictions do not always agree with the actual wave resistance coefficient.

At this point the physical events which occur when the protuberance is moved longitudinally along the model during a wave resistance test, which are disregarded in the idealized linear superposition theory, should be discussed. First, as the probuberance is moved aft along the model, the separation between the halves is increased and the amount of model interference between the two halves is increased. Secondly, the direction of the streamline flow approaching the protuberance differs at each location, effectively changing the angle of incidence of the flow. Finally, the form of the model varies at each location. All of these factors influence the wave pattern generated by the protuberance and could be the causes of the differences obtained in the above influence diagrams. To minimize these effects, only the protuberance at station 1 will be used in later shifting applications, since the difference signal generated by this configuration most closely approximates the protuberance in a free stream.

Salvesen (5) found that waves tend to die out in phase as well as amplitude as they propagate, and consequently their phase at a distance from the point of generation differs from the phase predicted by wave theory. Since it is expected that this phenomena is occuring in the wave resistance tests conducted for this project, a translation was applied to the influence diagram in an

attempt to obtain better agreement between the actual and predicted wave resistance coefficients.

By inspection of Figures 11 and 12 it was decided to use a twenty percent aft translation for a Froude number of 0.242 and a thirty percent aft translation for a Froude number of 0.363. However, for a Froude number of 0.484, it was obvious that translation of the influence diagram would be unrealistic, and therefore, no attempt was made to apply the technique to this speed. These translations yielded wave resistance coefficients at stations 1, 3 and 5 which are within a few percent of the experimentally obtained values.

To verify this technique, additional model tests were conducted with the large protuberance attached at stations 2 and 4. At both Froude numbers these tests yielded wave resistance coefficients at station 2 which were within six percent of the predicted translated values, while the wave resistance coefficients obtained at station 4 deviated considerably from the predictions. The experimentally obtained points have been shown on Figure 13. Table V compares the actual and predicted resistance coefficients.

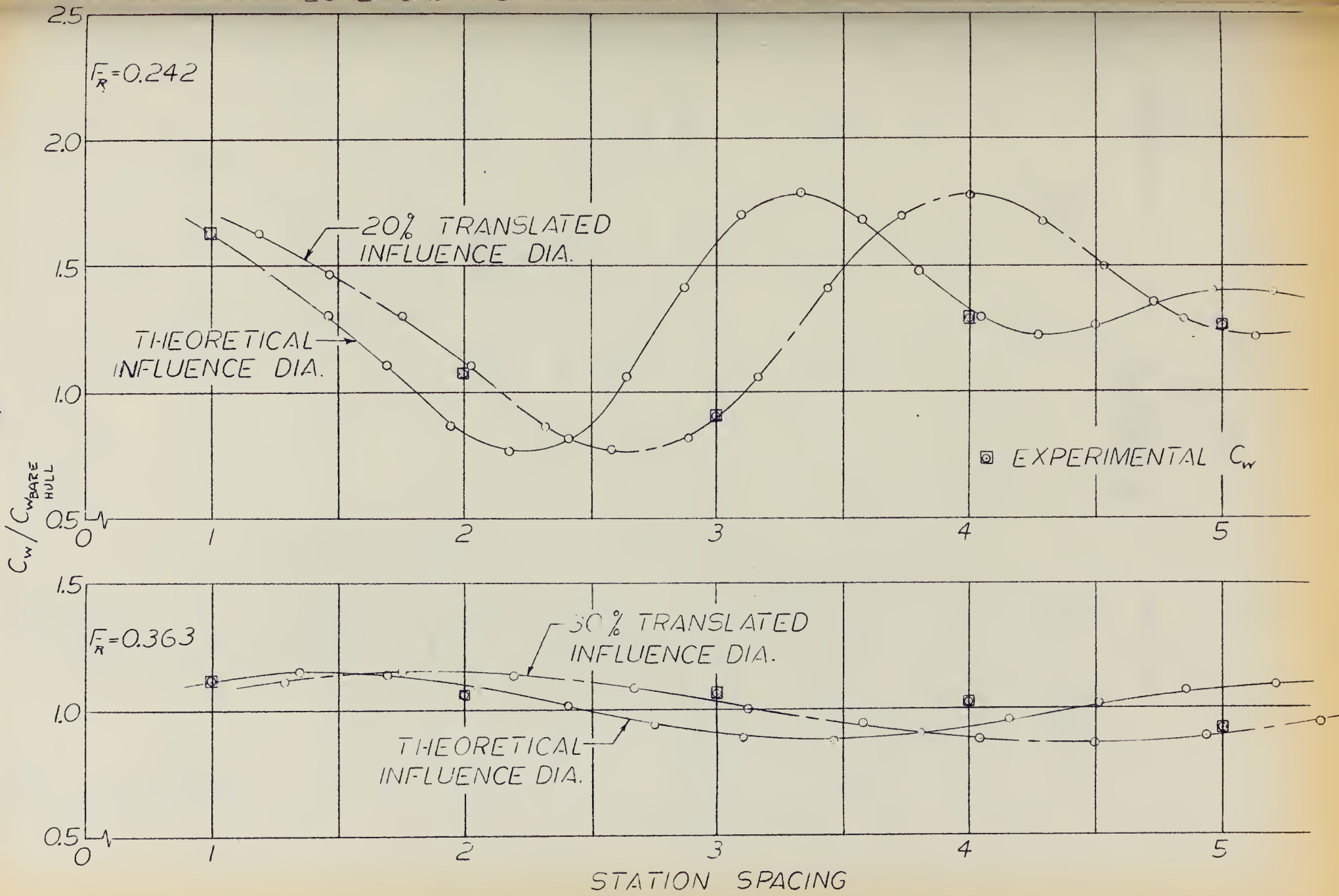
2.5
2.0
1.5
1.0
0.5
0
1
2
3
4
5
F_R=0.242
20% TRANSLATED INFLUENCE DIA.
THEORETICAL INFLUENCE DIA.
EXPERIMENTAL C_w
$C_w / C_{w_{BARE\ HULL}}$
1.5
1.0
0.5
F_R=0.363
30% TRANSLATED INFLUENCE DIA.
THEORETICAL INFLUENCE DIA.
STATION SPACING

TABLE V

Comparison of Actual and Predicted Wave Resistance Coefficients

Fr	Large Protub at Sta	Predicted C_w $x10^3$	Actual C_w $x10^3$	% Deviation of Predicted from Actual C_w
0.242	2	0.231	0.218	6.0
0.242	4	0.362	0.261	38.7
0.363	2	0.815	0.741	10.0
0.363	4	0.622	0.715	13.0

To check the validity of the linear superposition technique for short distances, a comparison was made of the actual wave resistance coefficients obtained from model tests and the wave resistance coefficients predicted by shifting the protuberance one station forward or aft, with no translation of the influence diagram. This comparison is shown as Table VI. It is evident that a higher Froude numbers a shift of the difference signal of one station aft predicts the wave resistance with considerable accuracy, while shifting the difference signal forward gives no reliable results.

TABLE VI

One Station Shift Comparison for Large Protuberances

Fr	(1) Shift From	(2) To	(3) C_w at (2)	(4) C_w Pred at (2)	(5) Diff (3)-(4)	(6) % Diff (5)/(3)
0.242	1	2	.218	.173	.045	20.6
"	3	4	.261	.352	-.091	-34.9
"	3	2	.218	.380	-.162	-74.3
"	5	4	.261	.295	.034	13.0
0.363	1	2	.741	.770	-.029	-3.9
"	3	4	.715	.695	-.020	-2.8
"	3	2	.741	.325	-.084	-11.3
"	5	4	.715	.770	-.055	-7.7
0.484	1	2	2.228	2.184	0.044	2.0
"	3	4	2.473	2.510	-0.037	-1.5
"	3	2	2.228	2.710	-0.482	-21.6
"	5	4	2.473	2.136	0.607	24.5

Data Investigation

At each Froude number under investigation, the wave record of the protuberance was obtained by the method outlined in the introduction. These wave records or difference signals are shown as Figures 14, 15, and 16. On each figure the assumed starting location, taken as the

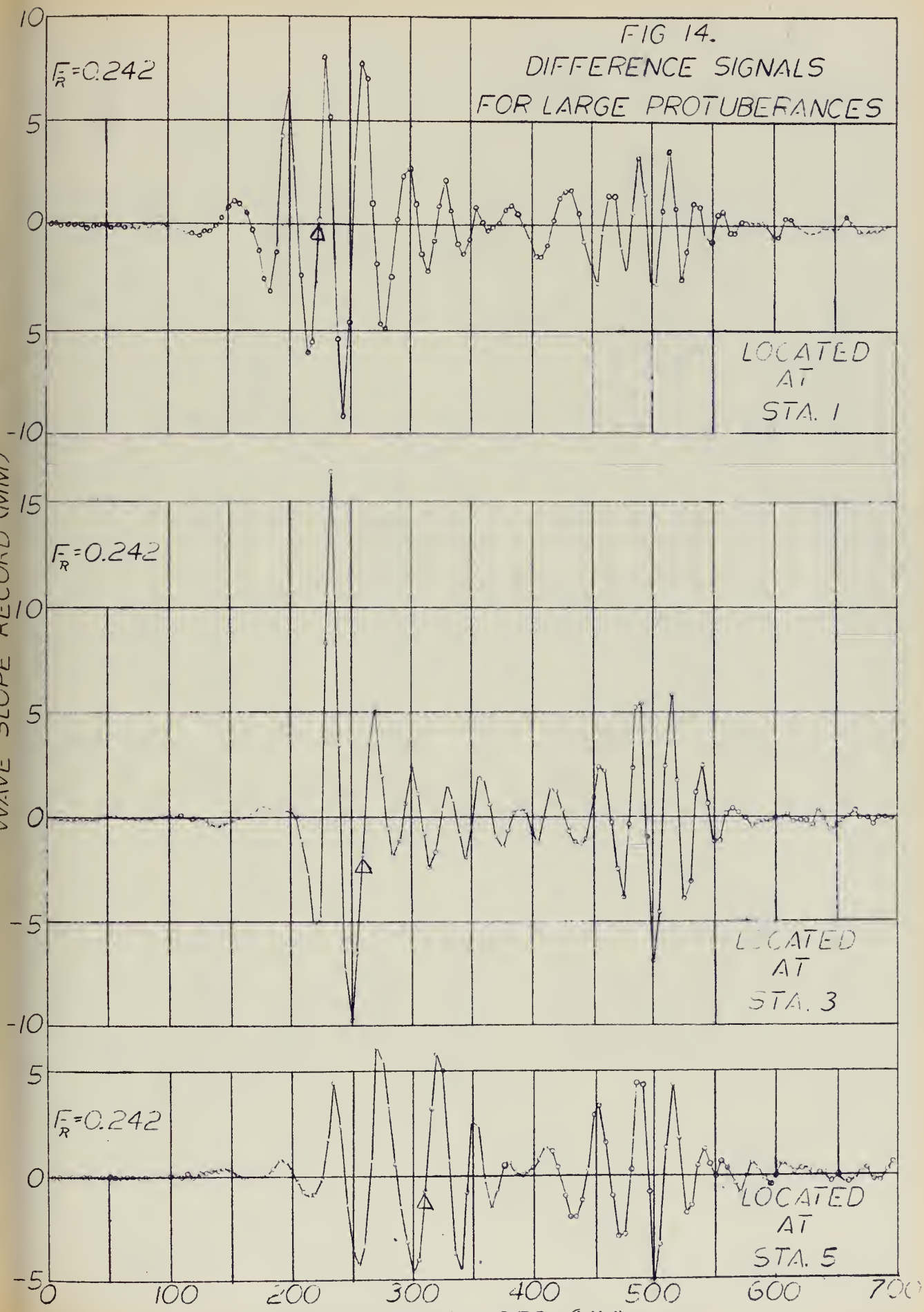
FIG 14.
DIFFERENCE SIGNALS
FOR LARGE PROTUBERANCES
F_R=0.242
LOCATED AT STA. 1
F_R=0.242
LOCATED AT STA. 3
F_R=0.242
LOCATED AT STA. 5
WAVE SLOPE RECORD (MM)
LENGTH OF RECORD (MM)
10
5
0
5
-10
15
10
5
0
-5
-10
5
0
-5
0
100
200
300
400
500
600
700

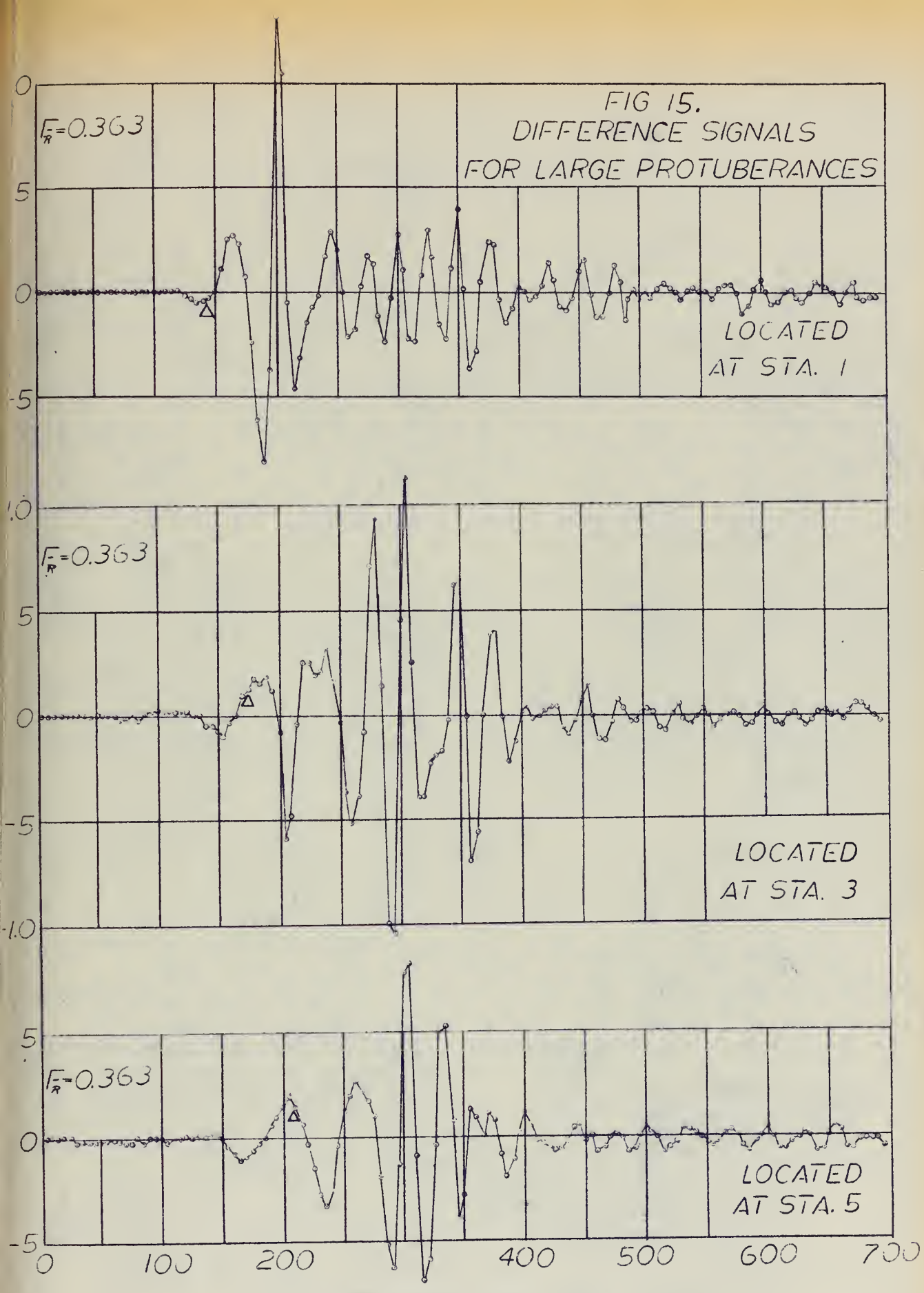
FIG 15.
DIFFERENCE SIGNALS
FOR LARGE PROTUBERANCES
F_R=0.363
LOCATED
AT STA. 1
F_R=0.363
LOCATED
AT STA. 3
F_R=0.363
LOCATED
AT STA. 5
0
5
0
-5
1.0
5
0
-5
-1.0
5
0
-5
0
100
200
400
500
600
700
LENGTH OF RECORD (MM)

FIG 16.
DIFFERENCE SIGNALS
FOR LARGE PROTUBERANCES

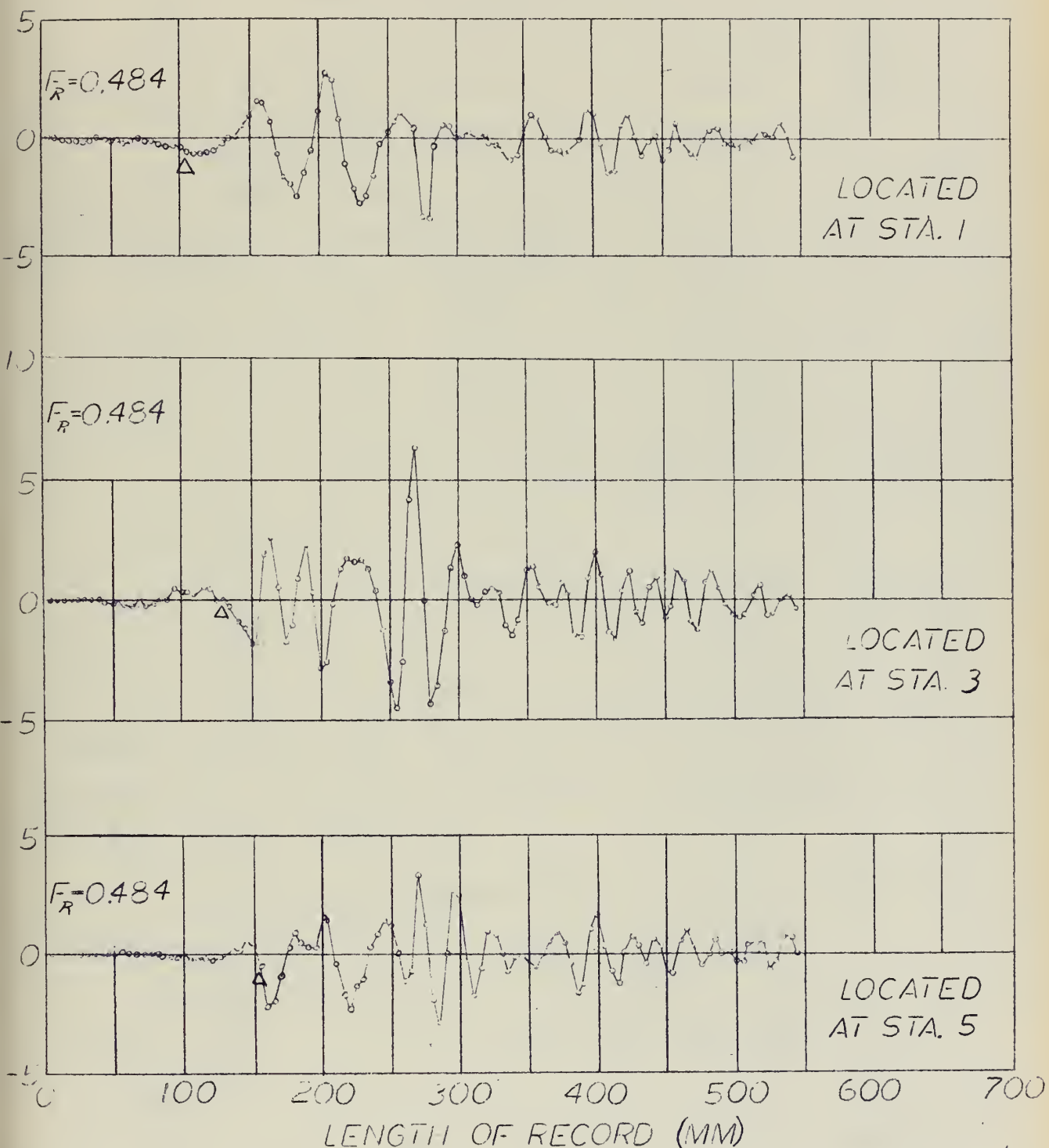

protuberance maximum cross section, of the difference signal is indicated by Δ .

If the original linear superposition theory were completely valid, the difference signals for each protuberance location at a given Froude number would be identical in phase and amplitude, varying only by their starting position. This shift in starting position would be directly related to the location of the protuberance on the model.

As can be seen from the difference signal plots, the correlation between the curves is not exact. However, the following points of agreement should be noted:

a. All of the difference signals are sinusoidal in nature and are quite similar in character to the wave records obtained from the model tests.

b. For a given Froude number, the difference signals exhibit fairly good phase and amplitude relationships.

c. The magnitude of the amplitudes of the signals decrease with increased Froude number, indicating that the effect of a protuberance upon the wave resistance decreases with increased speed.

d. At all Froude numbers the most severe difference signal occurs for the protuberance at station 3.

From this discussion it is evident that direct superposition may be possible but that additional analysis of the data is required.

The amplitude spectra and Fourier sine and cosine transforms were plotted so that the data could be compared

after it had undergone the first integration. This process gives an indication of the effect of the deviations between difference signals upon the wave resistance coefficient and allows comparison of the data after it has been smoothed. Figures 17, 18 and 19 show the curves obtained at a Froude number of 0.363 for the configurations with large protuberances attached at stations 1, 3 and 5. The remainder of the spectra are included in Appendix C.

The agreement among these spectra is remarkably good, particularly at the higher Froude numbers. The resultant amplitude spectra and Fourier transform spectra show a similar phase relationship at each Froude number as well as definite amplitude agreement.

In addition to the above,plots, the amplitude spectra of the difference signal alone were obtained for the large protuberance attached at stations 1, 3, and 5 at all three Froude numbers. These curves are shown as Figure 20. The nature of these spectra indicates that the difference signal obtained is essentially equivalent to that of the protuberance in a free stream, since in a free stream the protuberance can be represented by a point source, and thus it would give a straight line amplitude spectra.

Although free wave spectra cannot be directly applied to shifting methods, their consistent similarity indicates that further investigation of the proposed linear superposition technique should be pursued.

FIG 17

WAVE AMPLITUDE SPECTRA FOR LARGE PROTUBERANCE CONFIGURATIONS FROUDE NUMBER .363

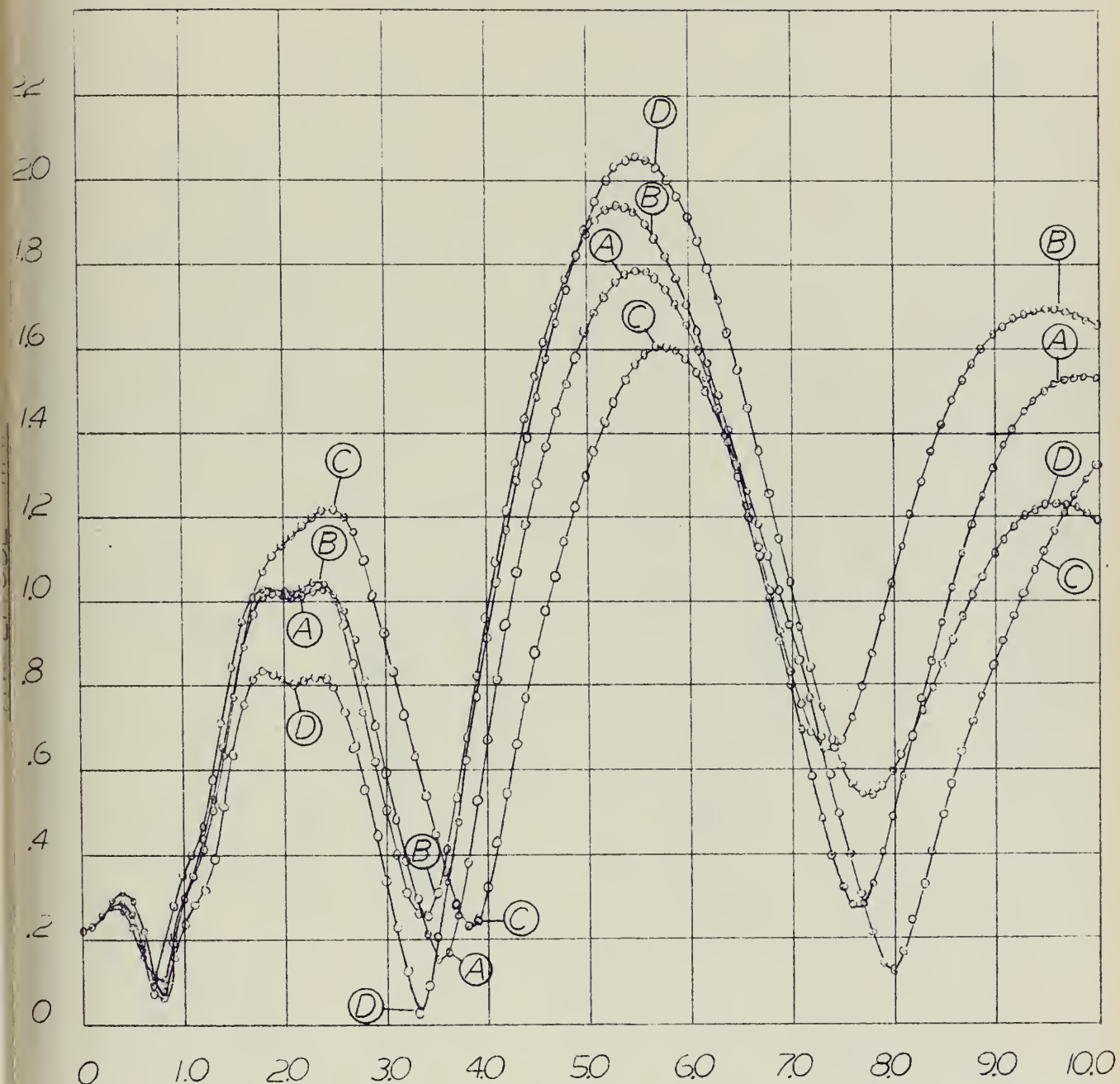

PROTUBERANCE LOCATION

A - BARE HULL
B - STA - 1
C - STA - 3
D - STA - 5

FIG 18.

WAVE SINE TRANSFORM

FOR

LARGE PROTUBERANCE CONFIGURATIONS

FROUDE NUMBER .363

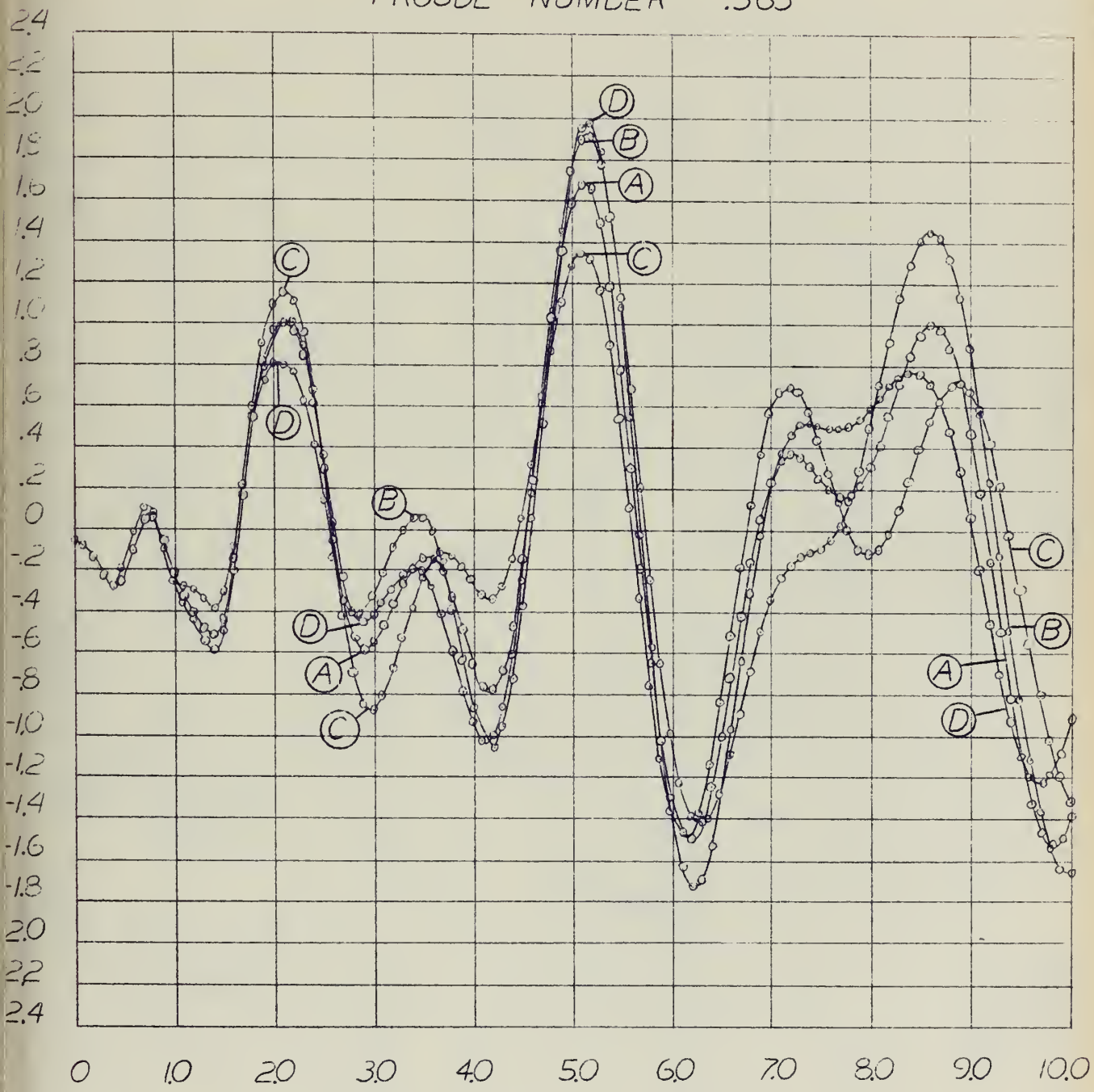

TRANSVERSE WAVE NUMBER — U

PROTUBERANCE LOCATION

A - BARE HULL

B - STA - 1

C - STA - 3

D - STA - 5

FIG 19.

WAVE COSINE TRANSFORM
FOR
LARGE PROTUBERANCE CONFIGURATIONS
FROUDE NUMBER .363

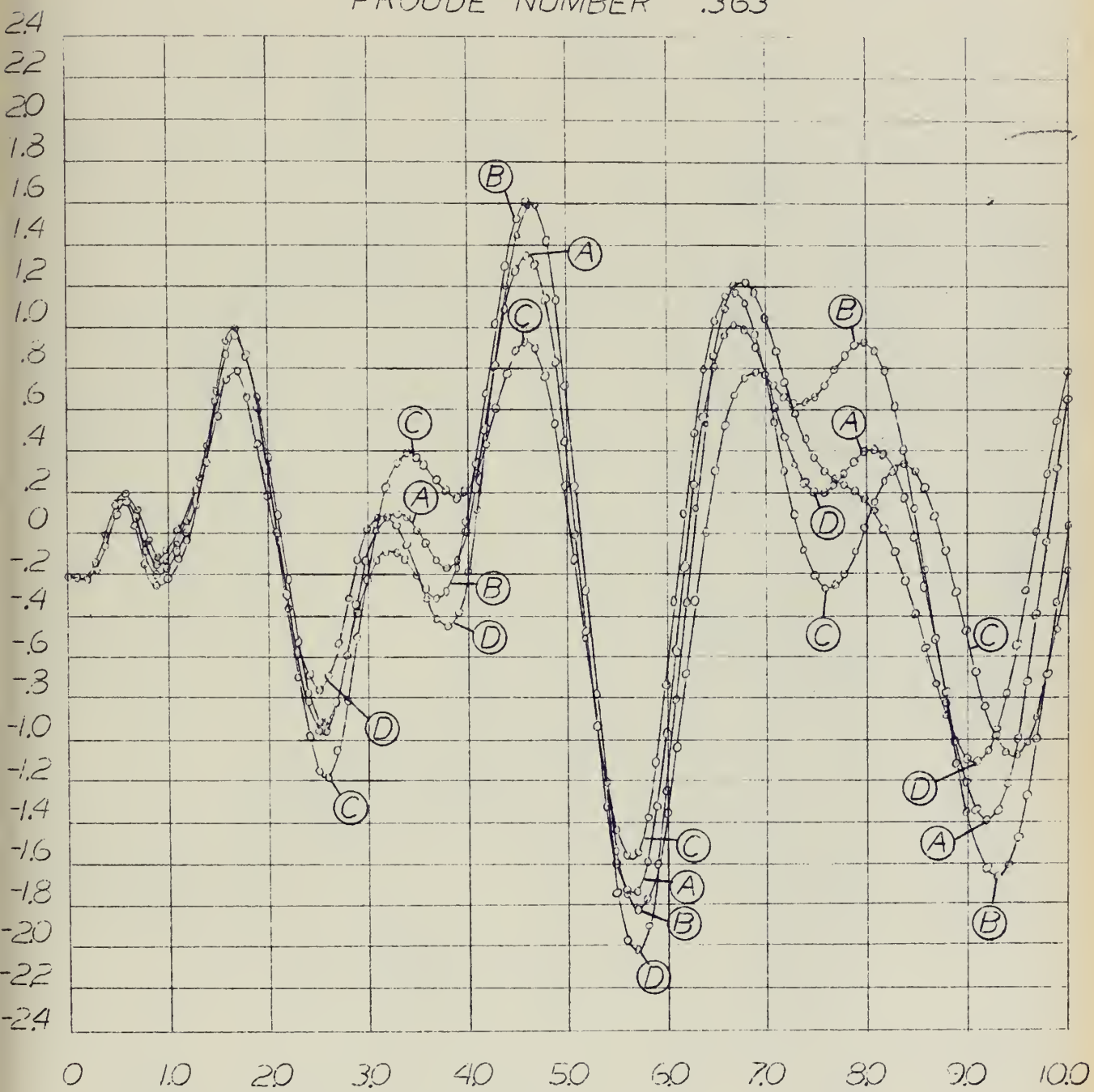

TRANSVERSE WAVE NUMBER—U

PROTUBERANCE LOCATION
A - BARE HULL
B - STA - 1
C - STA - 3
D - STA - 5

WAVE AMPLITUDE SPECTRA FOR DIFFERENCE SIGNALS

FIG. 20

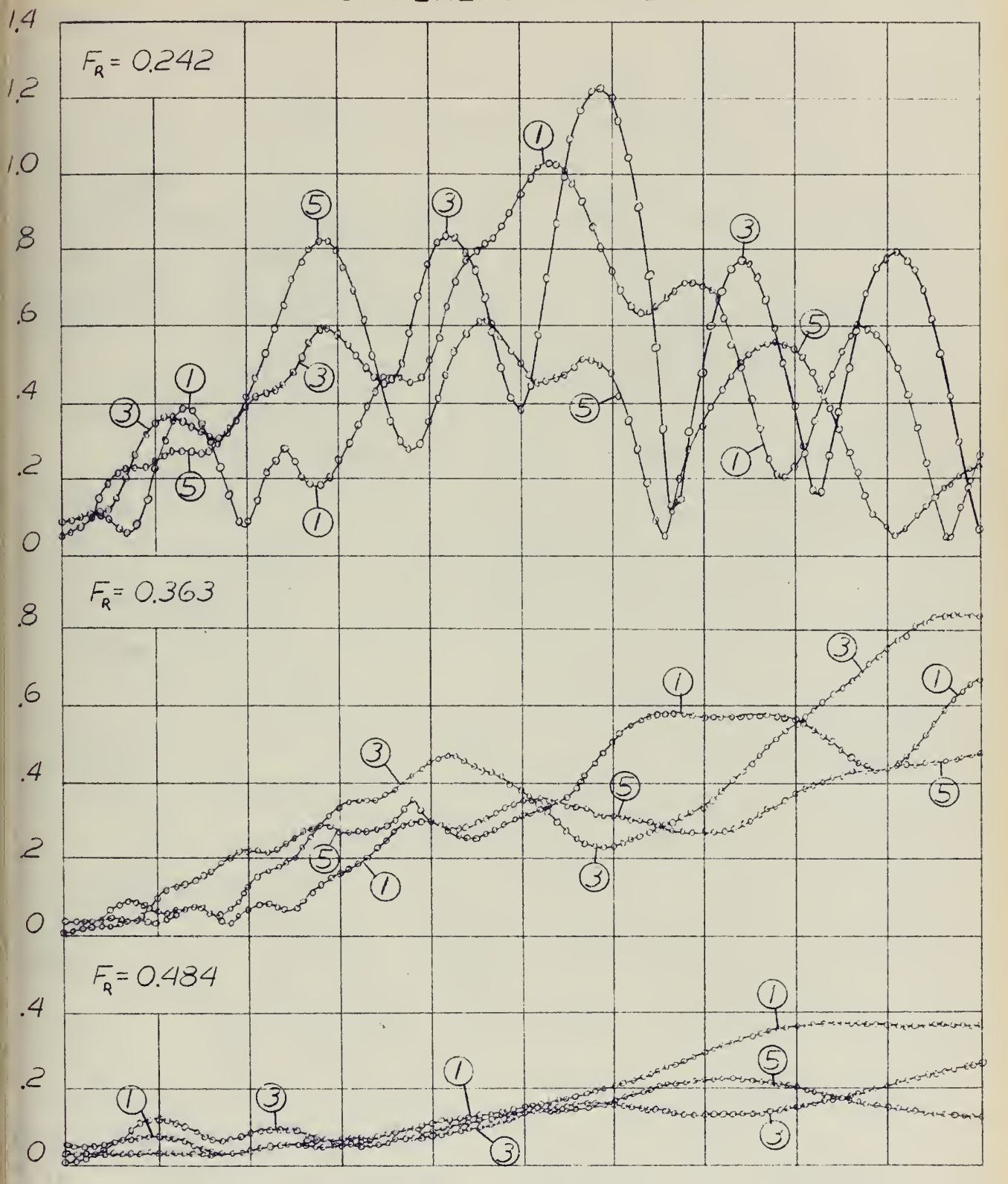

TRANSVERSE WAVE NUMBER - U

1 LARGE PROTUBERANCE AT STA. 1 MINUS BARE HULL

3 " " " " 3 " " "

5 " " " " 5 " " "

Size Comparison

The effect of protuberance size upon the wave resistance coefficient was analyzed by comparing the results obtained from model tests with the large and small protuberances attached at station 3. The methods of analysis were essentially the same methods employed in the previous sections and are best explained by the following:

a. Difference signals, shown as Figures 21 and 22, show no direct relationship.

b. Wave amplitude and Fourier sine and cosine transform spectra, shown for Froude number 0.363 as Figures 23, 24 and 25 and for Froude numbers 0.242 and 0.484 in Appendix C, show relatively good relationships at the higher Froude numbers.

c. Influence diagrams, Figures 26 and 27, are almost identical at Fr = 0.484, while there is no agreement between the diagrams at the lower Froude numbers.

d. The ratio of experimental wave resistance coefficients at the three speeds are:

Fr	C_w large / C_w small
0.232	0.832
0.363	1.355
0.484	1.069

As is evident from the various curves, the agreement between the results is a function of the Froude number

with the best agreement occuring at the highest speed. This is probably because the relative influence of the protuberance decreases with increasing speed.

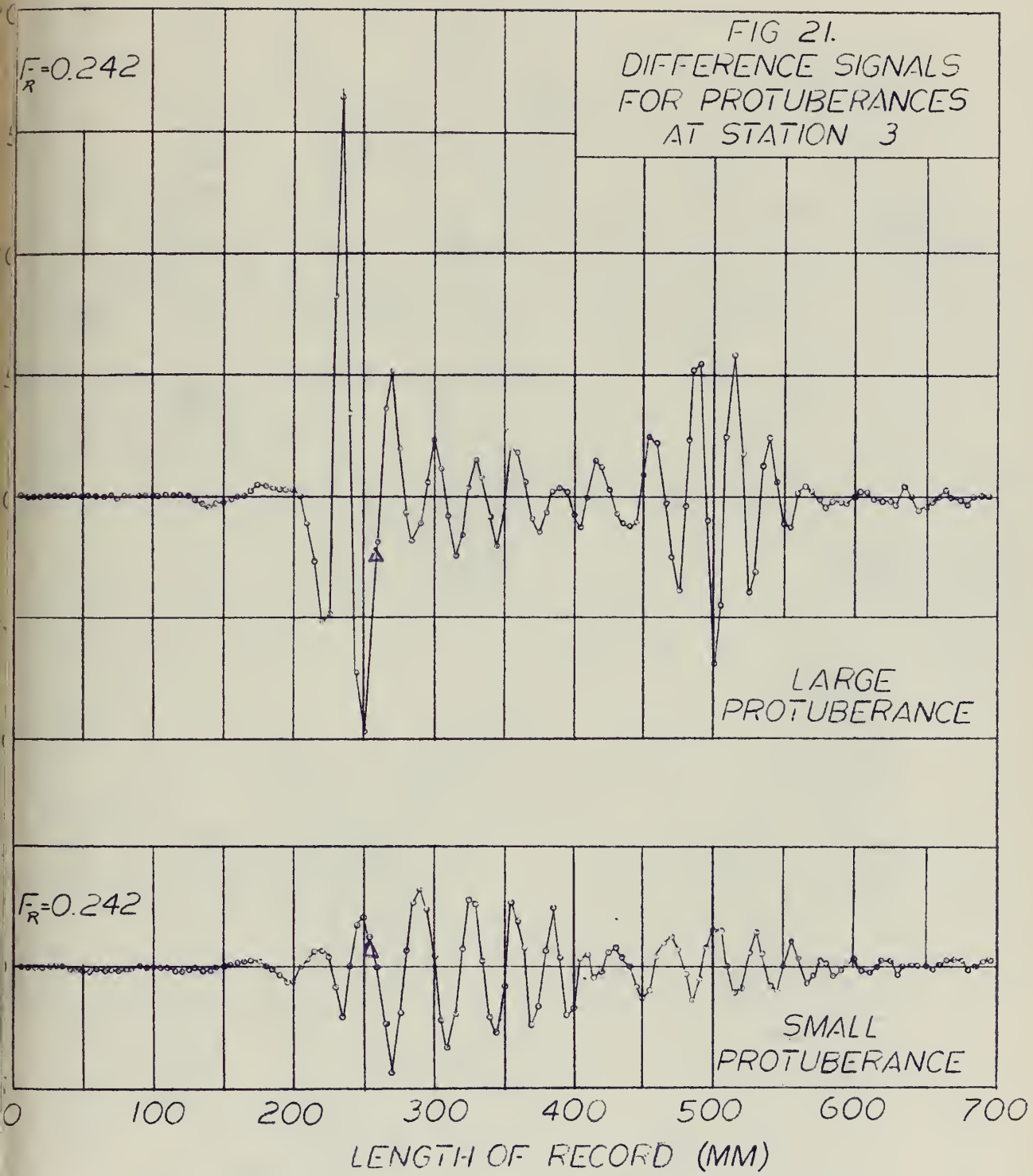
FIG 21.
DIFFERENCE SIGNALS
FOR PROTUBERANCES
AT STATION 3
F_R=0.242
LARGE
PROTUBERANCE
F_R=0.242
SMALL
PROTUBERANCE
0
100
200
300
400
500
600
700
LENGTH OF RECORD (MM)

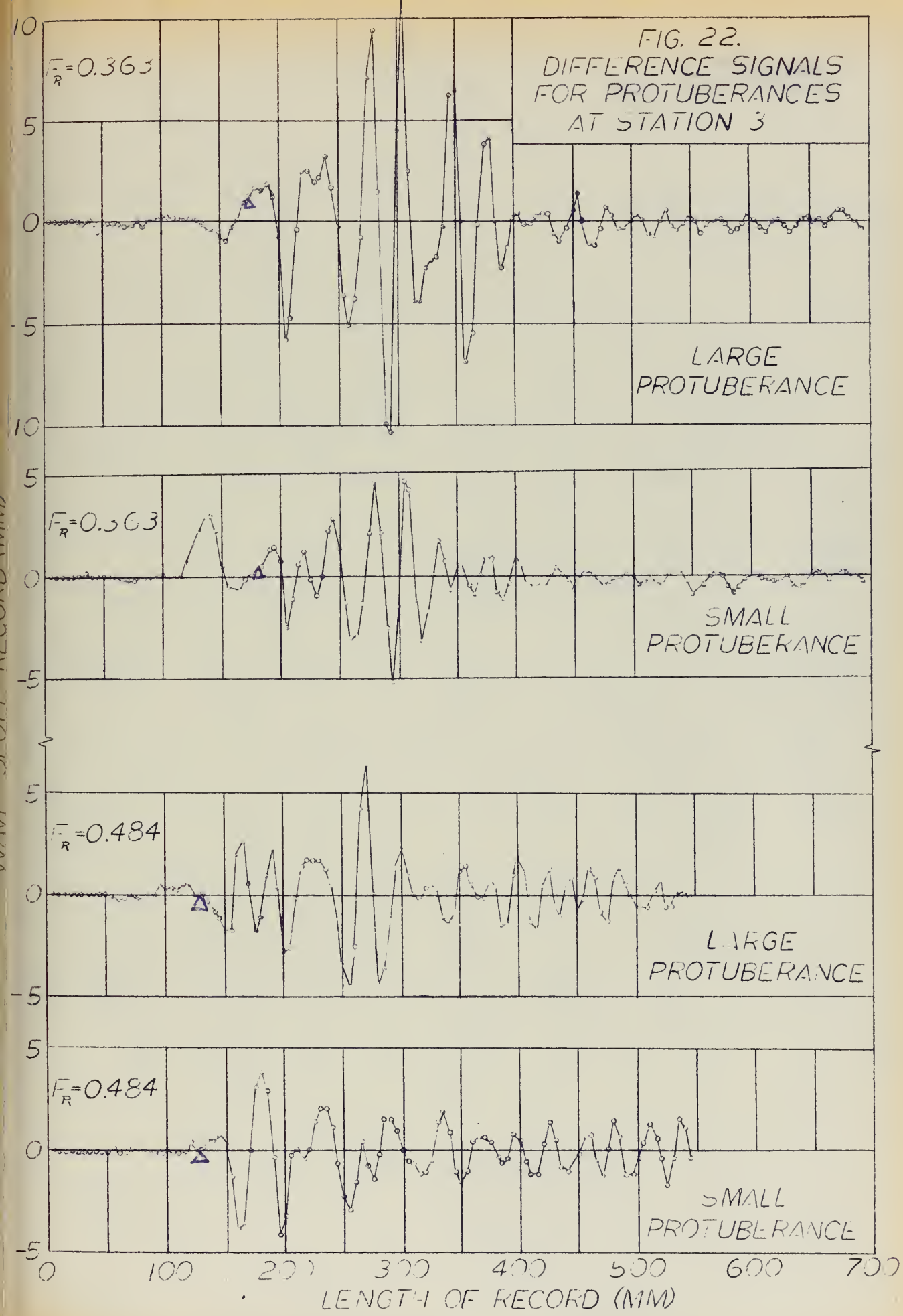
FIG. 22.
DIFFERENCE SIGNALS
FOR PROTUBERANCES
AT STATION 3
F_R=0.363
LARGE
PROTUBERANCE
F_R=0.363
SMALL
PROTUBERANCE
F_R=0.484
LARGE
PROTUBERANCE
F_R=0.484
SMALL
PROTUBERANCE
10
5
0
-5
-10
0
100
200
300
400
500
600
700
LENGTH OF RECORD (MM)

FIG 23.

WAVE AMPLITUDE SPECTRA
FOR
LARGE & SMALL PROTUBERANCE CONFIGURATIONS
FROUDE NUMBER .363

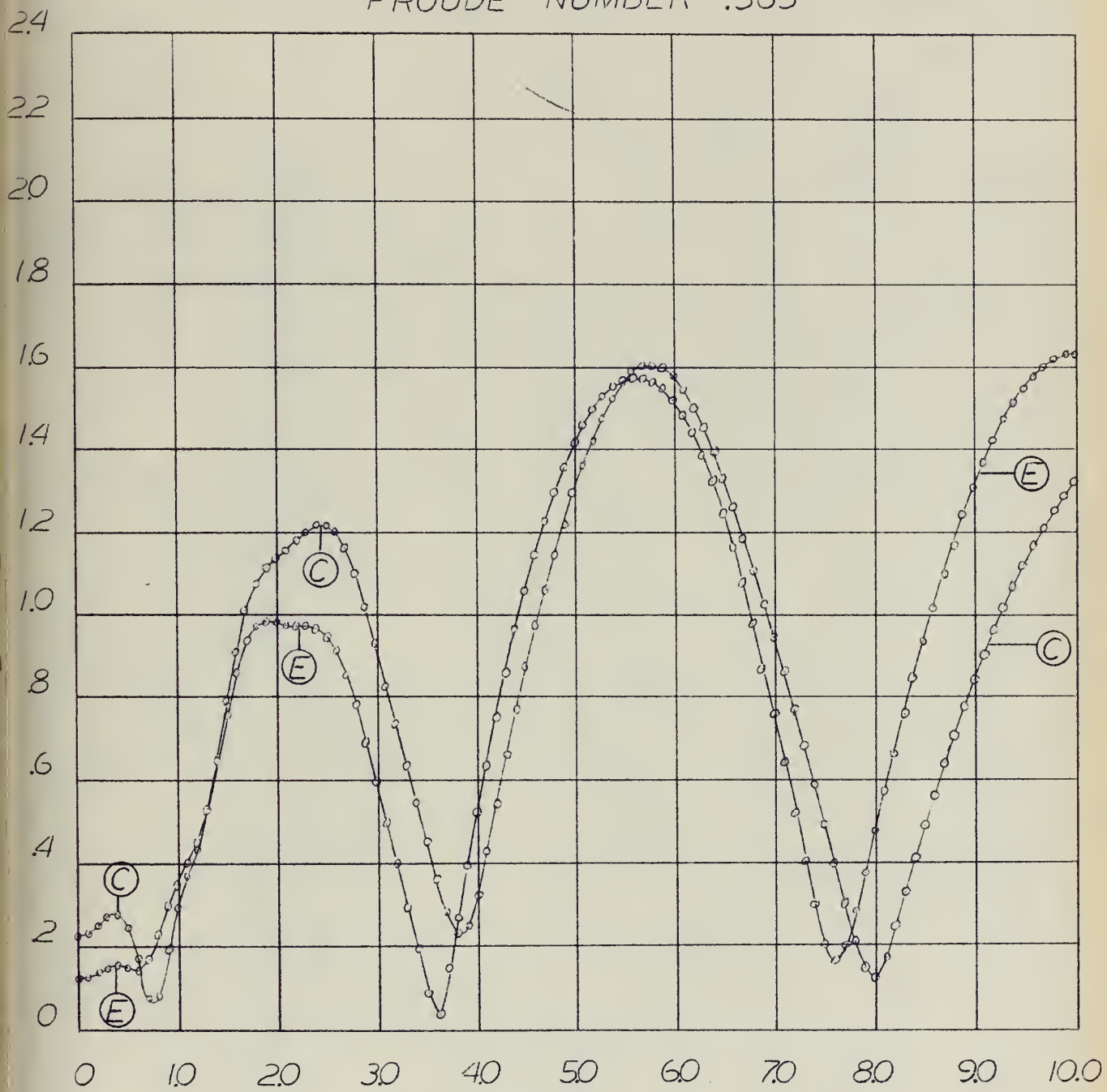

TRANSVERSE WAVE NUMBER — U

C-LARGE PROTUBERANCE STA 3
E-SMALL PROTUBERANCE STA 3

FIG 24.

WAVE SINE TRANSFORM

FOR

LARGE & SMALL PROTUBERANCE CONFIGURATIONS

FROUDE NUMBER .363

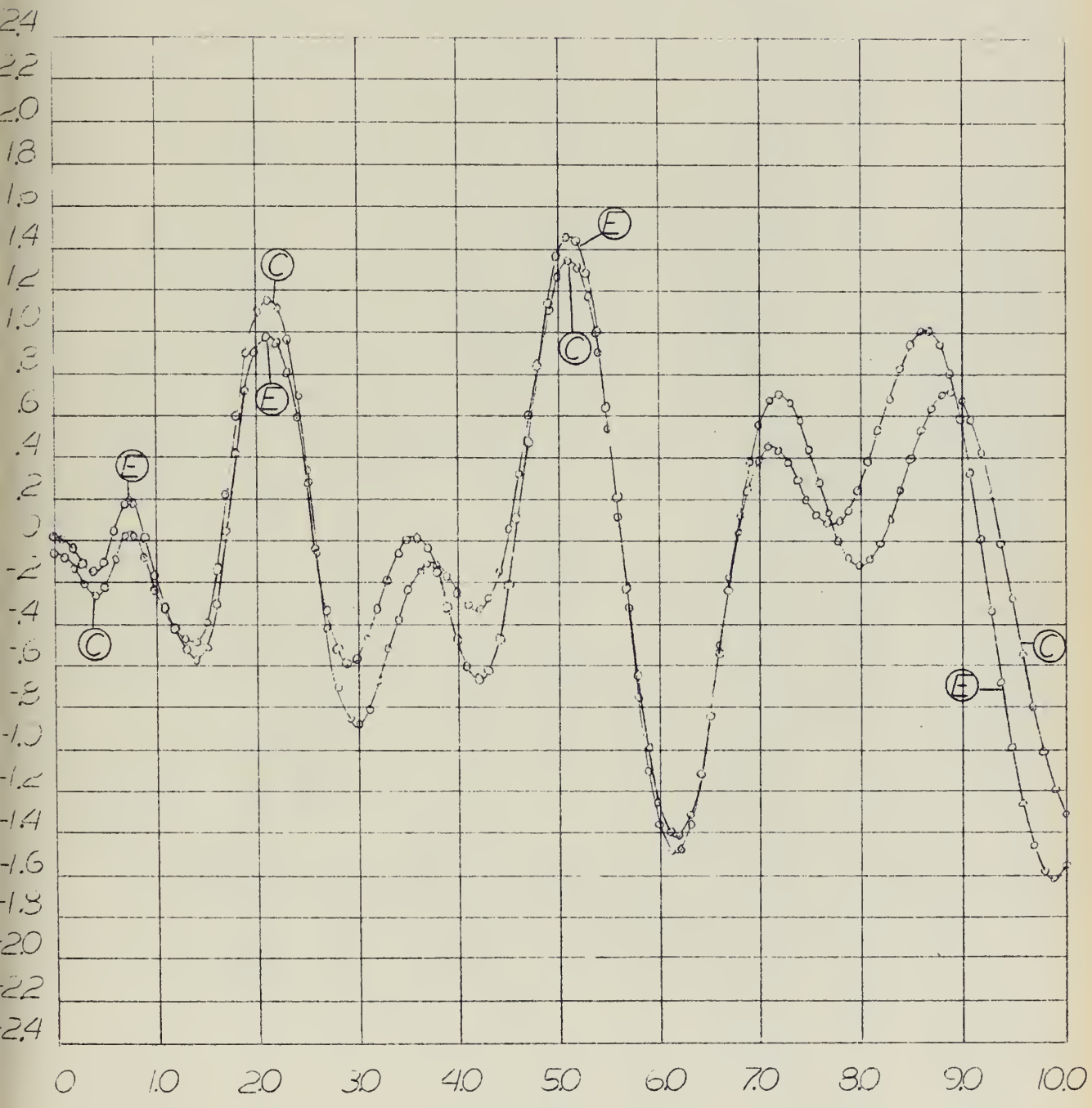

TRANSVERSE WAVE NUMBER — U

C - LARGE PROTUBERANCE STA 3

E - SMALL PROTUBERANCE STA 3

FIG 25.

WAVE COSINE TRANSFORM

FOR

LARGE & SMALL PROTUBERANCE CONFIGURATIONS

FROUDE NUMBER .363

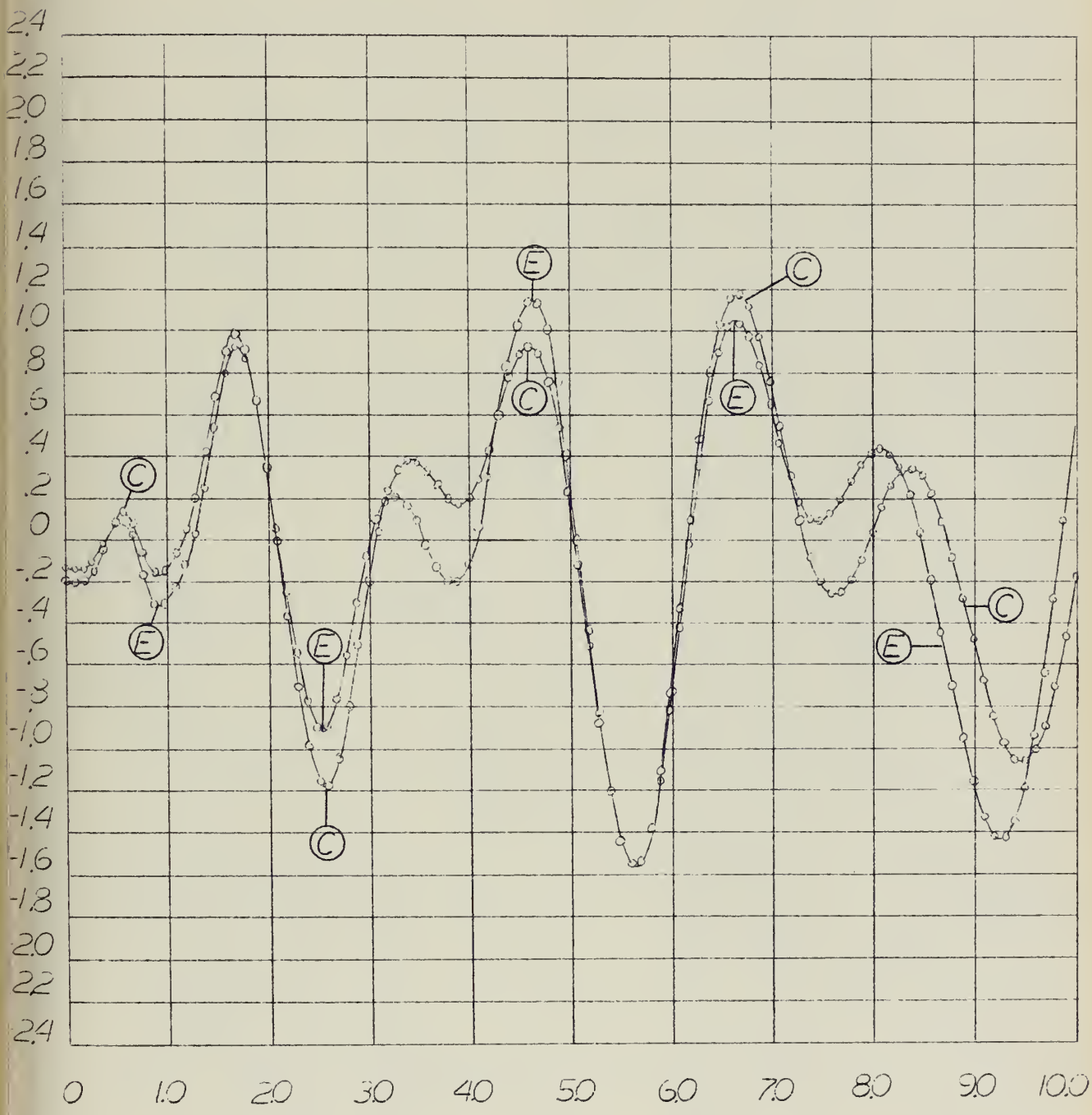

TRANSVERSE WAVE NUMBER — U

C-LARGE PROTUBERANCE STA 3

E-SMALL PROTUBERANCE STA 3

$C_w/C_{w_{BARE\ HULL}}$ vs. THEORETICAL PROTUBERANCE LOCATION

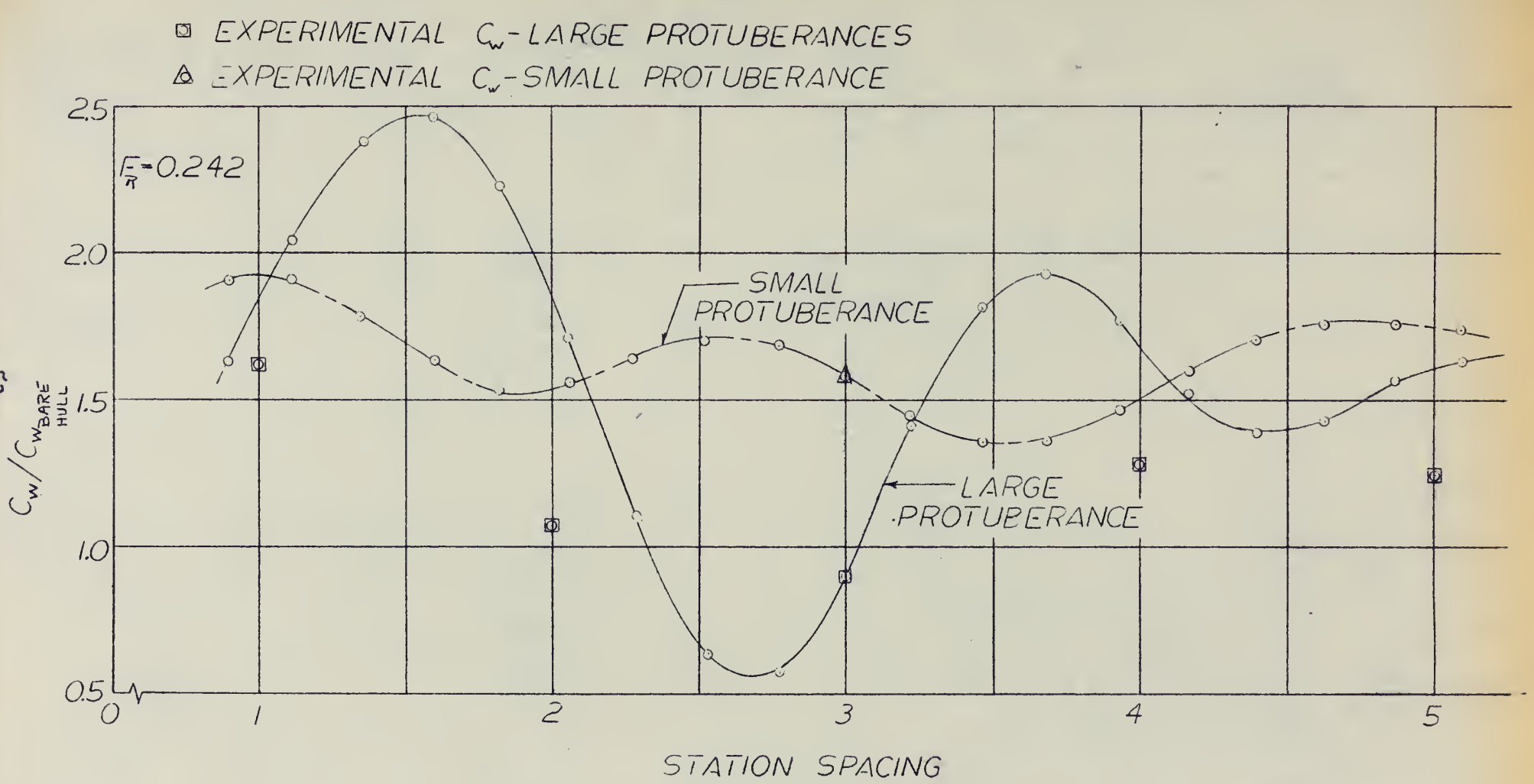

$C_w/C_{w_{BARE\ HULL}}$ vs. THEORETICAL PROTUBERANCE LOCATION

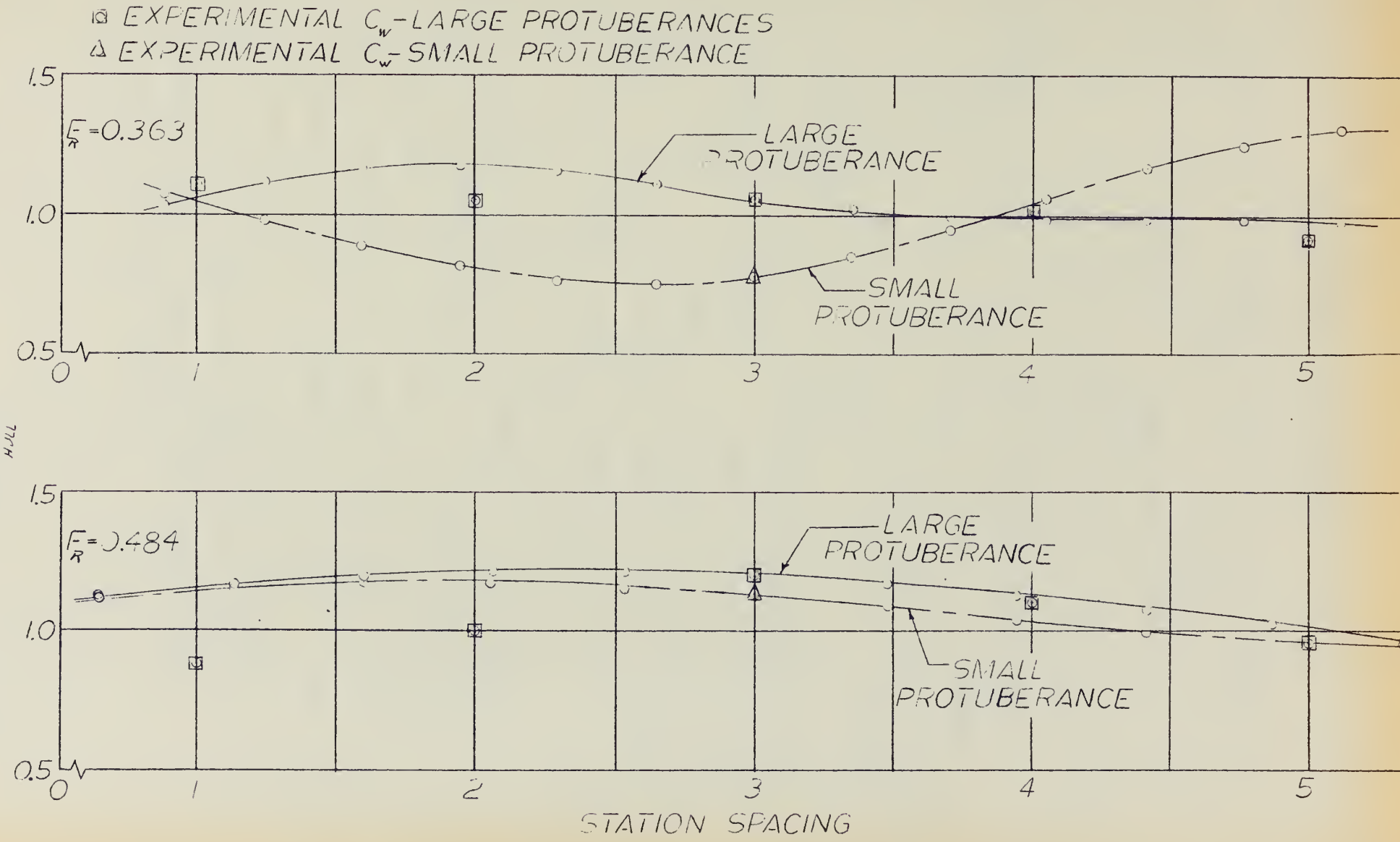

54.

CONCLUSIONS AND RECOMMENDATIONS

Contrary to the results obtained by Eggers, Sharma, and Ward (1,3) regarding the feasibility of the lateral cut, wave slope method of determing wave resistance, the authors experienced large variations in the computed wave resistance coefficients of individual data record sets. When principles of statistical probability were introduced (Appendix I), the average wave resistance coefficient used was found to have only a 50% degree of confidence of being within 6% of the actual value. Therefore, all results in this paper must be viewed with a certain degree of uncertainty.

At the present time, influence diagrams can be obtained only by extensive model testing. Attempts to accurately produce an influence diagram by applying the pinciple of linear superposition of wave records were met with varying degrees of success. The following positive trends were observed: (a) With increasing Froude number the relative effect of the protuberance upon the wave resistance decreased, yielding better correlation between the experimental and predicted wave resistance coefficients. (b) The linear superposition technique of developing influence diagrams appears to be valid only over small intervals. (c) At the lower Froude number, translation of the influence diagram was required to obtain any degree of correlation between experimental and predicted wave resistances. This technique produced relatively good agreement within an interval of two stations on the model.

When two protuberances of different size were tested at the same location, no discernable agreement or uniform trends were found at the lower Froude numbers. Only at the highest Froude number, where the effects of the protuberance are diminished, was any consistency observed.

Based on the foregoing results, the following recommendations are made for future work in this field: (a) The statistical nature of the data should be investigated to determine the approximate number of data records required to obtain sufficient confidence in the final wave resistance values. This appears to be especially true for the type of wave slope measurement used in the present investigation. (b) Since there have been no previous wave resistance tests on Destroyer-type models, the percentage relationship between the wave and residuary resistances is not known. It is possible that the low values obtained in the present tests reflect an error in the method or instrumentation. Further equipment checks in both areas should be made. (c) Curve fitting techniques should be applied to the experimentally-obtained wave resistance coefficients to improve the quality of the influence diagrams. (d) Theoretical investigation into non-linear wave theory should be conducted to discover, if possible, simple adjustments to the linear superposition principle so that acceptable agreement between the experimental and predicted wave resistances and between results for different-sized protuberances can be obtained. The similarities between the difference signals and the wave spectra noted earlier encourage this effort. Success would allow one to construct a valid influence diagram for wave resistance which does not seem possible using the present linearized approach.

LIST OF REFERENCES

(1) Eggers, K. W. H., Sharma, S. D., and Ward, L. W., "An Assessment of Some Experimental Methods for Determining the Wavemaking Characteristics of a Ship Form", Transactions of the Society of Naval Architects and Marine Engineers, Vol. 75, November 1967

(2) Hogner, E., "Influence Lines for the Wave Resistance of Ships", Proceedings of Royal Institute of Naval Architects, Vol. 155, 1936

(3) Ward, L. W., "Experimental Determination of Wave Resistance of a Ship Model from Lateral Wave-Slope Measurements", ONR-Report, Webb Institute of Naval Architecture, Glen Cove, New York, September 1967

(4) Sharma, S. D., "A Comparison of the Calculated and Measured Free-Wave Spectrum of an Inuid in Steady Motion", International Seminar on Theoretical Wave-Resistance, University of Michigan, Ann Arbor, Michigan, August 1963

(5) Salvesen, N., "On Second Order Wave Theory for Submerged Two-Dimensional Bodies", University of Michigan, Ann Arbor, Michigan, 1966

(6) Ward, L. W., "Wave Resistance Surveys on a Ship Model of Minimum Resistance", ONR-Report, Webb Institute of Naval Architecture, Glen Cove, New York, August 1965

APPENDIX A: DESCRIPTION OF THE WAVE SLOPE MEASURING PROBE[4]

A successful wave slope measuring probe based on the resistance wire principle was developed in 1965 for use at Webb in conjunction with the 2KC excitation from a two-channel Brush BL-4622-00 amplifier and Mark II recorder. The probe and the calibration scheme is shown in Figure A-1, the corresponding circuit diagram is shown in Figure A-2, and photographs of the equipment in use are shown as Figure A-3. The scheme is an adaptation of the wave height measuring probe previously developed in connection with this effort (5), and employs three parallel stainless-steel wires of .004 inch diameter, spaced at 3/4 inch intervals between carefully drilled holes in Plexiglass blocks held by a C-shaped frame. The frame is mounted on a slider which allows known variations of vertical height of $\pm$ 3" at approximately $\frac{1}{4}$" intervals and this in turn is on a plate which can be rotated in either direction to produce a slope variation of $\pm$ .20 radians in steps of 0.10 for the slope calibration. The height variations are used to calibrate wave height probes mounted on the same frame or in the present case to check the insensitivity of the wave slope probe to changes in wave elevation.

---

4. This appendix has been extracted from "Experimental Determination of Wave Resistance of a Ship Model from Lateral Wave Slope Measurements" by L. J. Ward, Sep. 1967

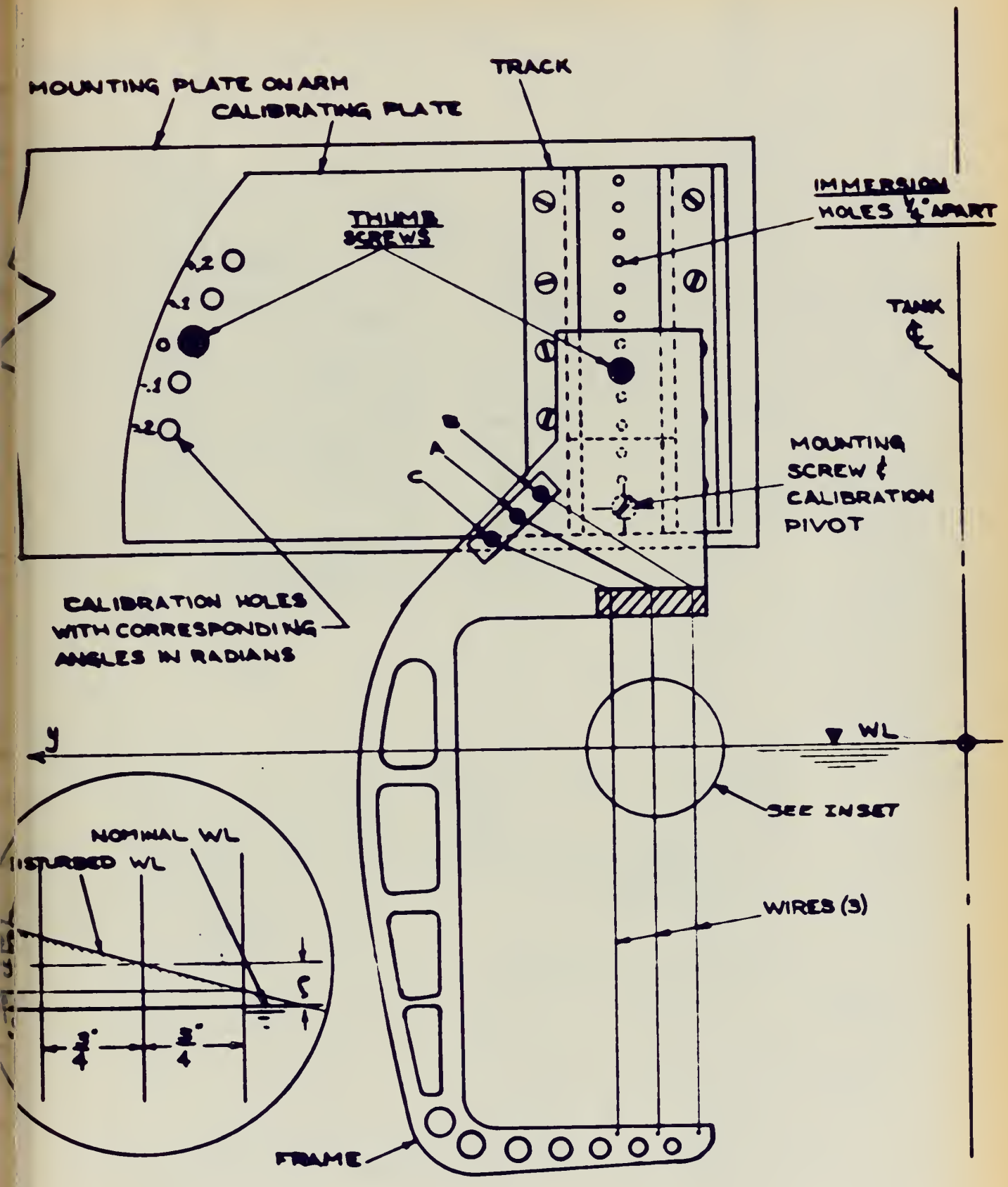

FIGURE A-1 : WAVE-SLOPE PROBE & CALIBRATING PLATE

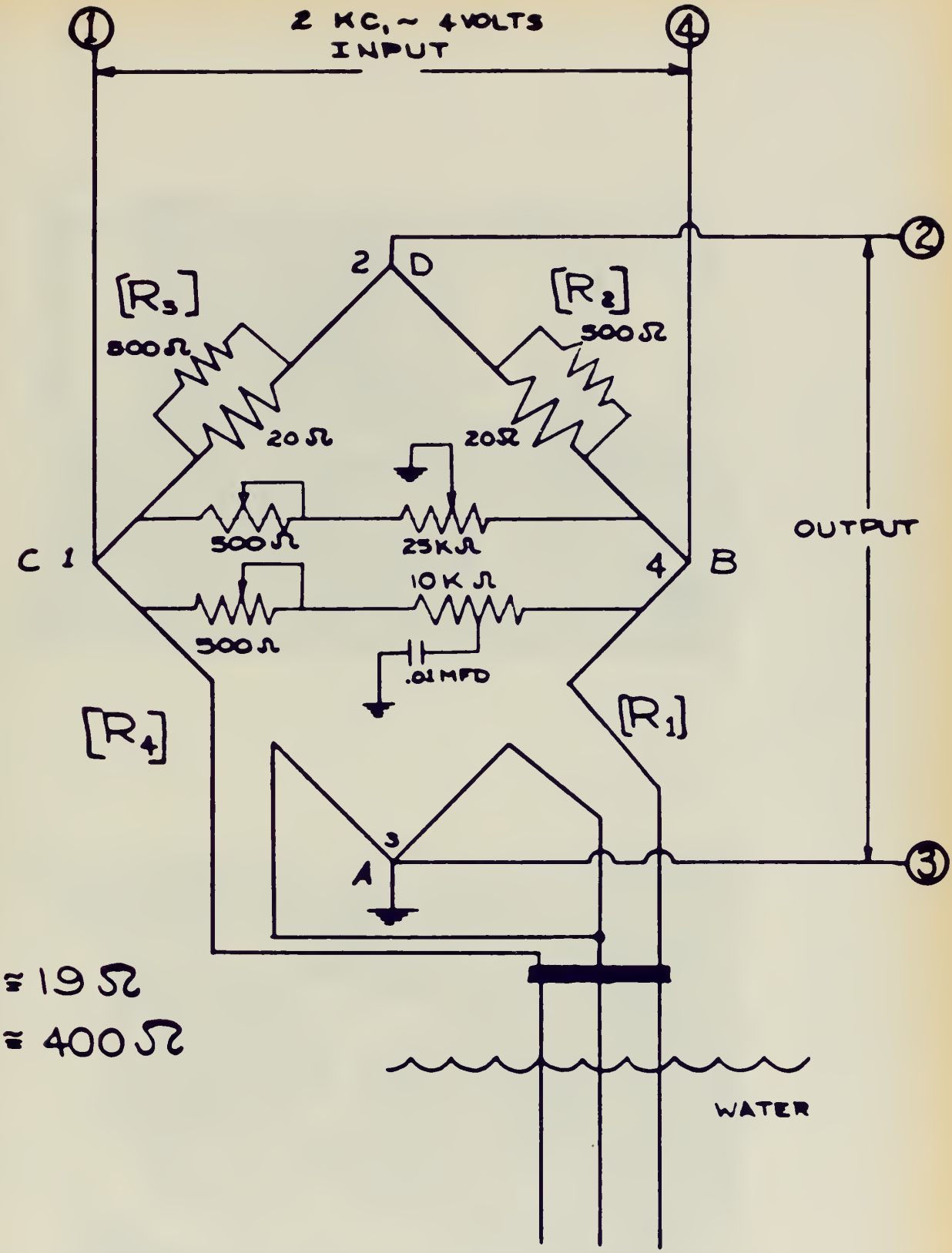

$R_2 + R_3 \cong 19\ \Omega$

$R_1 + R_4 \cong 400\ \Omega$

FIG A-2 WAVE-SLOPE PROBE CIRCUIT

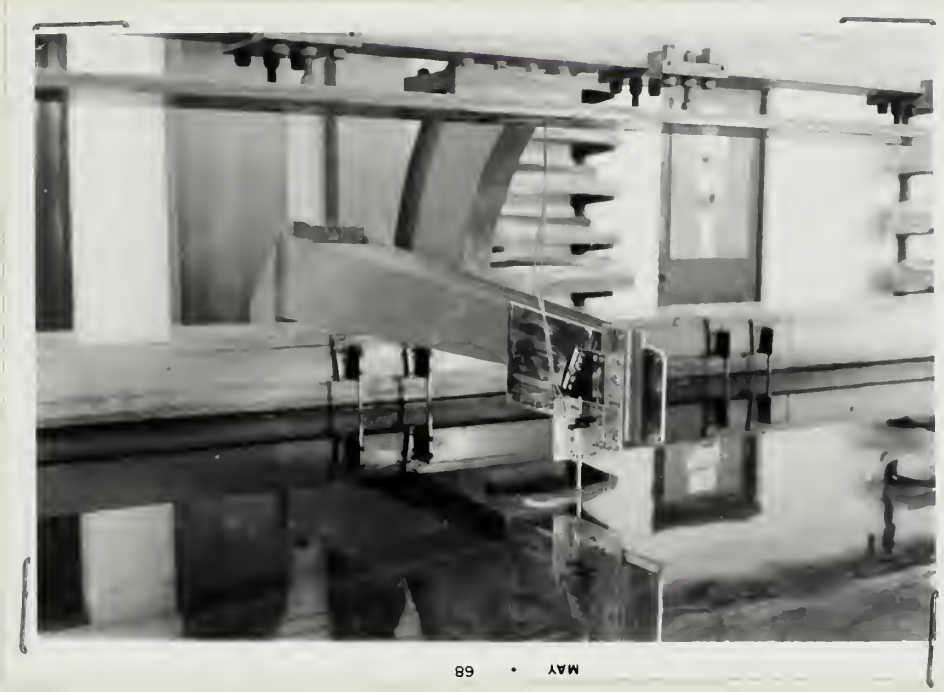

Wave Slope Probe

Brush Recorder and Amplifier

As shown in Figure A-2, the measuring circuit consists of a Wheatstone bridge with two of the resistances R_1 and R_4 replaced by the equivalent path resistance of the water between each set of wires AB and AC. This scheme is known in the case of the height probe to give a good linear response to changes in wave height over a range of several inches when the ratio of resistance:

$$R_{3/R_4} = R_{2/R_1} = K \qquad (A\text{-}1)$$

is properly chosen; in this case the value of K is approximately 20 based on the equivalent D. C. resistance of the water elements. In the case of the slope probe the elements are used differentially, as shown. This circuit is more symmetric and actually easier to balance than the height-probe circuit where an electrical resistor must be used to attempt to reproduce the water effect. A combined resistance and capacitance balancing circuit is provided within the bridge circuit to assist that available in the amplifier.

As mentioned previously, good linear response has been established for this probe in operation over the range of $\pm$ 0.20 radians ample for the usual model wave system and relatively good insensitivity with changes in wave height over the range of $\pm$ 1½ inches required for the present tests. Care is taken to keep the wires clean and at constant tension. No difficulty with this arrangement has been noted due to variations in surface film, nor does the exact spacing of the wires seem to be a critical factor as has been noted by

others. This might be a fortuitous result of the relatively high exciting frequency of 2KC provided by the Brush amplifier.

The foregoing statements refer to the characteristics noted under static conditions and do not include any effects due to dynamic action, such as meniscus oscillation at the frequency of the waves being measured. Although Pearlman ran a series of such tests on a similar device and found no important effects at the frequencies of importance, the present device should be subjected to a similar series of tests for the sake of completeness.

APPENDIX B: COMPUTER PROGRAM

A basic program computerizing Equation (14) is given by Ward (3). An extensively modified version of it was adapted for this paper, although the fundamental computations have remained intact. In addition to computing a wave resistance coefficient, the program (named "PROTUB") developed for this project can subtract a bare hull record, point by point, from a with-protuberance configuration record, and compute the difference signal wave resistance coefficient. Additionally, it can shift this difference record forward or aft along the model, multiply each slope value by any desired constant, add the modified signal back to the bare hull record, and determine the wave resistance coefficient of the altered data.

PROTUB, as listed in Figure B-1, is written in GE time-sharing fortran. The input data consists of NZETA[5] wave slope values which are stored and referenced in the $FILE statement. Each data point is divided by the calibration factor for that configuration (CAL1 or CAL2) to obtain the ZETAY(N) set in radians, which are the proper units for processing.

Equation (14) may be re-written in series form as:

$$C_W = \frac{1}{\pi S} \sum_{J=0}^{JU} (S_y^2 + C_y^2)\, \Delta u / \omega^4 (2\omega^2 - 1) \qquad (B\text{-}1)$$

5. Capitalized words correspond to names as programmed in PROTUB.

The incremental value of u is given in Ref (3) as

$$\Delta u = \pi / k_o b_{eff} \qquad \text{(B-2)}$$

where b_{eff} is a hypothetical effective tank width. If it is assumed that $k_o b_{eff} = 10\pi$, then $\Delta u = \frac{\pi}{10\pi} = 0.10$ [6]

$$\left.\begin{aligned} S_y = SY &= \sum_{N=1}^{NZETA} ZETAY(N)\, SIN(w k_o X)\, \Delta X \\ C_y = CY &= \sum_{N=1}^{NZETA} ZETAY(N)\, COS(w k_o X)\, \Delta X \end{aligned}\right\} \qquad \text{(B-3)}$$

---

6. This simplifying assumption may be justified by consideration of the tank geometry. The actual effective tank width considering the model offset equals 11.88 ft.

$$b_{eff} = \frac{\pi}{k_o \Delta U} = \frac{\pi V_m^2}{g\, 1/10} = \frac{10\pi V_m^2}{g} = \left.\begin{matrix} 10.12 \\ 22.8 \\ 40.5 \end{matrix}\right\} \text{Ft.}$$

Therefore b_{eff} is generally equal to or greater than the actual value, giving a Δu about equal to or smaller than required from Equation (B-2). This provides a finer integration than is required by Equation (B-2).

where: X = DELX = VM(model speed in ft/sec) * PAPER (interval between readings in mm) / VP (paper speed in mm/sec)

Therefore DELX equals the distance between data points in feet

X = N * DELX, N = 1,2,3.....NZETA

w is a function of J and is computed from Equation (11) for each increment of u.

Letting CAYO = k_o and factoring DELX out of the expression,

$$\left.\begin{aligned} S_y &= \sum_{N=1}^{NZETA} ZETAY(N) * SIN(W * CAYO * N * DELX) \\ C_y &= \sum_{N=1}^{NZETA} ZETAY(N) * COS(W * CAYO * N * DELX) \end{aligned}\right\} \quad (B-4)$$

Equations (B-4) solve the Fourier transforms. However, the trigonometric identities,

$$\sin(X + \Delta X) = \sin X \cos\Delta X + \cos X \sin\Delta X$$

$$\cos(X + \Delta X) = \cos X \cos\Delta X - \sin X \sin\Delta X$$

are utilized in PROTUB to reduce computer core time.

Letting $k_o b_{eff}$ = CAYOB = 10π

S = WETSR = model surface-ft^2

$$C_W = \frac{2(DELX)^2}{WETSR * CAYOB} \sum_{J=0}^{JU} \frac{SY^2 + CY^2}{w^4 * (2w^2 - 1)} \quad (B-5)$$

where the entire expression is doubled because only $\frac{1}{2}$ the wave pattern is recorded by the probe. Note that the final resistance coefficient is the product of a constant and the wave amplitude spectra, squared, times a weighting function, $\left\{\frac{1}{w^4(2w^2-1)}\right\}$, which decreases quite rapidly with increase in u or w.

FIGURE B-1 COMPUTER PROGRAM

```
100 "PROTUR" WILL CALCULATE WAVE RESISTANCE COEFFICIENT OF A
200 MODEL WITH THE WAVE SLOPE RECORD AS INPUT.  IT WILL GIVE
300 THE COEFFICIENT FOR A SINGLE RUN (KEE = 1), THE DIFFERENCE
400 BETWEEN TWO RUNS (KEE = 1), OR WITH A SIMULATED DIFFERENCE
500 SHIFT ALONG THE MODEL LENGTH (KEE = 3).
600 TO ELIMINATE DETAILED INCREMENTAL PRINT OUT, LET 'INC' EQUAL 0."
70 "FILE A1,A2,A3,B2
80 DIMENSION ZETAY(240),PHULL(240),VBULL(240),XBULP(240),BULP(240)
90 READ, NTEST, NZETA,KEE,INC,VM,PAPER,YMOVE,XMULT,WETSI,CAL1,CAL2
100 VP=125.0; CAYOI=31.4159
110 PRINT"WAVE RESISTANCE TEST WITH 5.5 FT MODEL, STEVENS NO 393"
120 DO 2000 NT=1,NTEST
130C RESERVED FOR VARIABLE INPUT STATEMENT
140 CAYO=32.17/VM**2
150 JU=100
160 CW=0.0
170 DELX=VM*PAPER/VP
180 CON=2000*DELX**2/WETSI/(AYO)
190 IF (KEE-2) ONERUN
200 PRINT"TWO RECORDS USED ARE?"
210 INPUT, (L,M)
220 READ (L) (PHULL(N),N=1,NZETA); REWIND L
230 READ (M) (VBULP(N),N=1,NZETA); REWIND M
250 DO 100 N=1,NZETA
260 100: BULP(N)=VBULP(N)/CAL2-PHULL(N)/CAL1
270 IF (KEE-2) ONERUN, ONEBULP
280 JUMP=IFIX(XMOVE/12.0/DELX)
290 DO 300 N=1,NZETA
300 300: XBULP=0.0
310 DO 320 N=1,NZETA
320 NU=N+JUMP
330 IF (NU-NZETA) 310,310, 320
340 310: IF (NU) 320,320
350 XBULP(NU)=BULP(N)
360 320: CONTINUE
370 DO 330 N=1,NZETA
380 330: ZETAY(N)=PHULL(N)/CAL1+XMULT*XBULP(N)
390 GO TO START
400 ONEBULP: DO 350 N=1,NZETA
410 350: ZETAY(N)=XMULT*BULP(N)
420 GO TO START
430 ONERUN: PRINT"RECORD USED IS?"
440 INPUT, (K)
```

FIGURE B-1 (CONTINUED)

```
450 READ (K) (PHULL(N),N=1,NZETA); PRINT *
460 DO 400 N=1,NZETA; 400: ZETAY(N)=PHULL(N)/CAL1
470 START: IF (KEY-2) RUN, DIFF, SHIFT
480 RUN: PRINT"WAVE RECORD BASED ON ONE MODEL RUN"
490 GO TO 500
500 DIFF: PRINT"WAVE RECORD BASED ON PULL SIGNAL ONLY"
510 GO TO 500
520 SHIFT: PRINT"WAVE RECORD BASED ON SHIFTED PULL SIGNAL"
530 500: PRINT"MODEL SPEED IS",VM,"FT/SEC"
540 PRINT"WETTED SURFACE IS",WETSR,"SQ FT"
550 PRINT"RECORD BASED ON",NZETA," DATA POINTS AT",PAPER,"MM INTERVALS"
560 PRINT"CALIBRATION FACTOR IS",CAL1/10.0,"MM/READ"
570 IF (KEY-2) SAME
580 PRINT"CALIBRATION FACTOR WITH PULL CONFIG. IS",CAL2/10.,"MM/READ"
590 IF (XMOVE) FWD,NO,AFT
600 FWD: PRINT"PULL SHIFTED",XMOVE,"INCHES FWD"
610 GO TO MOVE
620 AFT: PRINT"PULL SHIFTED",XMOVE,"INCHES AFT"
625 MOVE: PRINT 4, XMOVE," INCHES EQUALS",JUMP," DATA PT INCREMENTS"
630 NO: IF (YMULT-1.0) CHANGE,SAME,CHANGE
640 CHANGE:PRINT"PULL SIGNAL MULTIPLICATION FACTOR EQUALS",YMULT
650 SAME: IF (INC-1) NOPRINT
660 PRINT,1," NO     AMP       COMPONENT    RESISTANCE"
670 NOPRINT: DO 1000 J=0,JU
680 U=.1*J
690 V=SQRT(.5+SQRT(.25+U**2))
700 SINDEL=SIN(V*DELX*CAY0)
710 COSDEL=COS(V*DELX*CAY0)
720 SINX=0.0;  COSX=1.0
730 SY=0.0; CY=0.0
740 DO 1001 N=1,NZETA
750 SY=SY+ZETAY(N)*SINX; CY=CY+ZETAY(N)*COSX
760 SINE=SINX*COSDEL+COSX*SINDEL
770 COSINE=COSX*COSDEL-SINX*SINDEL
780 SINX=SINE
790 1001: COSX=COSINE
800 AY=SY**2+CY**2
810 AMP = SQRT (AY)
820 C=CON*AY/V**4/(2.0*V**2-1.0)
830 CV=CV+C
840 IF (INC-1) 1000
850 PRINT 1, J,AMP,C,CV
860 1000: CONTINUE
870 RW=1.9337/2000.*CV*VM**2*WETSR
```

FIGURE I-1 (CONTINUED)

```
1830 1: FORMAT (I3,F10.4,F10.5)
1890 2: FORMAT (F10.8)
1892 3: FORMAT (F8.5)
1894 4: FORMAT (F7.2,I4)
1900 PRINT 2, 1,"TOTAL WAVE RESISTANCE COEFFICIENT FORMLS",CW/1000.
1920 2000: PRINT 3,"TOTAL WAVE RESISTANCE FORMLS",LV," LV",11
1930 STOP
1940 $DATA
9999 THIS IS THE END
```

APPENDIX C: WAVE SPECTRA PLOTS

The remaining amplitude and Fourier sine and cosine spectra, not included in the body of the report, are shown in this section. The curves were plotted by the NSRDC 7090 computer. Due to the limitations of the curve plot subroutines used, the following notation was adopted for identification of the curves:

First letter denotes:

- A Bare hull configuration
- B Large protuberance at station 1
- C Large protuberance at station 3
- D Large protuberance at station 5
- E Small protuberance at station 3

First number denotes:

- 1 Froude number equals 0.242
- 2 Froude number equals 0.363
- 3 Froude number equals 0.484

AVE denotes that the curves are plotted from data averaged over three model tests.

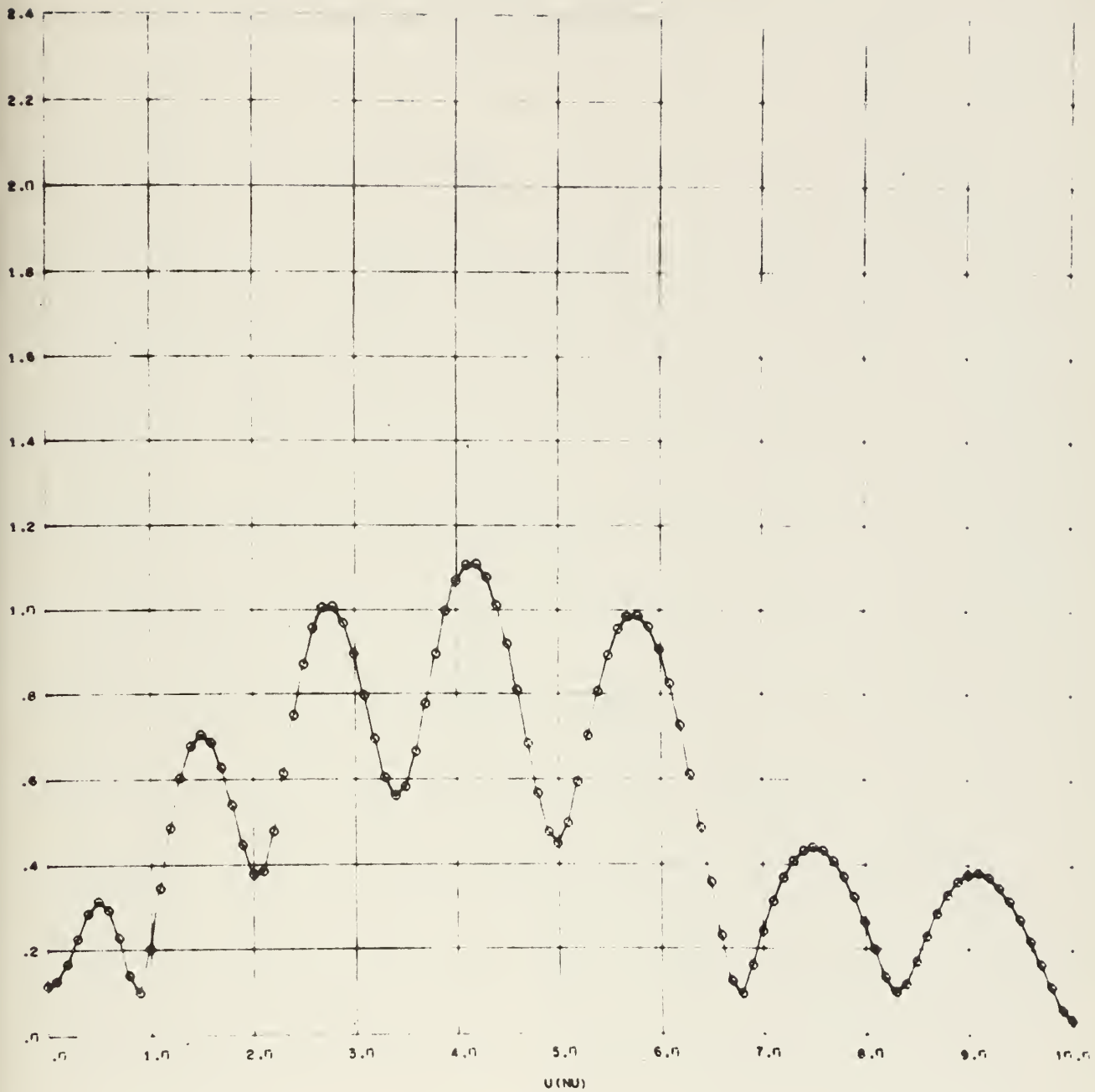

FROUDE NO. = 0.242 CONFIGURATION AIAVE

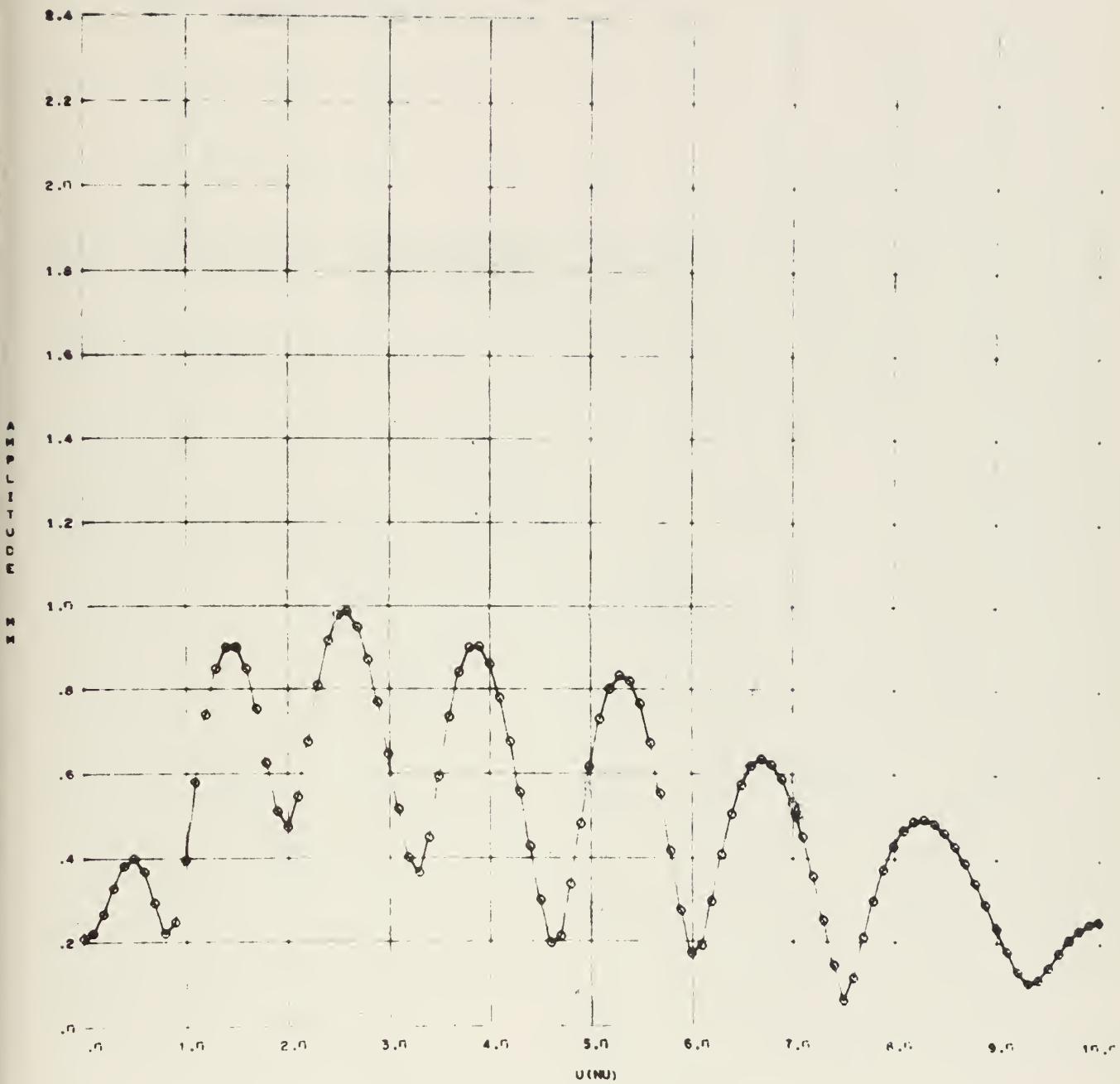

FROUDE NO. - 0.242 CONFIGURATION BIAVE

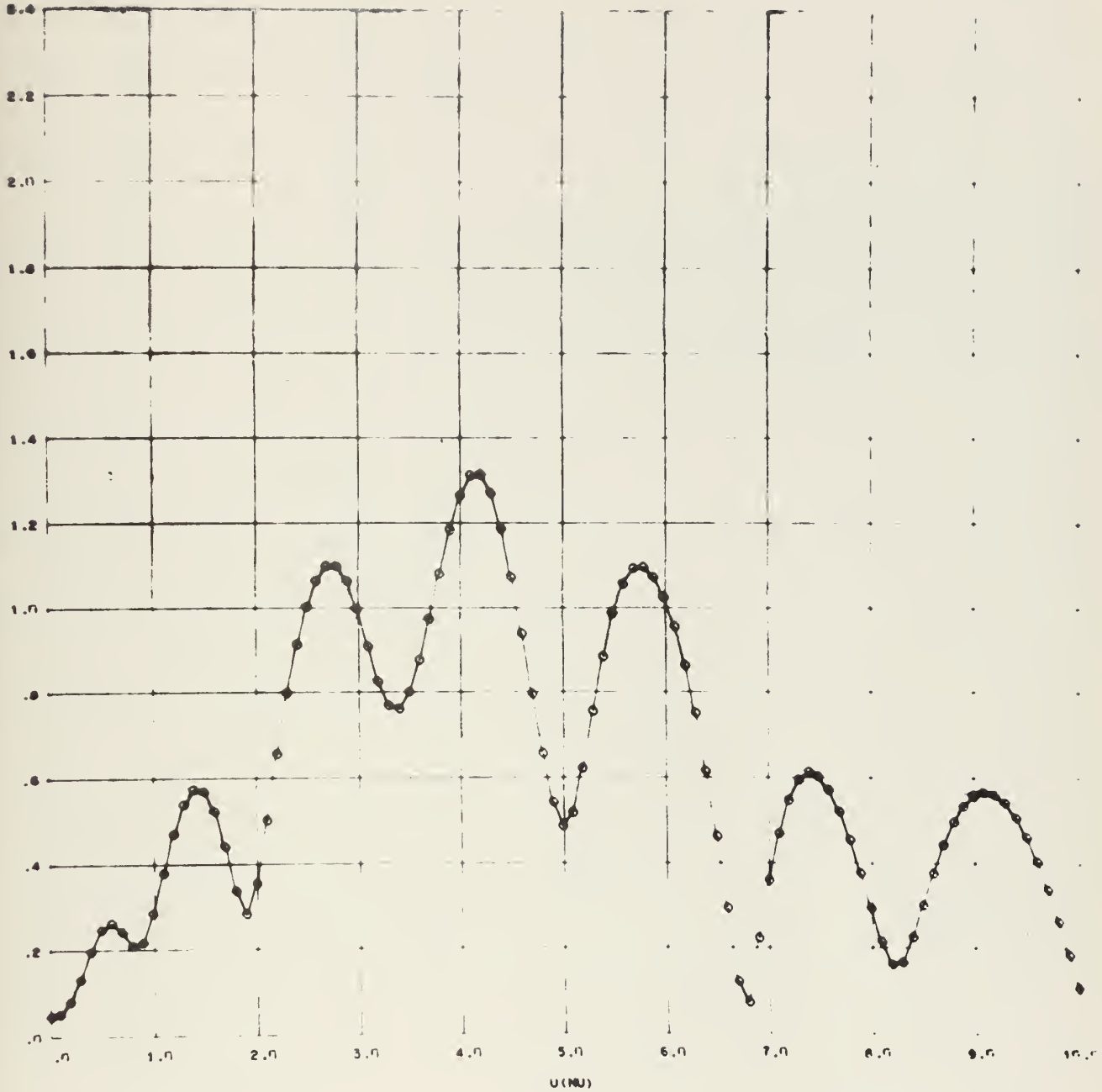

FROUDE NO. • 0.242 CONFIGURATION CIAVE

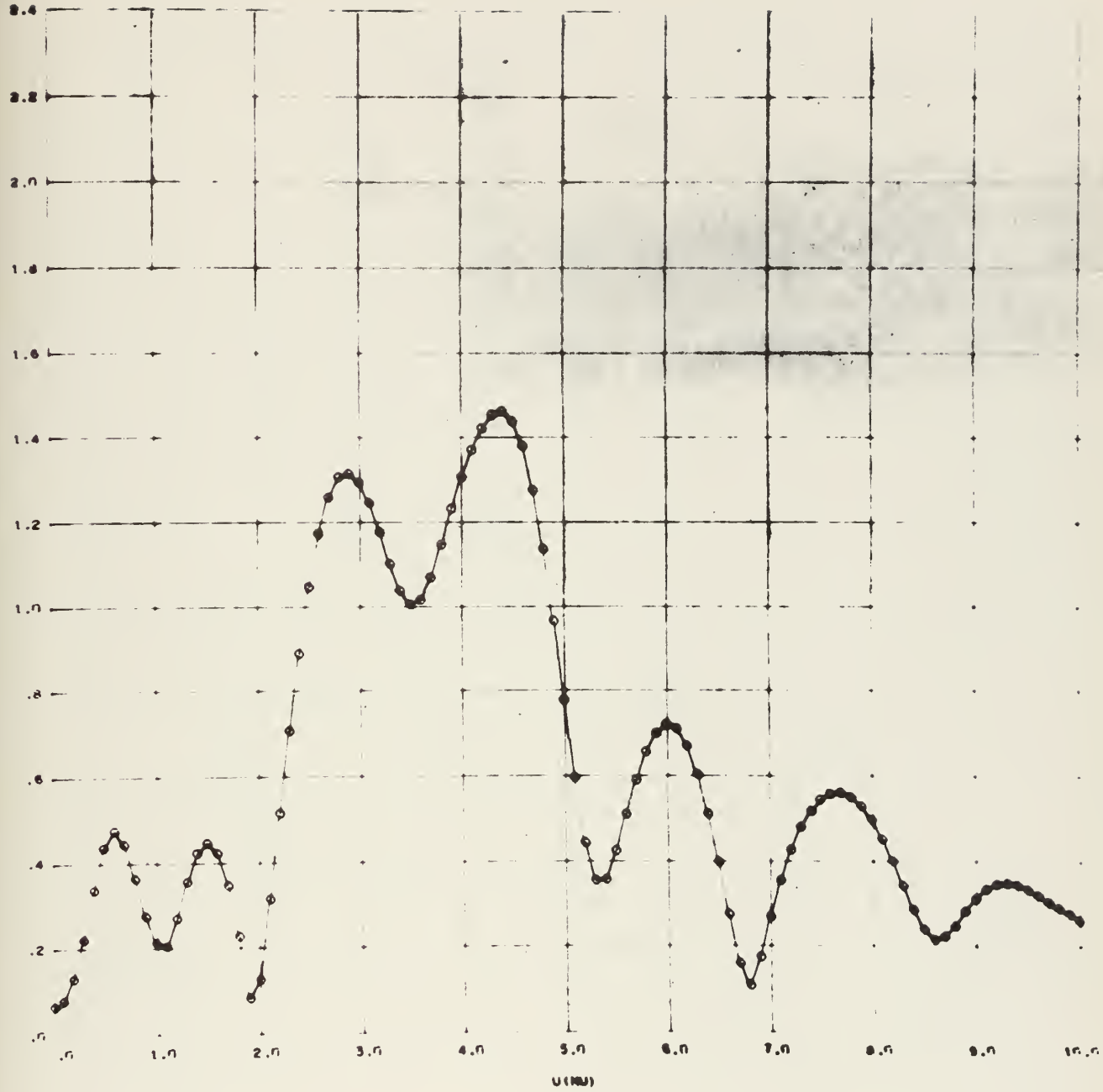

FROUDE NO. - 0.242 CONFIGURATION DIAVE

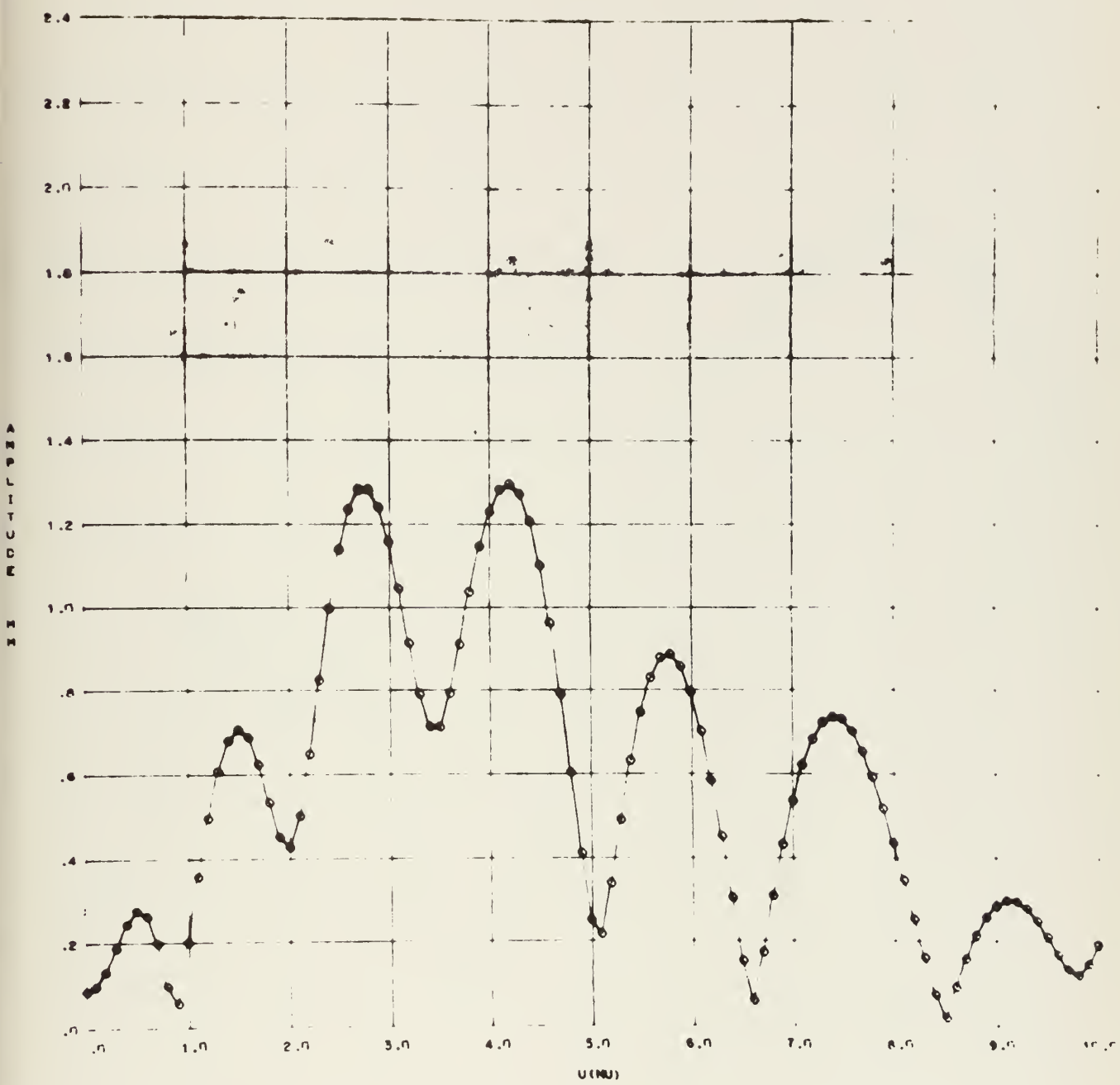

FROUDE NO. = 0.242 CONFIGURATION E1AVE

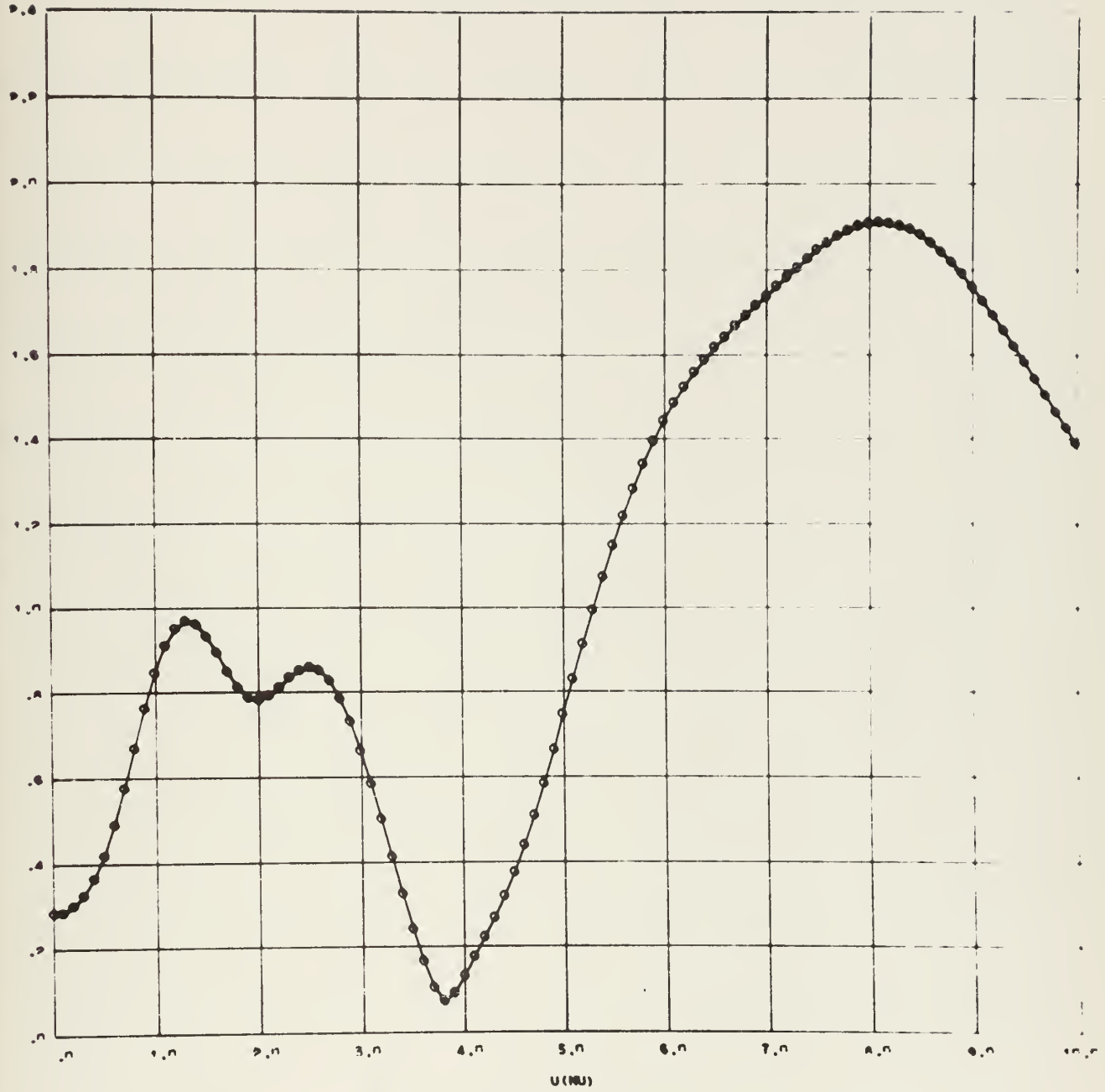

FROUDE NO. = 0.484 CONFIGURATION A3WE

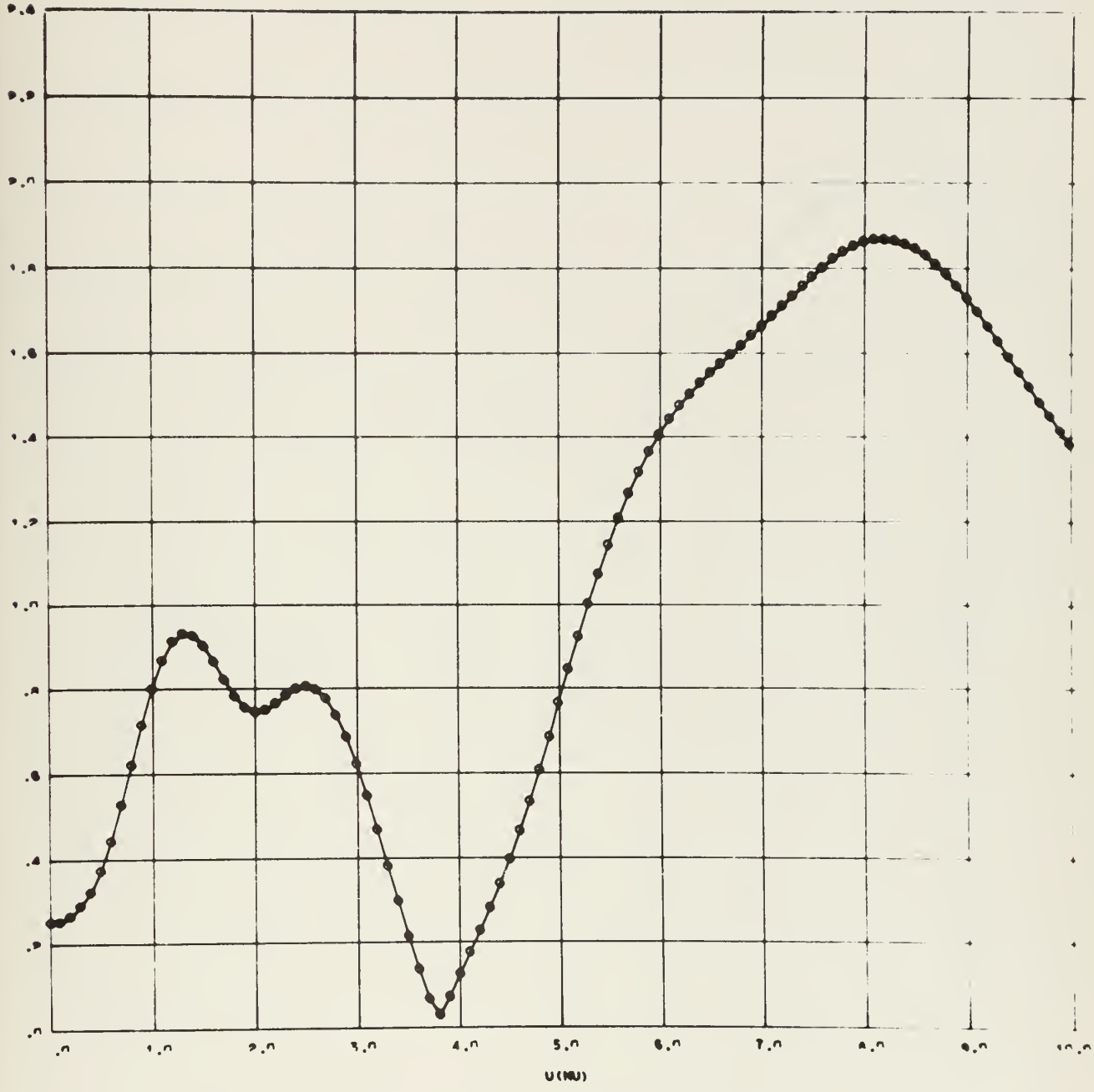

FIGURE NO. = 0.404 CONFIGURATION BOMB

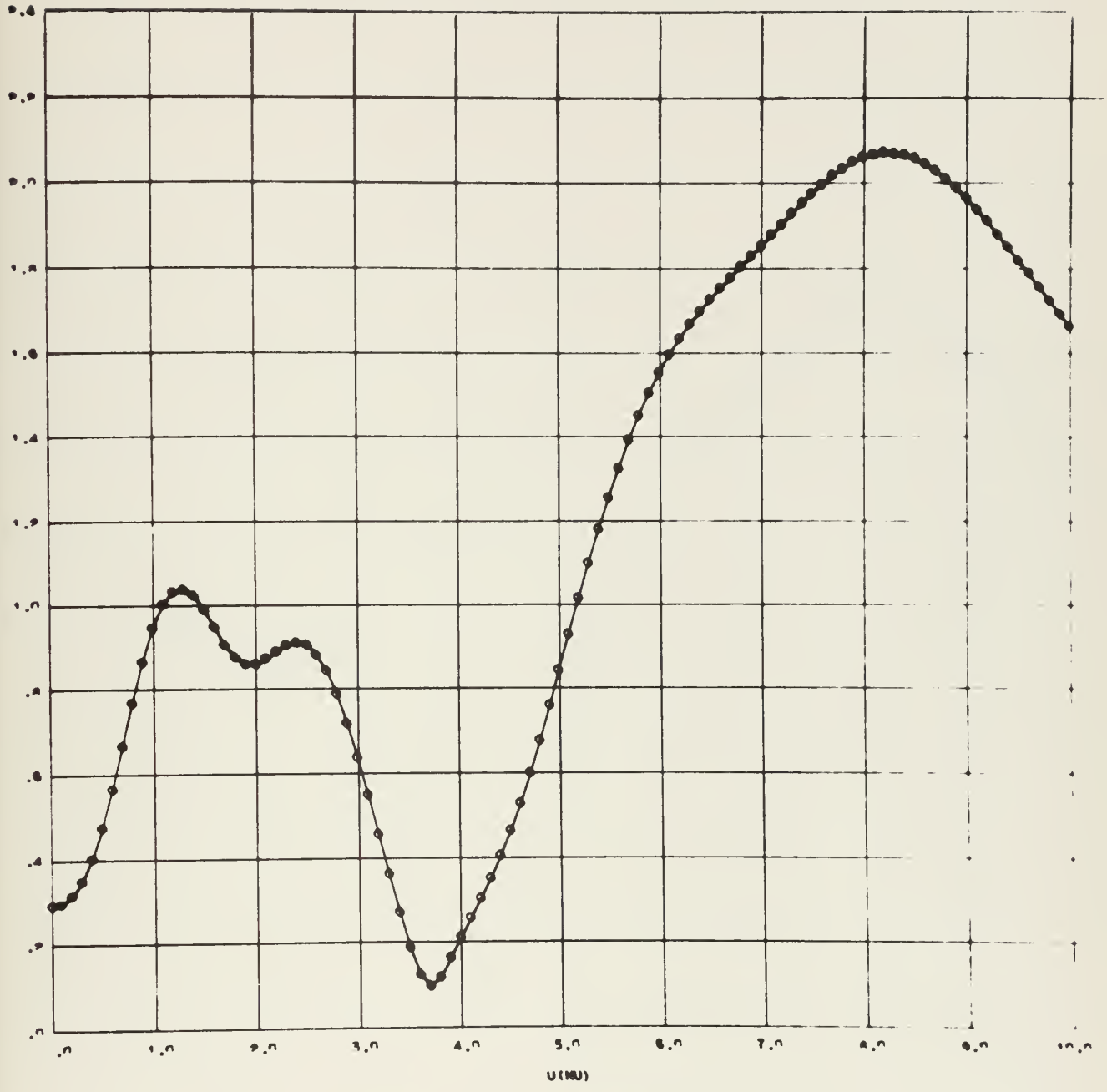

FIGURE NO. = 0.494 CONFIGURATION CONE

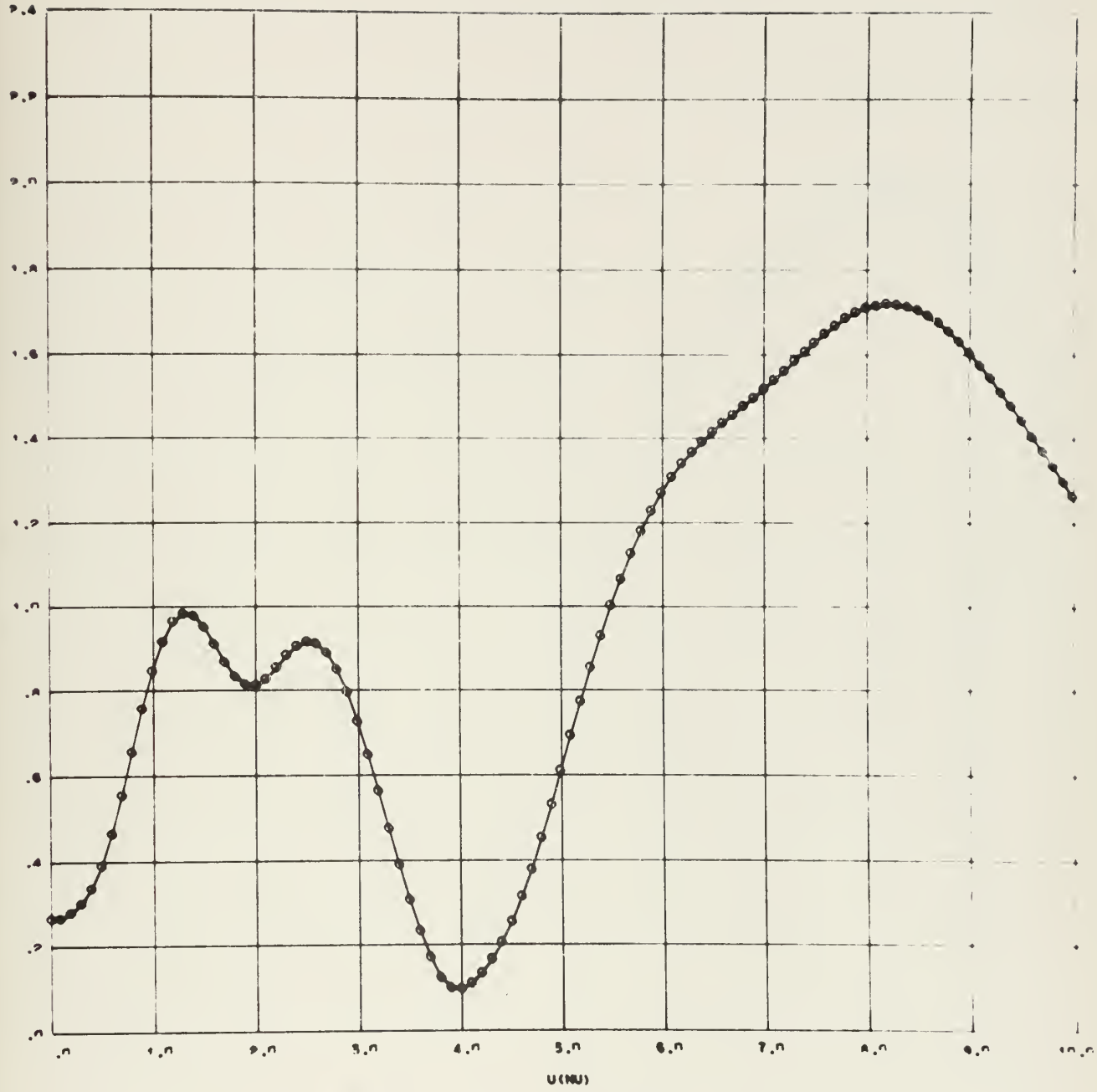

FROUDE NO. = 0.494 CONFIGURATION DDHC

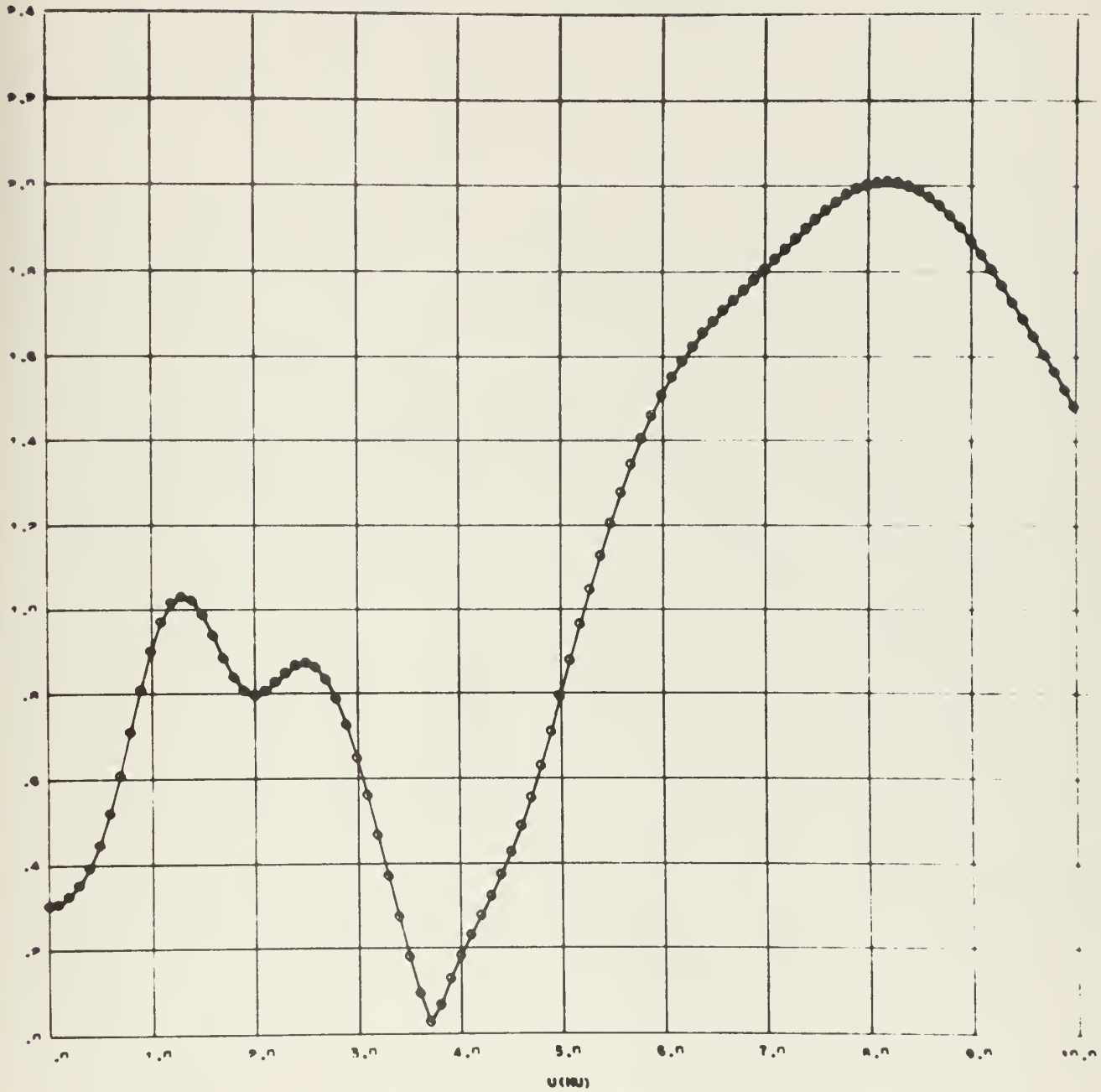

FIGURE NO. - 0.494 CONFIGURATION ESNE

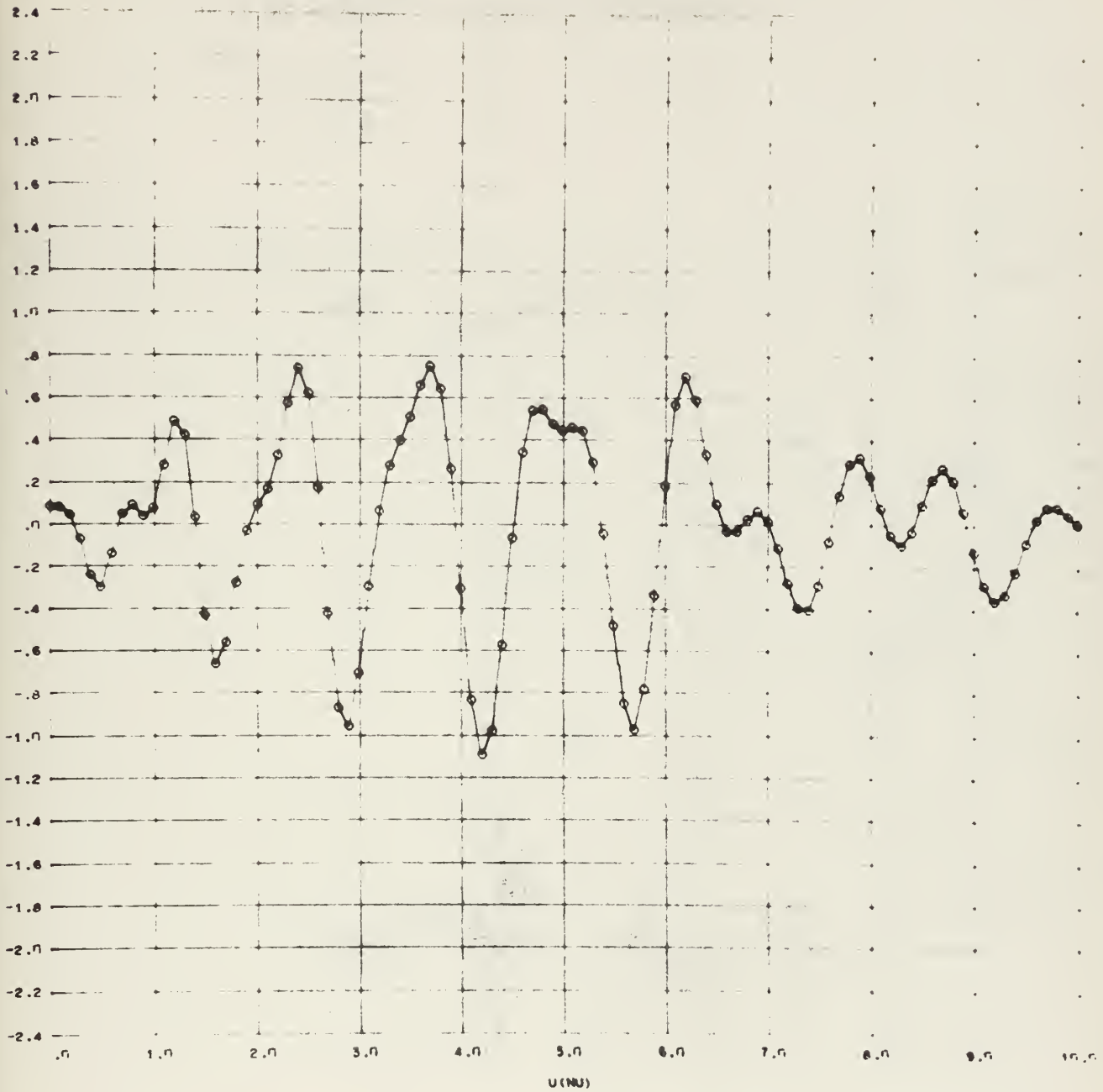

FROUDE NO. = 0.242 CONFIGURATION A1AVE

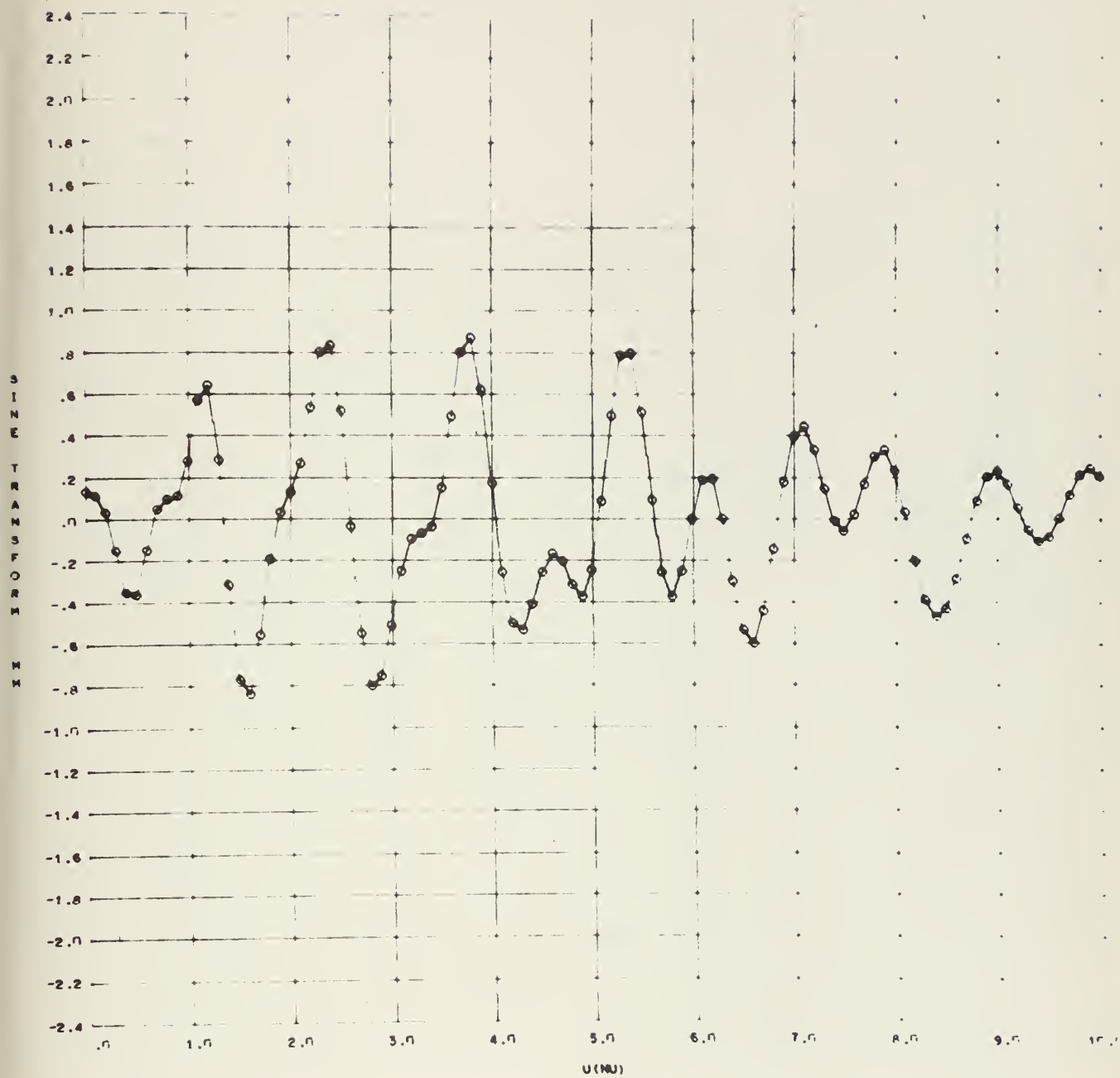

FROUDE NO. = 0.242 CONFIGURATION BIAVE

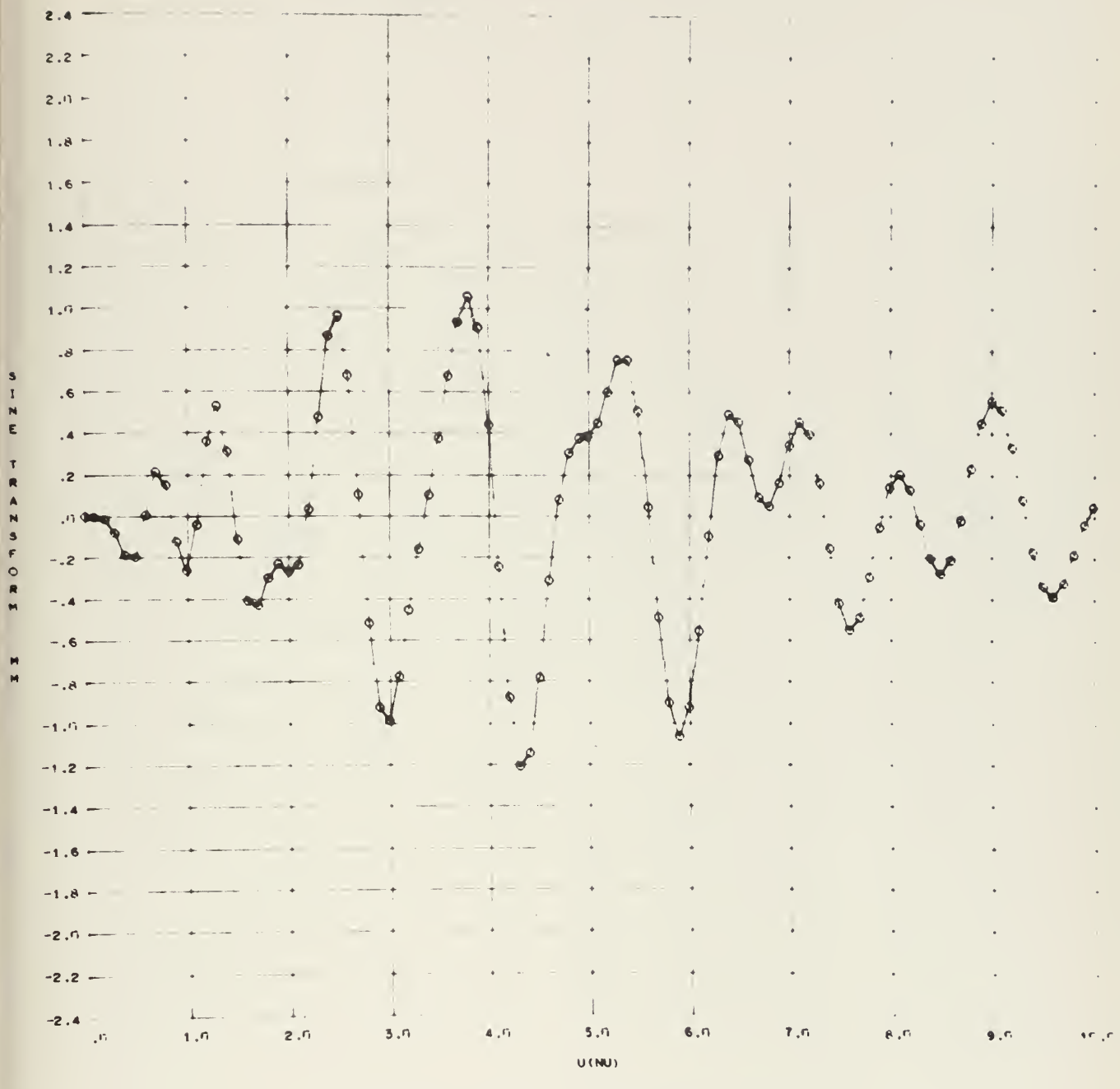

FROUDE NO. - 0.242 CONFIGURATION CIAVE

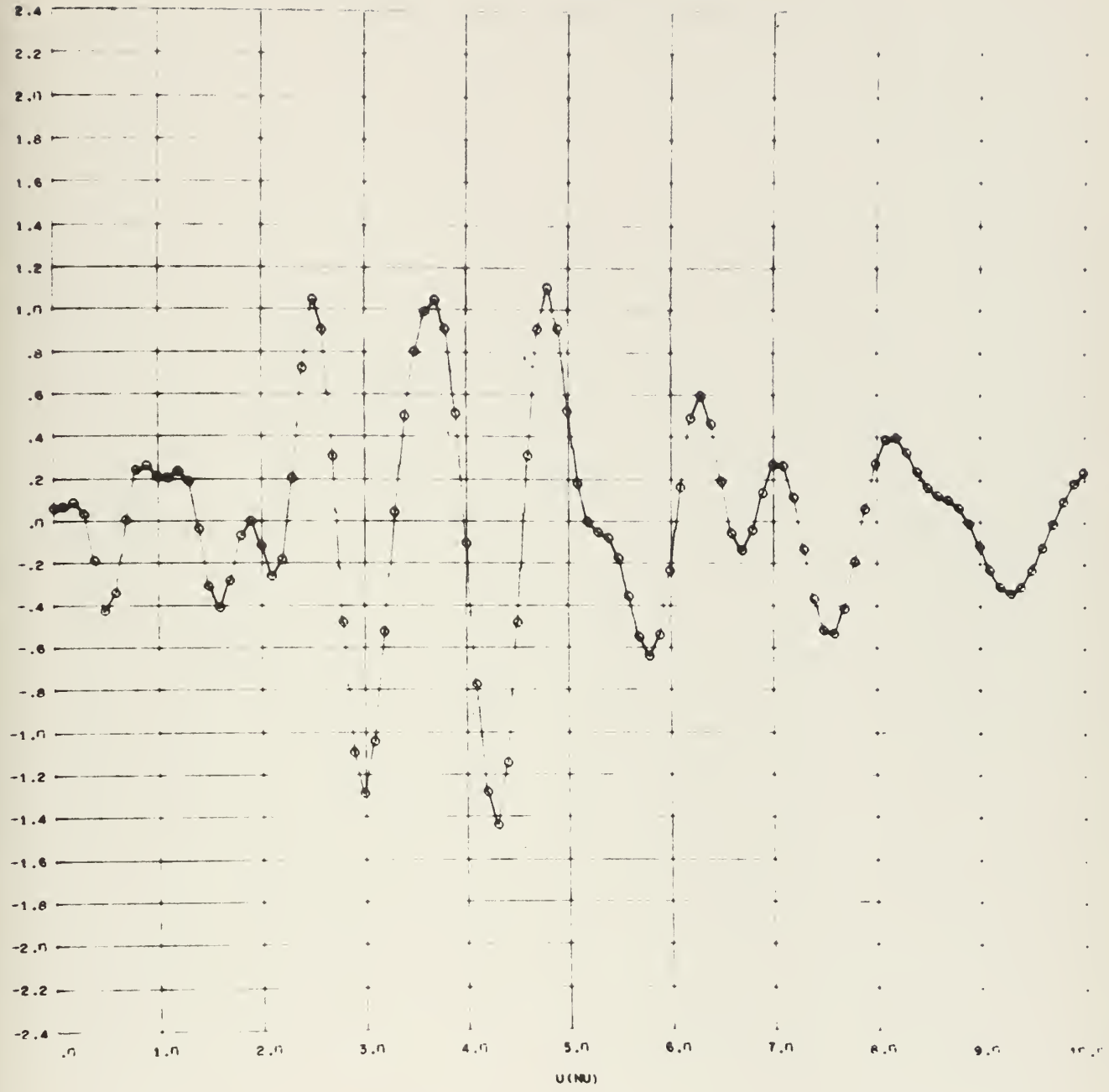

FROUDE NO. = 0.242 CONFIGURATION DIAVE

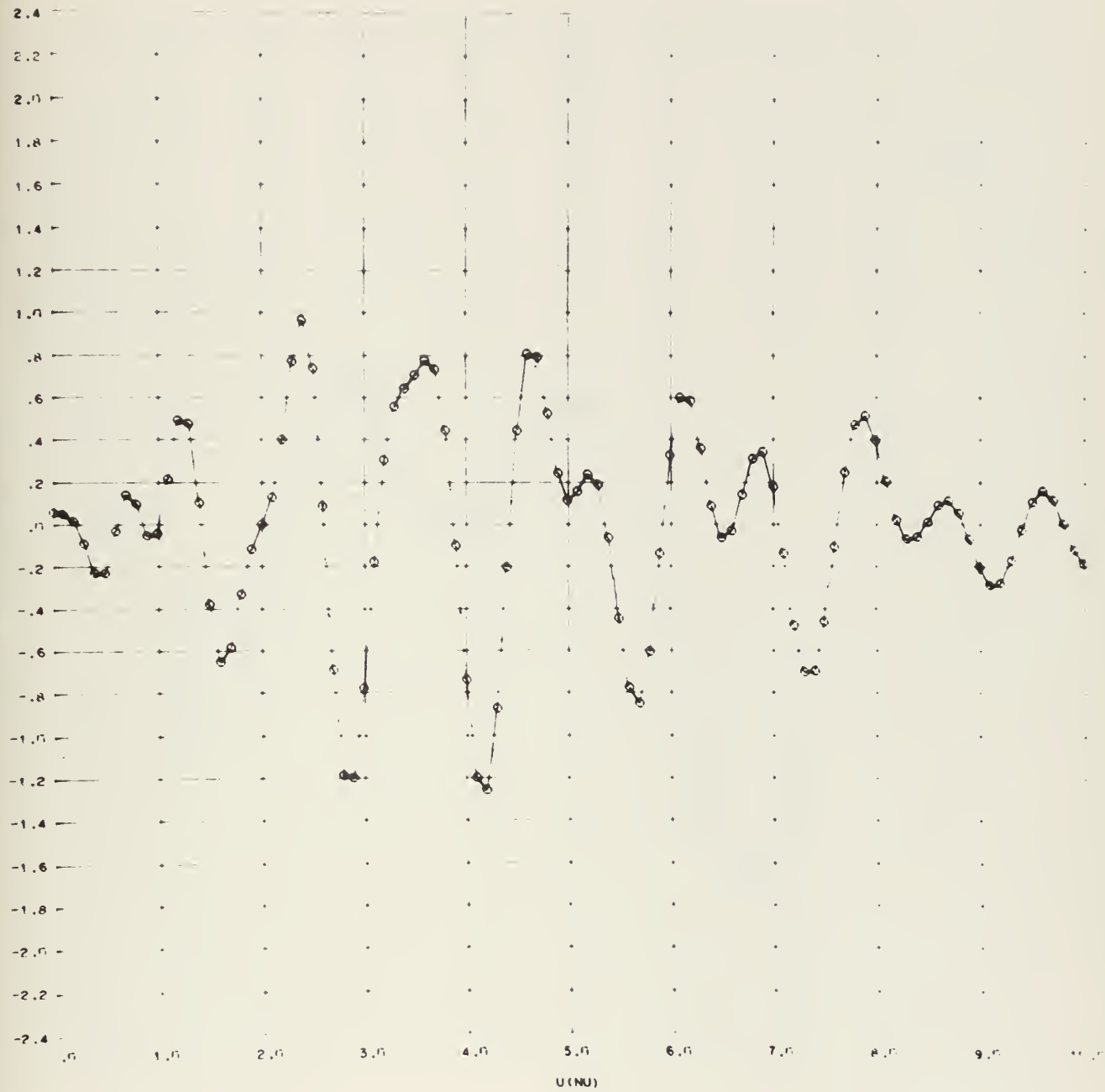

FROUDE NO. = 0.242 CONFIGURATION E1AVE

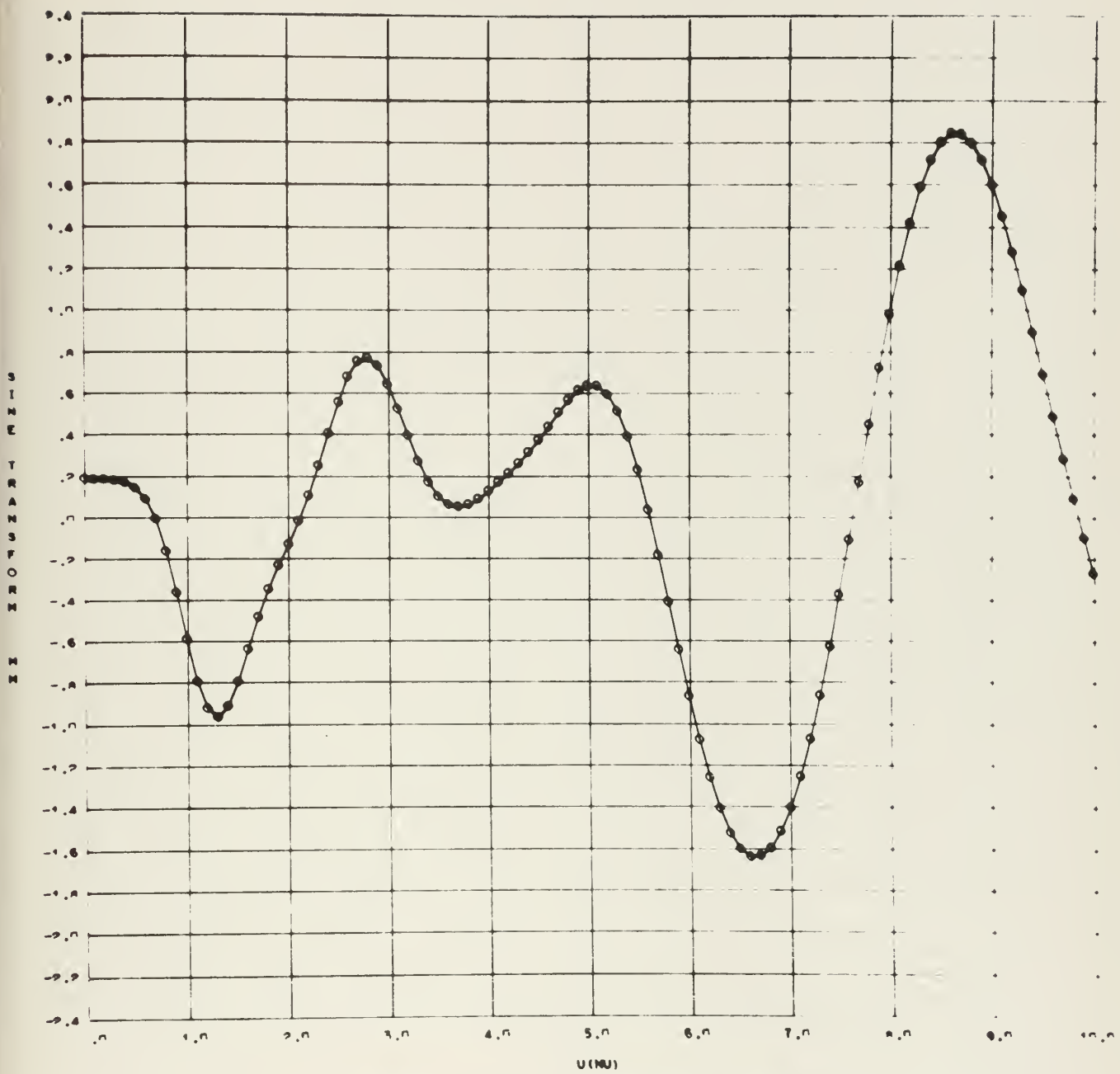

FROUDE NO. = 0.484 CONFIGURATION ASHVE

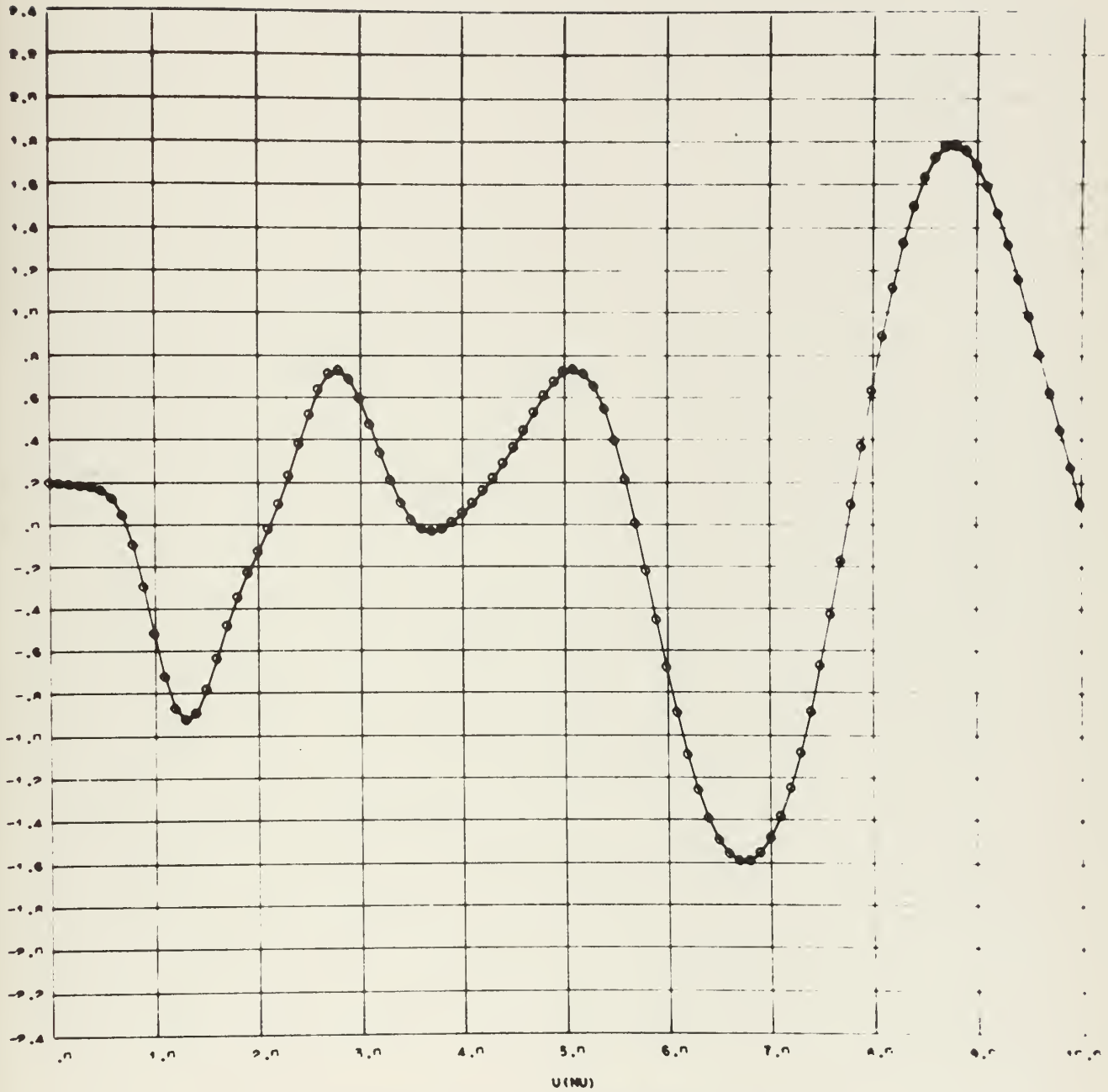

FROUDE NO. = 0.484 CONFIGURATION BOWIE

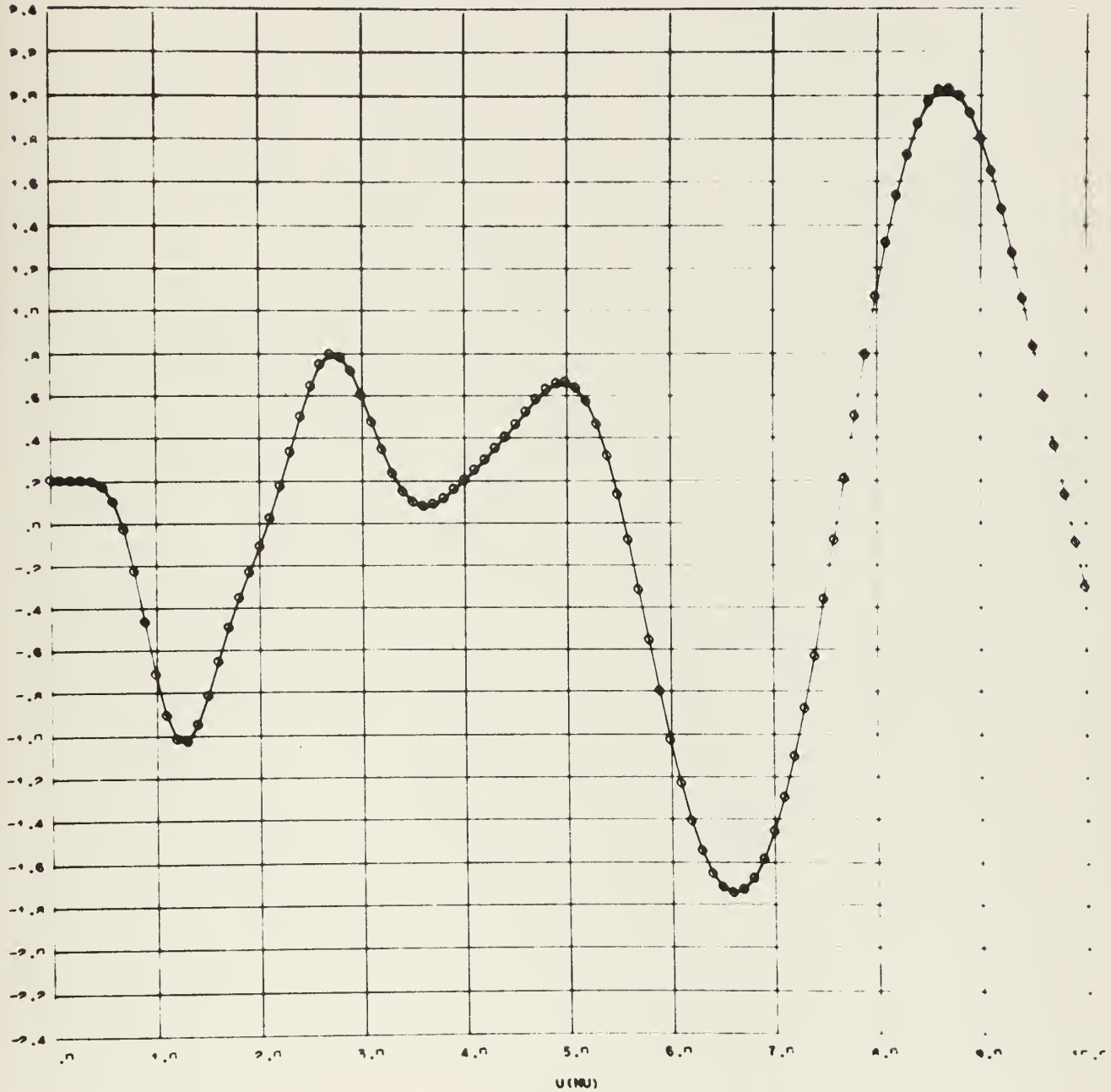

FROUDE NO. = 0.484 CONFIGURATION CONE

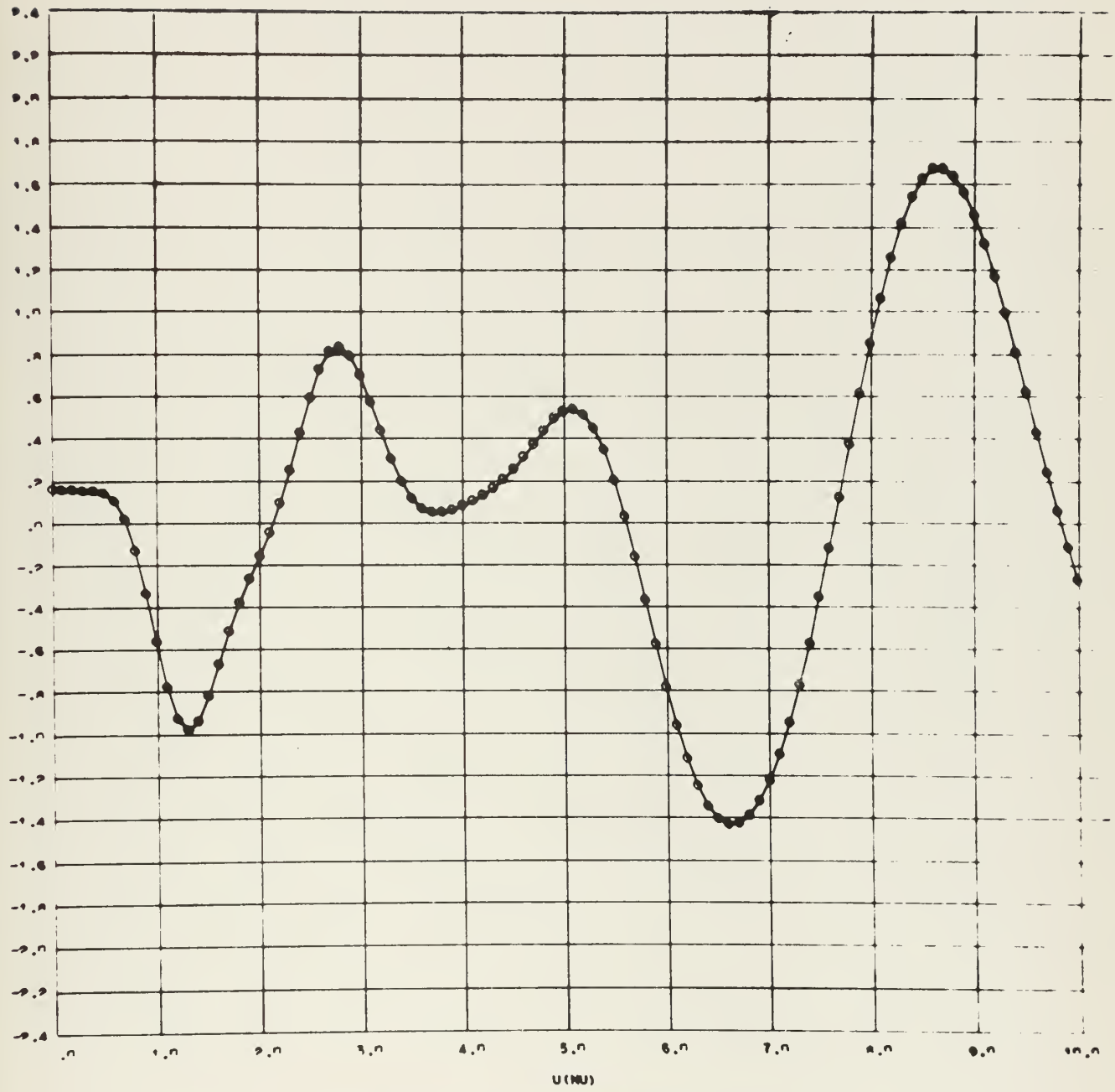

FIGURE NO. = 0.484 CONFIGURATION DOME

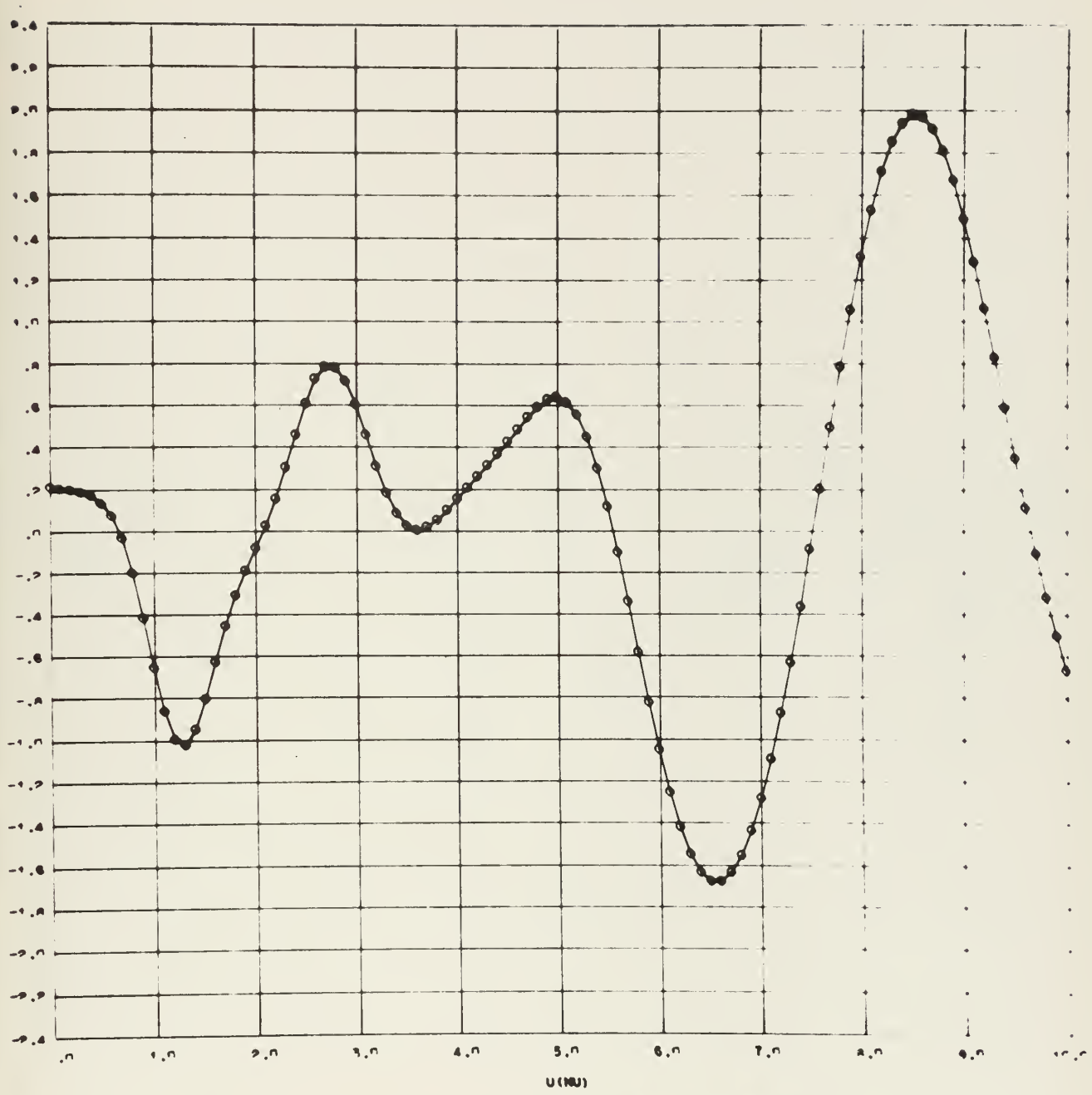

FROUDE NO. = 0.484 CONFIGURATION ESWE

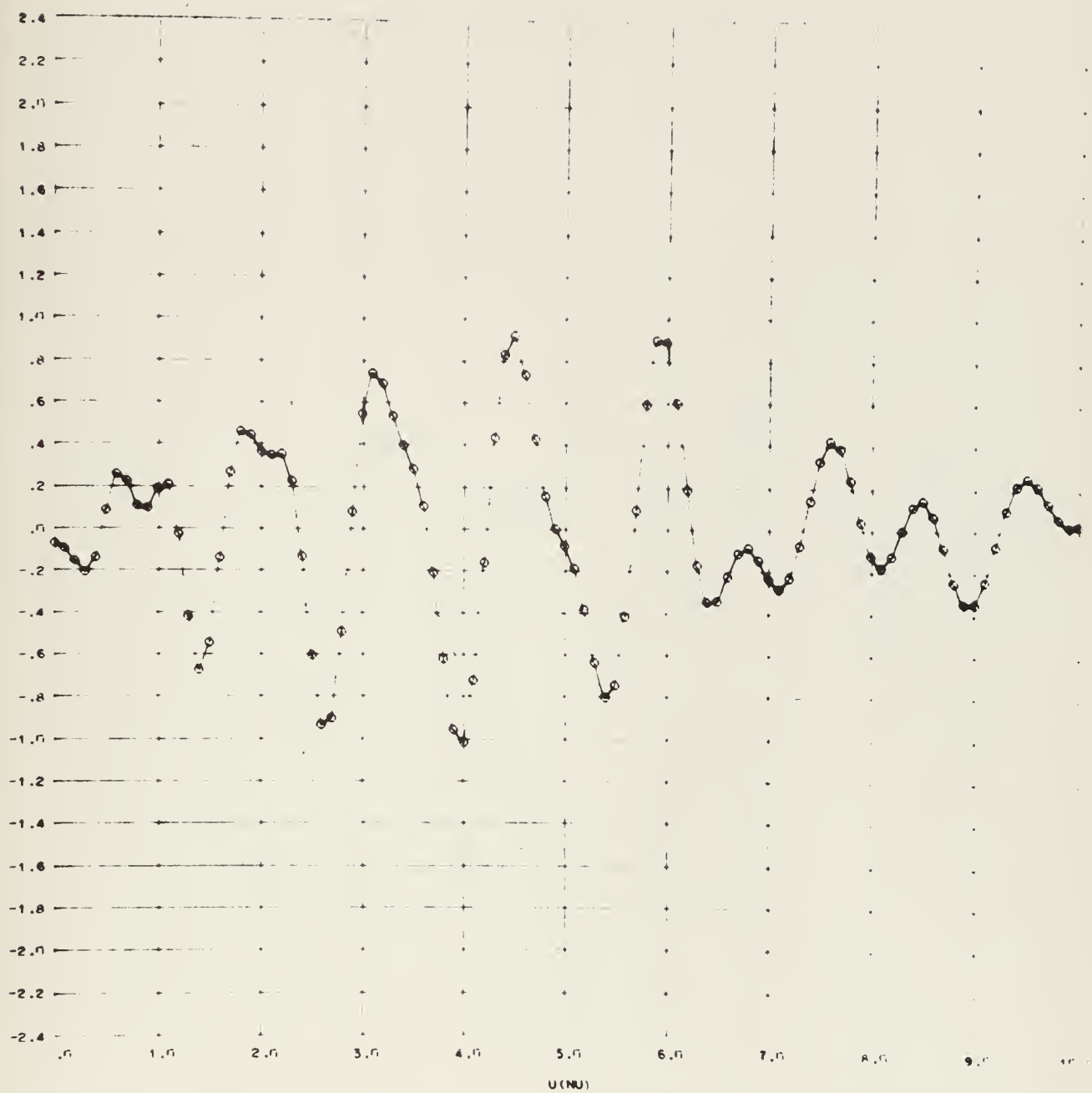

FROUDE NO. = 0.242 CONFIGURATION A1AVE

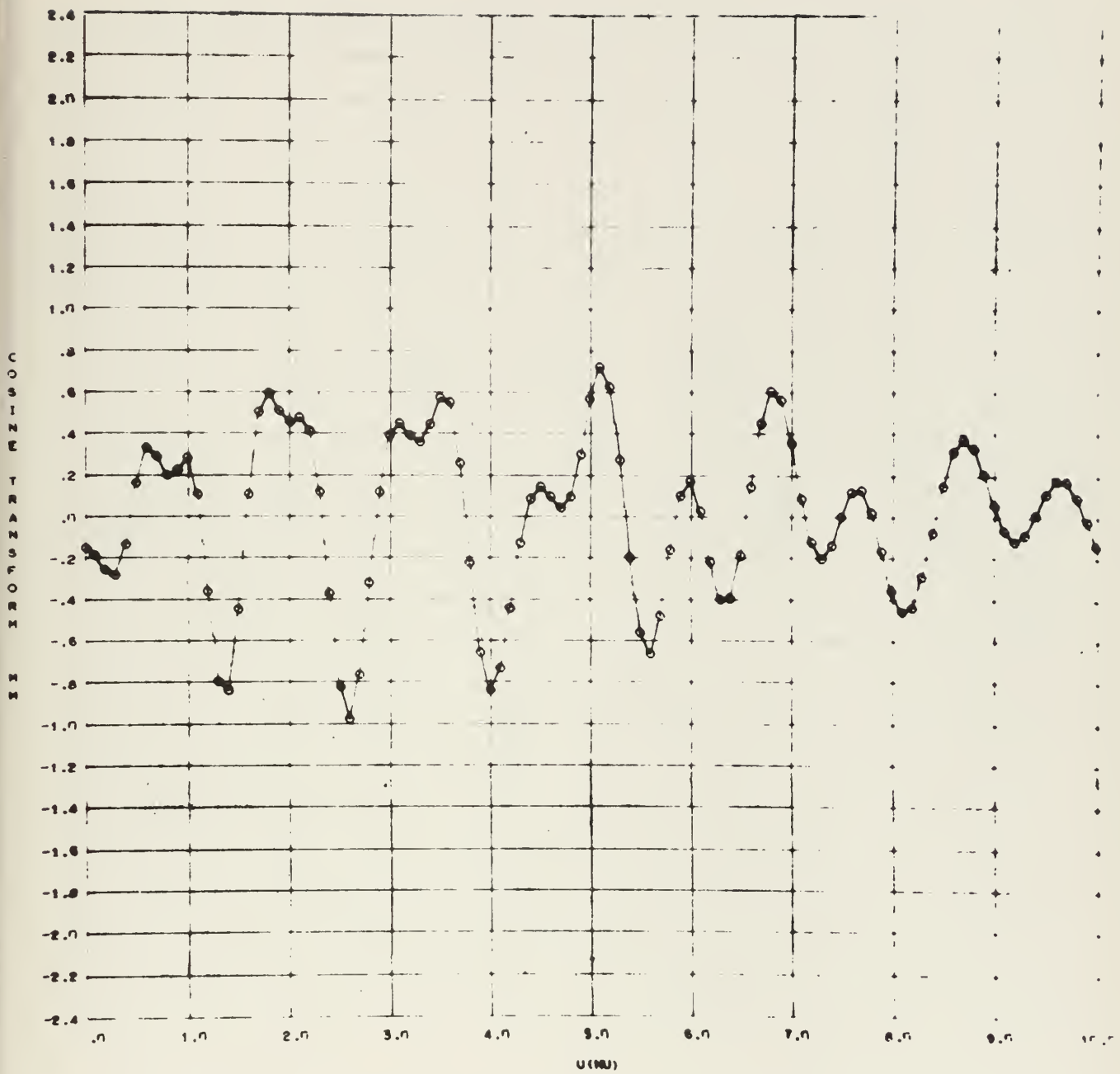

FROUDE NO. = 0.242 CONFIGURATION BIAVE

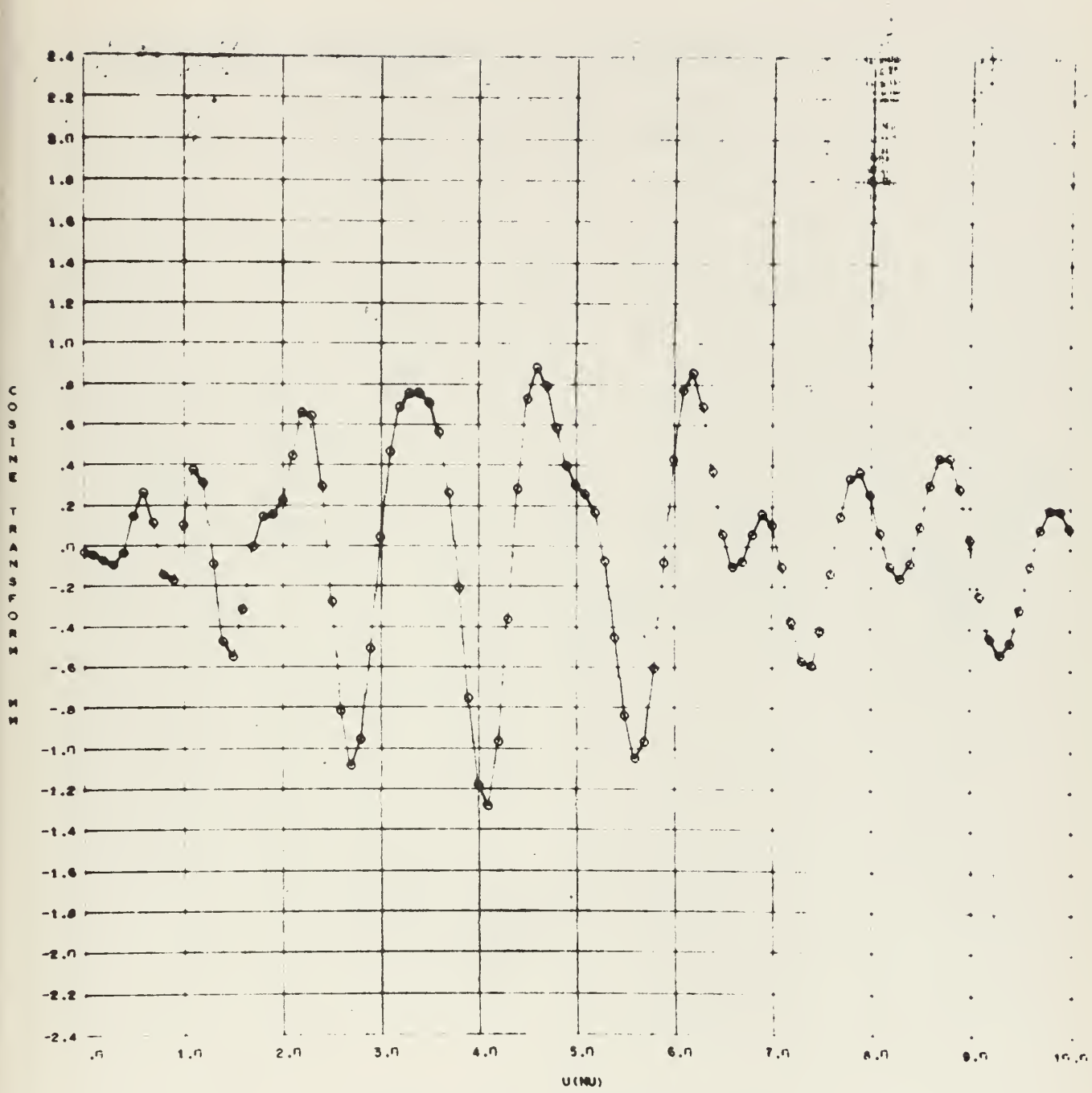

FROUDE NO. • 0.242 CONFIGURATION CIAVE

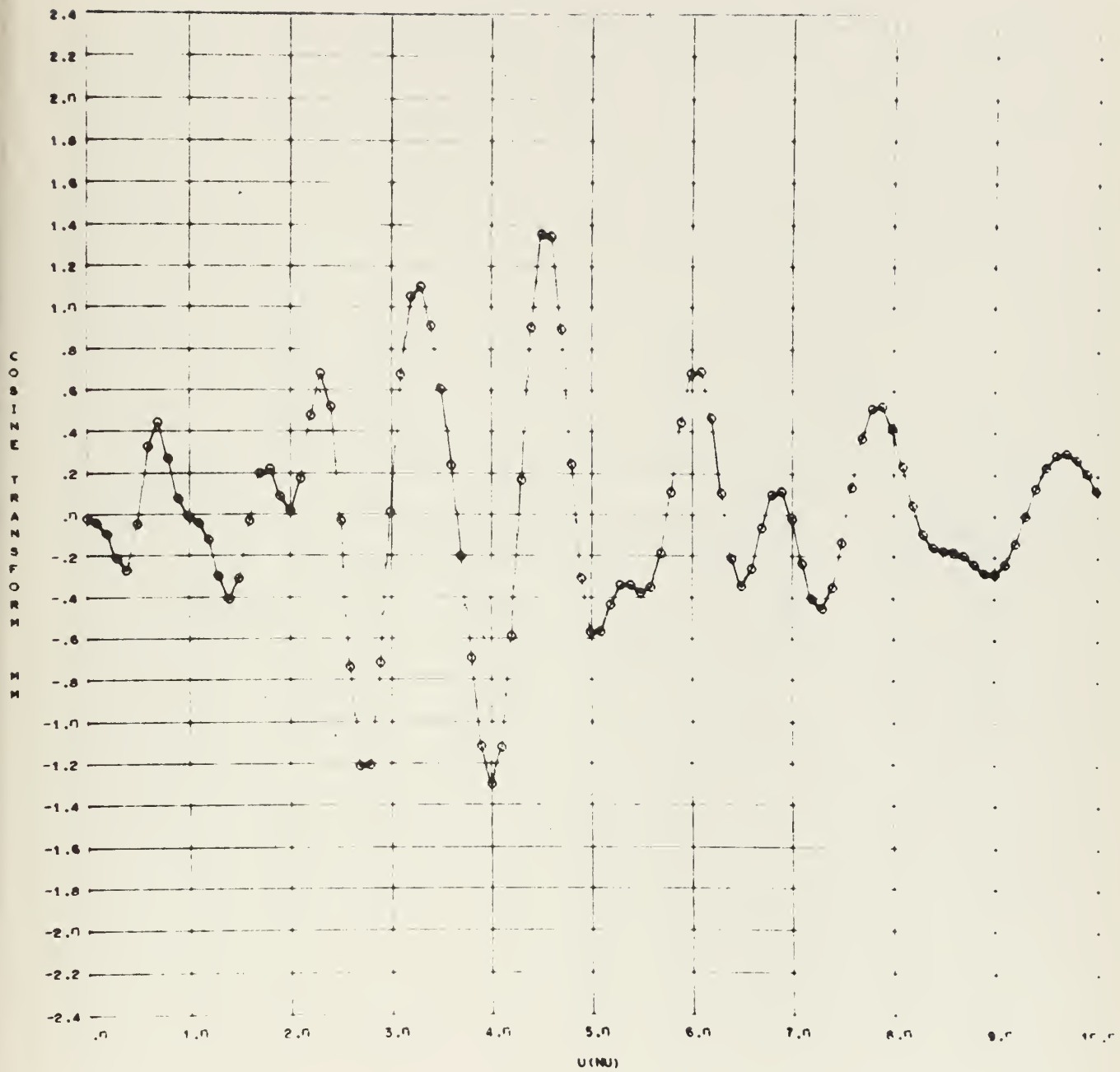

FROUDE NO. = 0.242 CONFIGURATION DIAVE

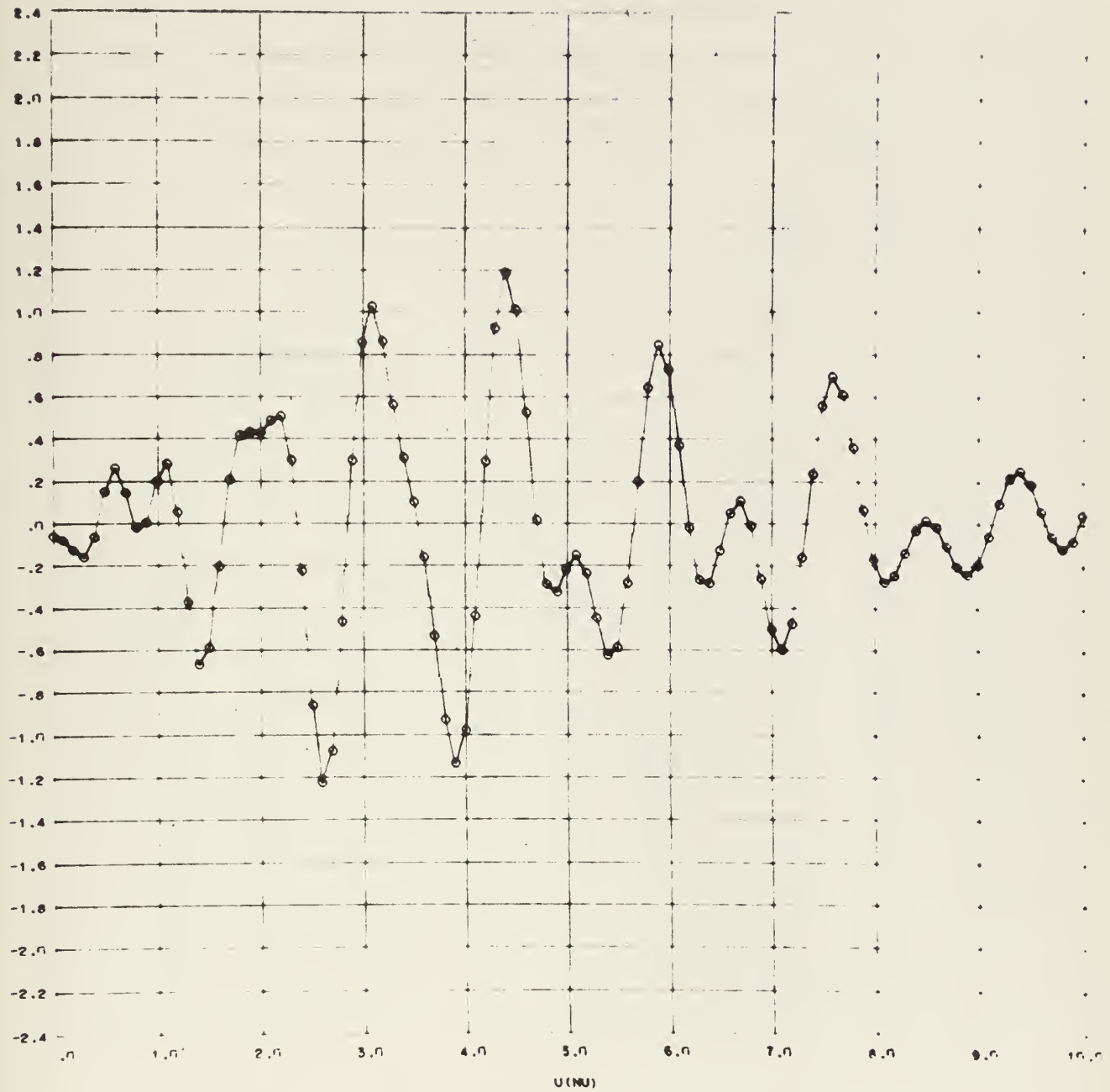

FROUDE NO. • 0.242 CONFIGURATION E1AVE

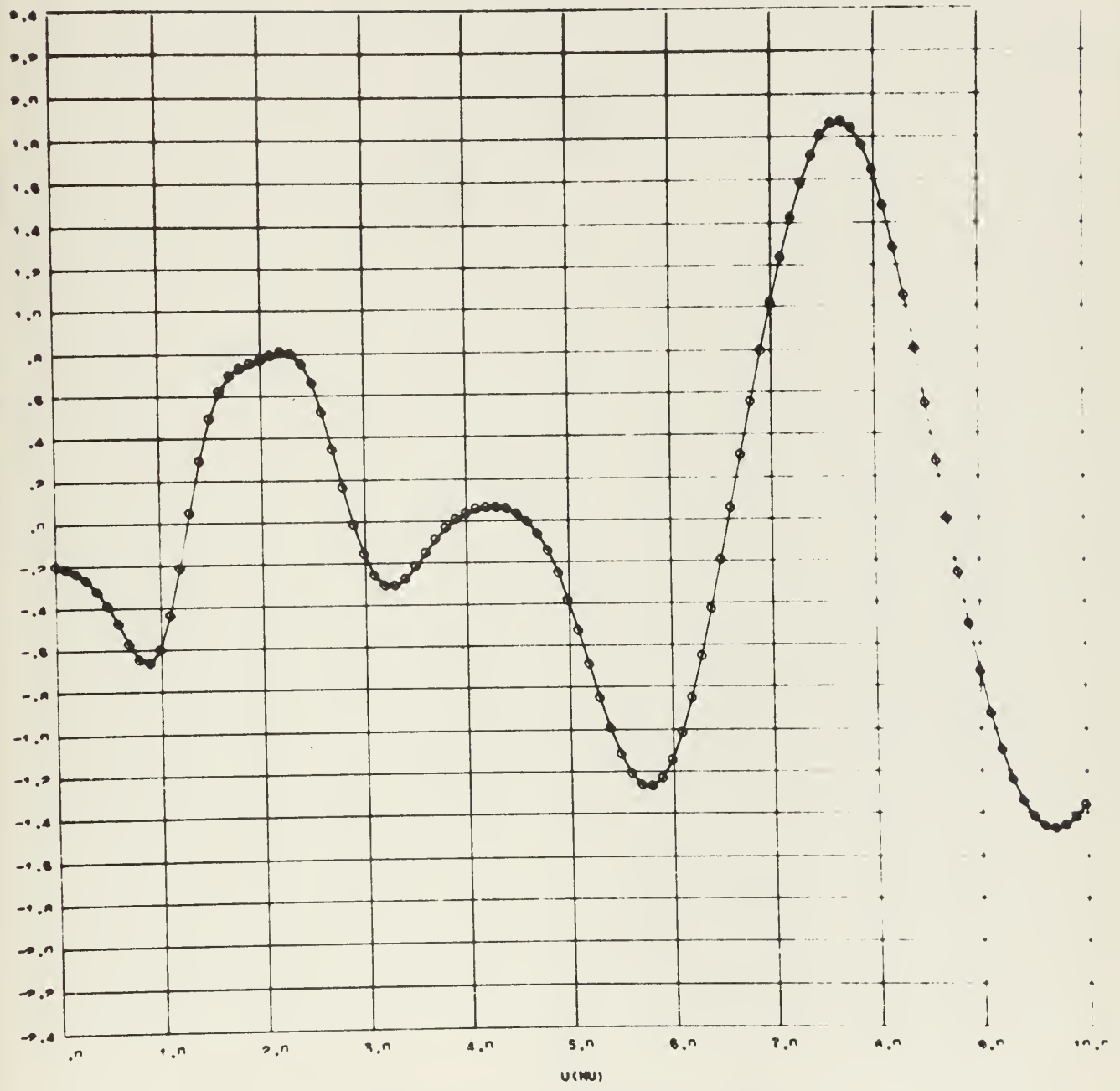

FROUDE NO. = 0.484 CONFIGURATION ASHVE

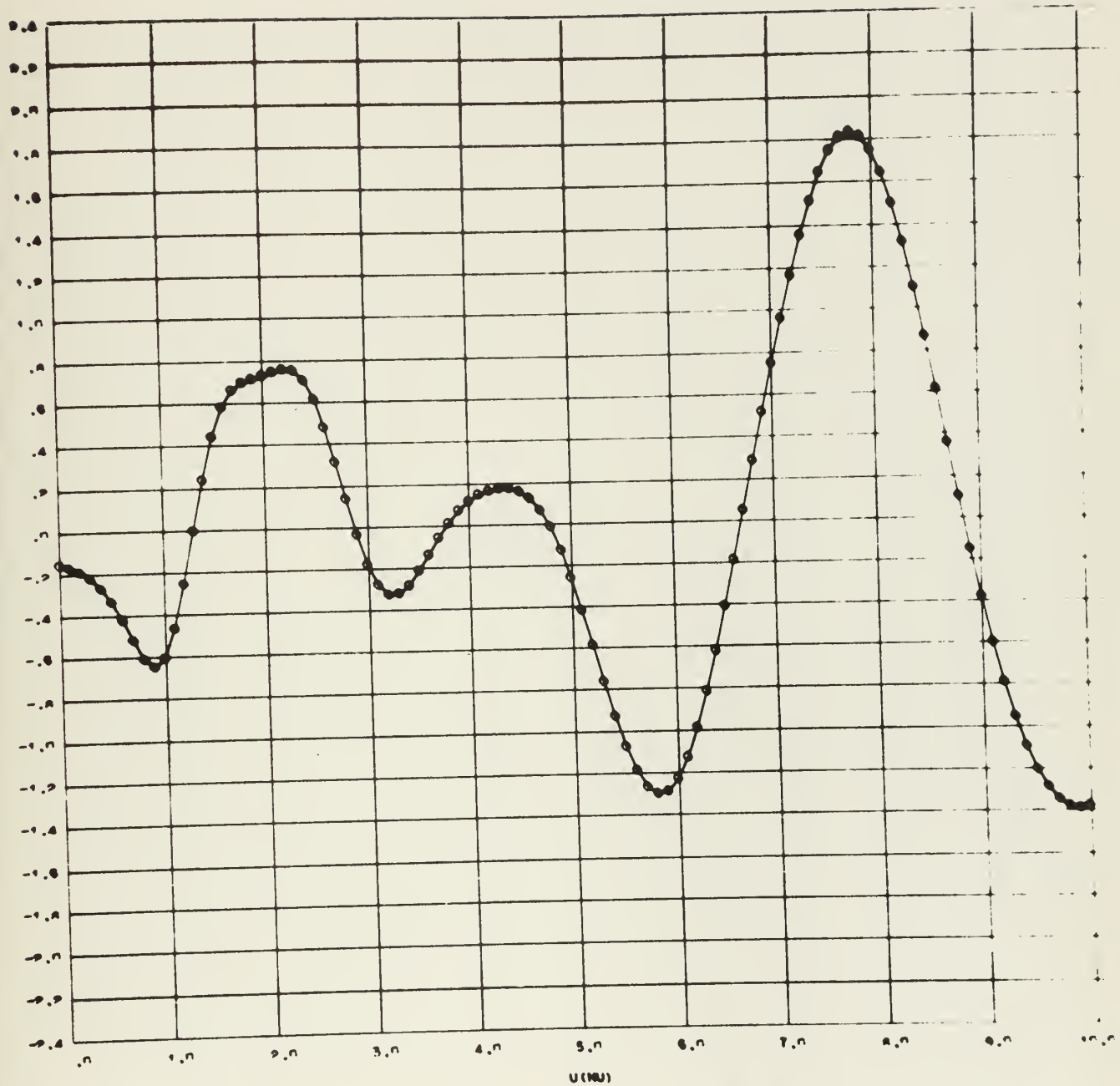

FIGURE NO. - 0.484 CONFIGURATION BOMB

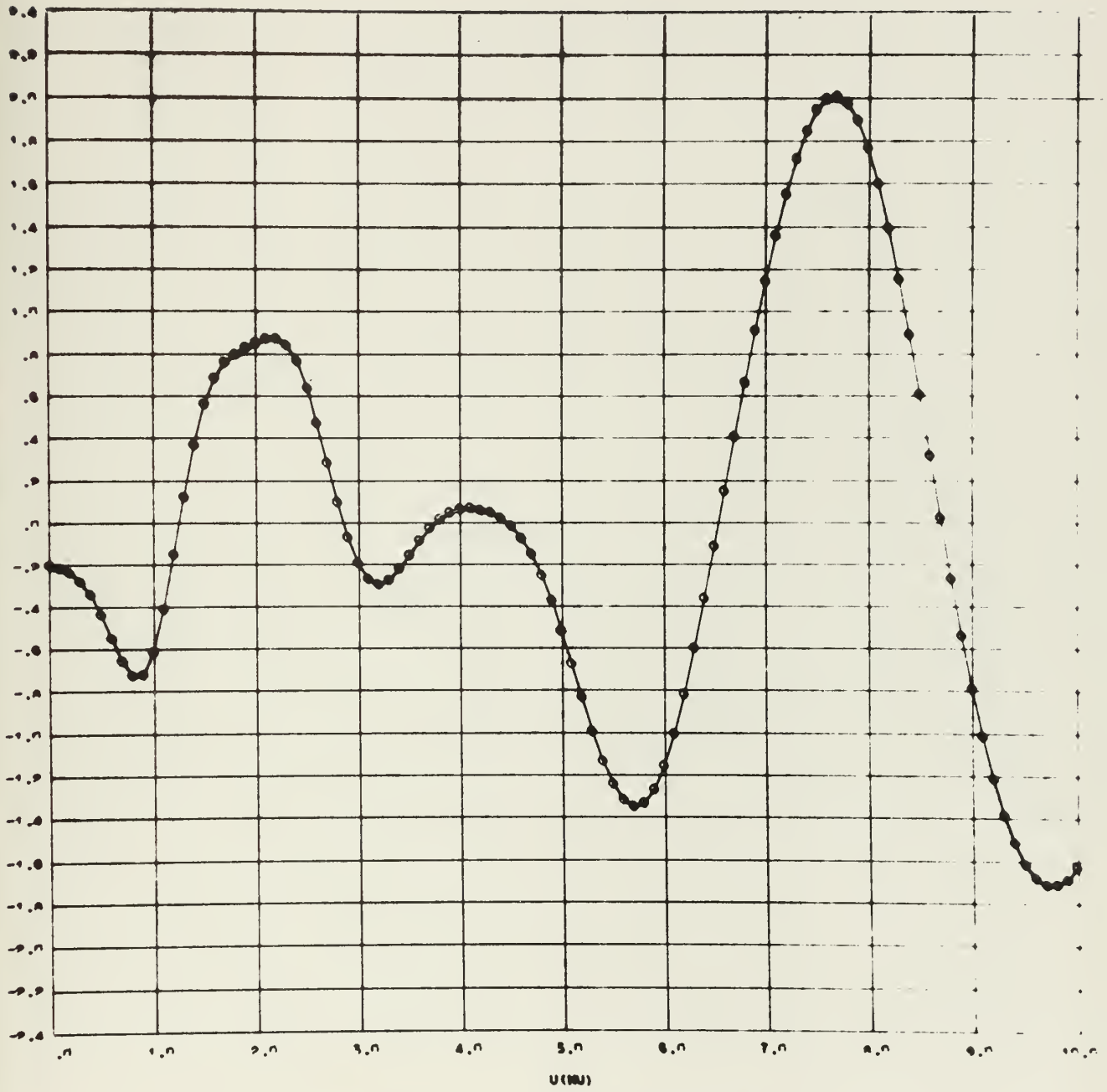

FROUDE NO. = 0.484 CONFIGURATION CONE

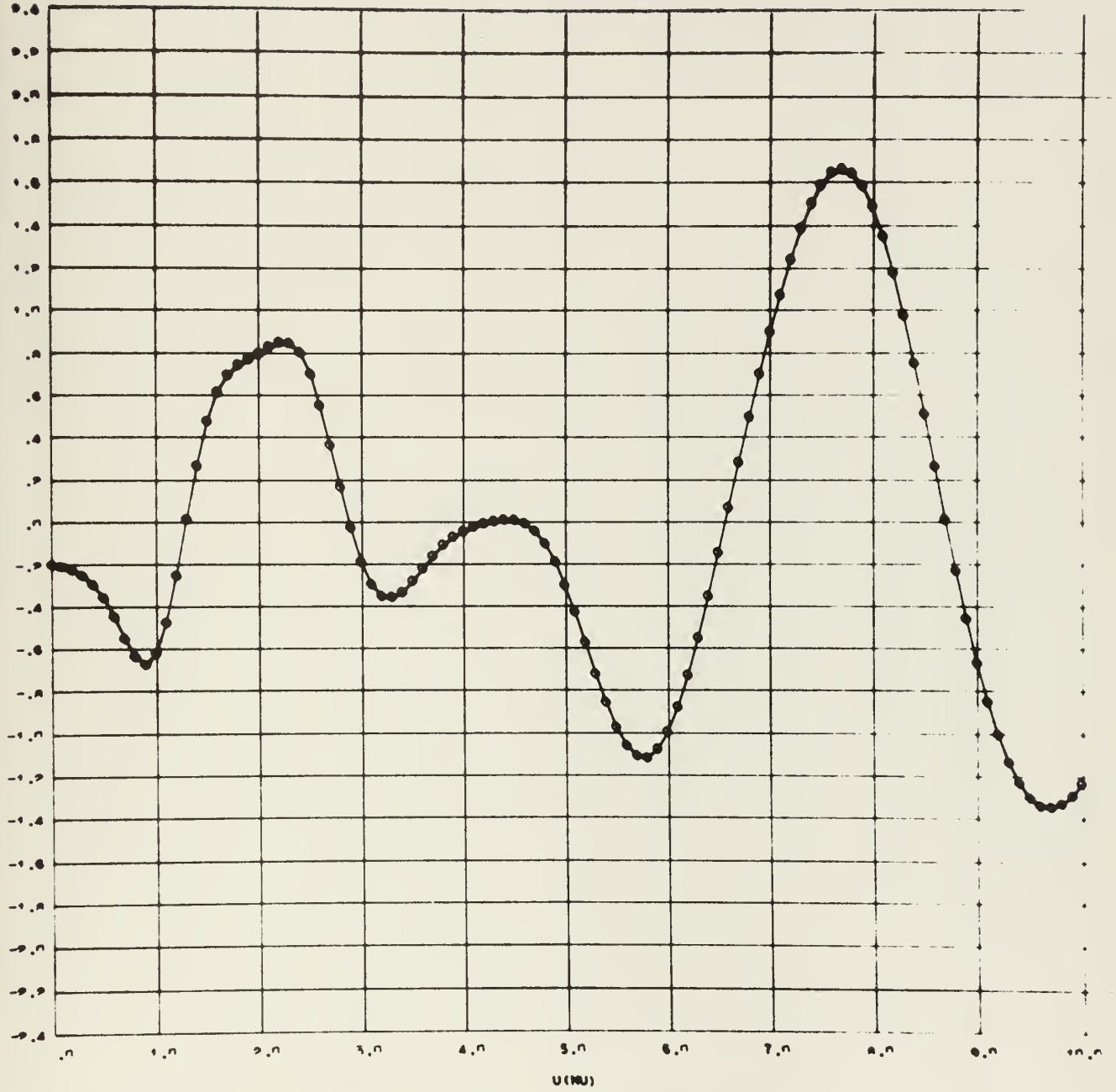

FROUDE NO. = 0.484 CONFIGURATION DDHE

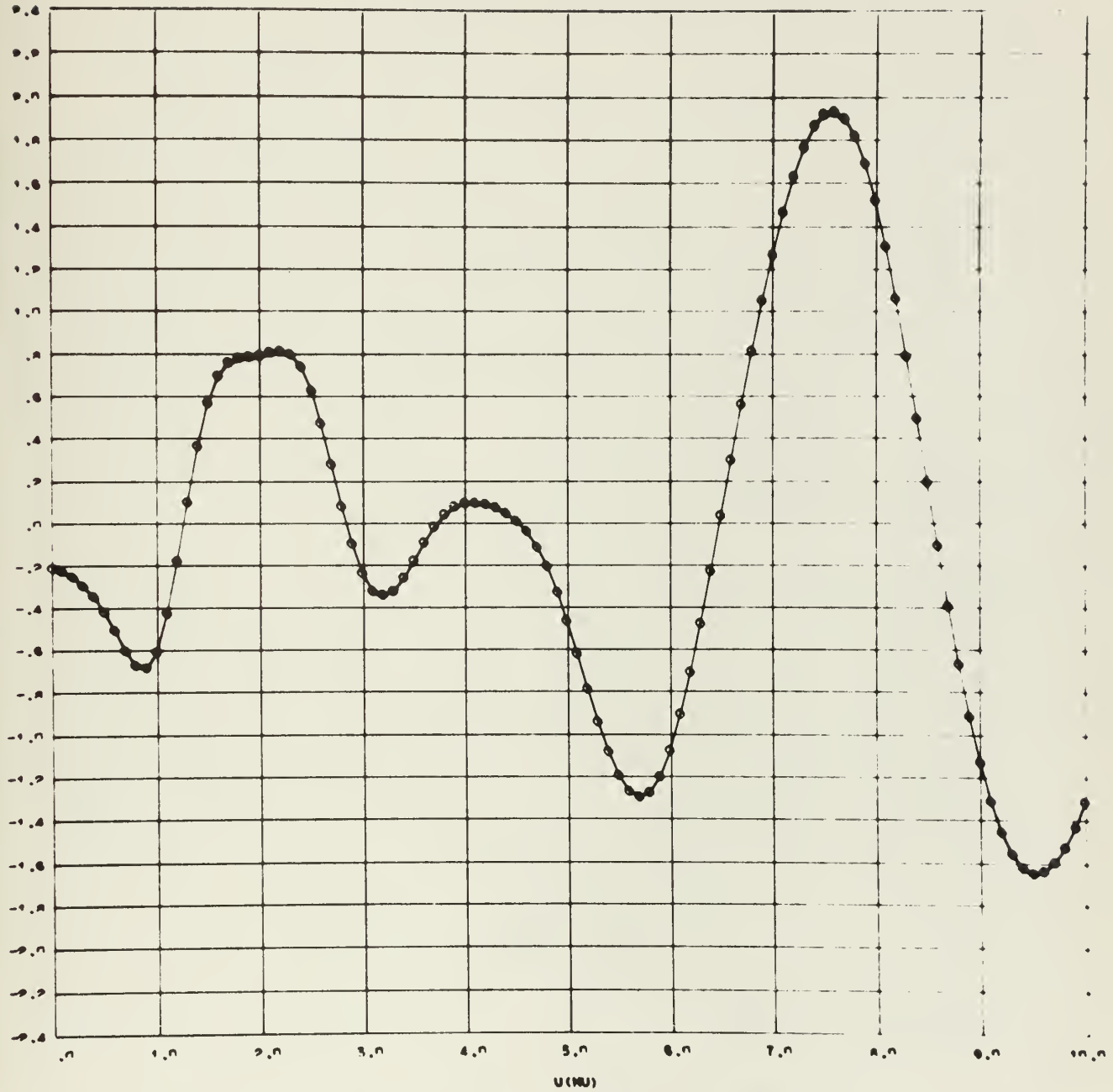

FROUDE NO. = 0.404 CONFIGURATION ESSAVE

APPENDIX D: ERROR ANALYSIS

Data Inconsistency Record

Although the three data tapes retained for each configuration and speed had an average speed within $\pm$ 0.01 ft/sec, the wave slope records were not identical, and significant phase shifts developed toward the middle of most of the records. To investigate this source of error four sets of data were artibrarily selected. These were:

Set	Speed	Configuration
1	.242	Large protuberance at station 1
2	.363	Bare Hull
3	.363	Large Protuberance at station 2
4	.484	Bare Hull

When individual tapes of each set were analyzed, the extreme wave resistance coefficient had an average deviation of almost 10% from the mean. The deviation amoung the four sets of data so analyzed are shown in Table D-I.

TABLE D-I DATA DEVIATION

	C_w of Individual Data Tapes				
Set	Tape 1	Tape 2	Tape 3	$\bar{C}_w$	Max Dev from $\bar{C}_w$
1	.3129	.3545	.3114	.3290	7.8
2	.6755	.7780	.6816	.7033	10.7
3	.8404	.7394	.6790	.7529	11.6
4	2.348	2.382	2.047	2.244	8.8
				Average	9.7

There is strong reason to believe that the wave records are statistical in nature, and that many more data tapes are required to attain a suitable degree of confidence in the average value. Applying the student 'T' distribution for small samples, if $\bar{C}_w$ and s^2 are the mean and variance of a sample of size N from an assumed normal distribution, $n(\mu,\sigma^2)$, where μ and σ^2 are unknown, then the percent deviation of $\bar{C}_w$ from the mean with a given confidence interval may be readily determined.

Each of the four sets of data individually investigated and compared in Table D-I experienced considerable variation. Therefore, probable deviations of $\bar{C}_w$ from the theoretical mean were determined for each set at four confidence levels and averaged. These steps are tabulated in Figure D-1, which shows the percent deviation of the accepted $\bar{C}_w$ from the mean versus its respective degree of confidence. For comparative purposes, the same values of s and $\bar{C}_w$ are used to calculate the confidence levels were ten samples to be taken. It is quite apparent that, from a statistical viewpoint, three runs per set do <u>not</u> produce sufficiently reliable values of wave resistance coefficients.

<u>Calibration Factor</u>

The Brush recorder and amplifier exhibited some fluctuation and non-linearity during testing. A sample calibration factor plot for the bare hull configuration is shown in

FIGURE D-1 CONFIDENCE LEVELS FOR WAVE RESISTANCE COEFFICIENTS

SET	$\bar{C}_w$	$S/\sqrt{3}$	% DEVIATION FROM MEAN AT ___% CONFIDENCE			
			50	80	90	95
1	.3290	.0143	3.55	8.2	12.7	18.7
2	.7033	.0337	3.92	9.0	14.3	20.7
3	.7529	.0471	5.20	11.8	18.3	27.0
4	2.244	.0830	3.02	7.0	10.8	15.9
AVERAGE DEVIATION			3.90	9.0	14.2	20.5

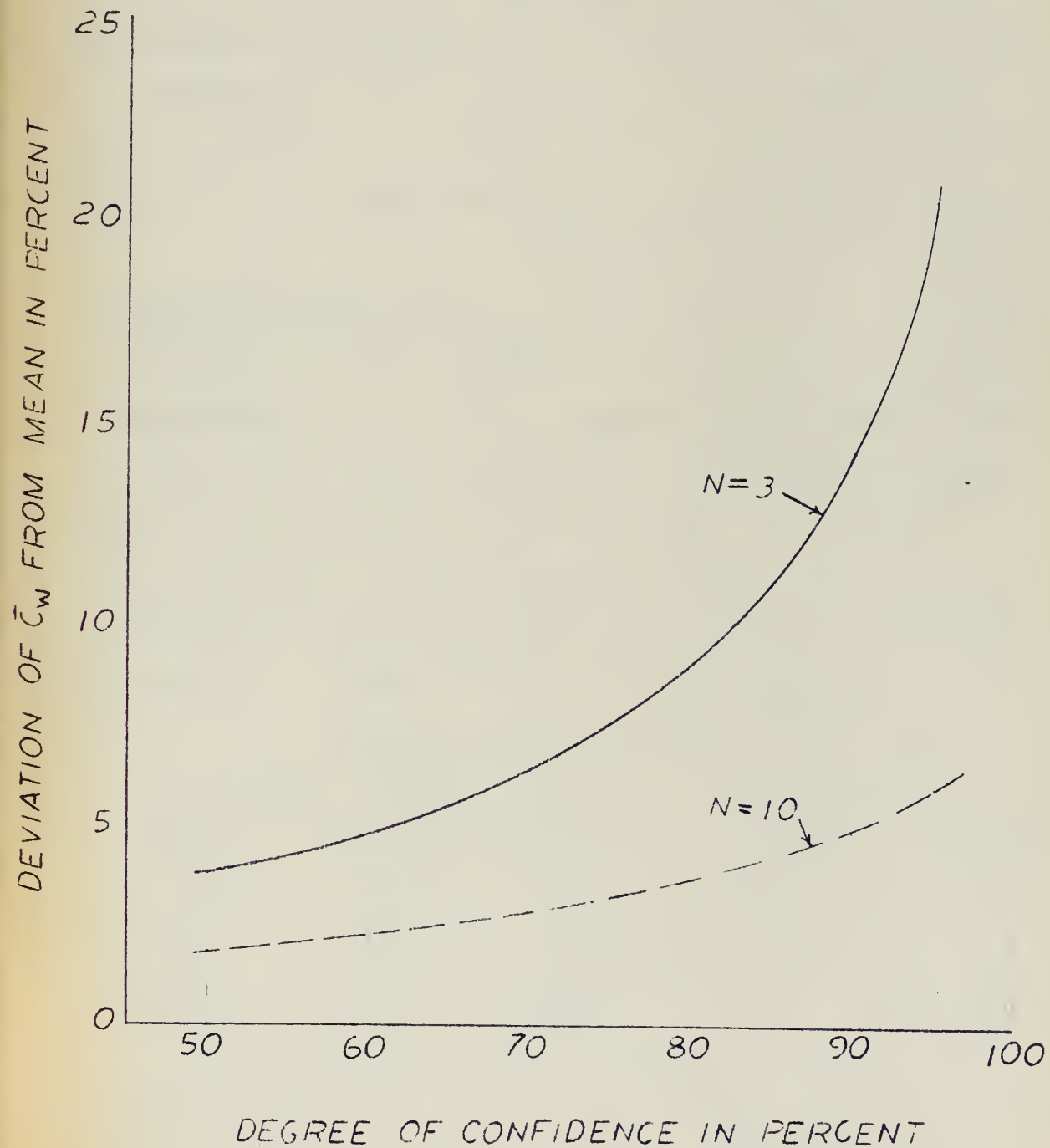

Figure D-2. Depending on the manner of securing the probe after each rotation when calibrating, an error of $\pm \frac{1}{4}$ mm. at .2 radians was observed. This gives an expected calibration error of $\pm$ 1.25 mm/rad.

As the probe is raised or lowered with no rotation, a perceptible scale deflection was detected. However, the resulting effect on the wave record tends to be self-compensating and this factor is mentioned for information only.

Therefore, since the average calibration factor is about 95 mm/rad and is squared in the calculations, percentage error is approximately $(\pm\ 1.5/95)^2 \approx 2\frac{1}{4}\%$.

Wave Record Reading Error

Because the human element is involved in reading the data tapes, a reading error of measurable magnitude is likely to be incurred. To investigate this problem, each of the tapes in the fourth set of data mentioned above was read individually by each of the authors and separate values of C_W computed. Table D-II summarizes the results. From this, a gross reading error of $\pm$ 1 3/4% is anticipated.

Table D-II Reading Error

Protuberance located at station 2, Froude number = 0.363

Reader	1st Tape	2nd Tape	3rd Tape	Average
FJM	.8337	.7216	.6732	.7278
CAB	.8383	.7648	.6712	.7500
AJJ	.8492	.7317	.6926	.7448

Average for all readings = .7409

Maximum deviation from average = $\frac{7409-7278}{.7409}$ = 1.77%

FIGURE D-2 BARE HULL CALIBRATION FACTOR

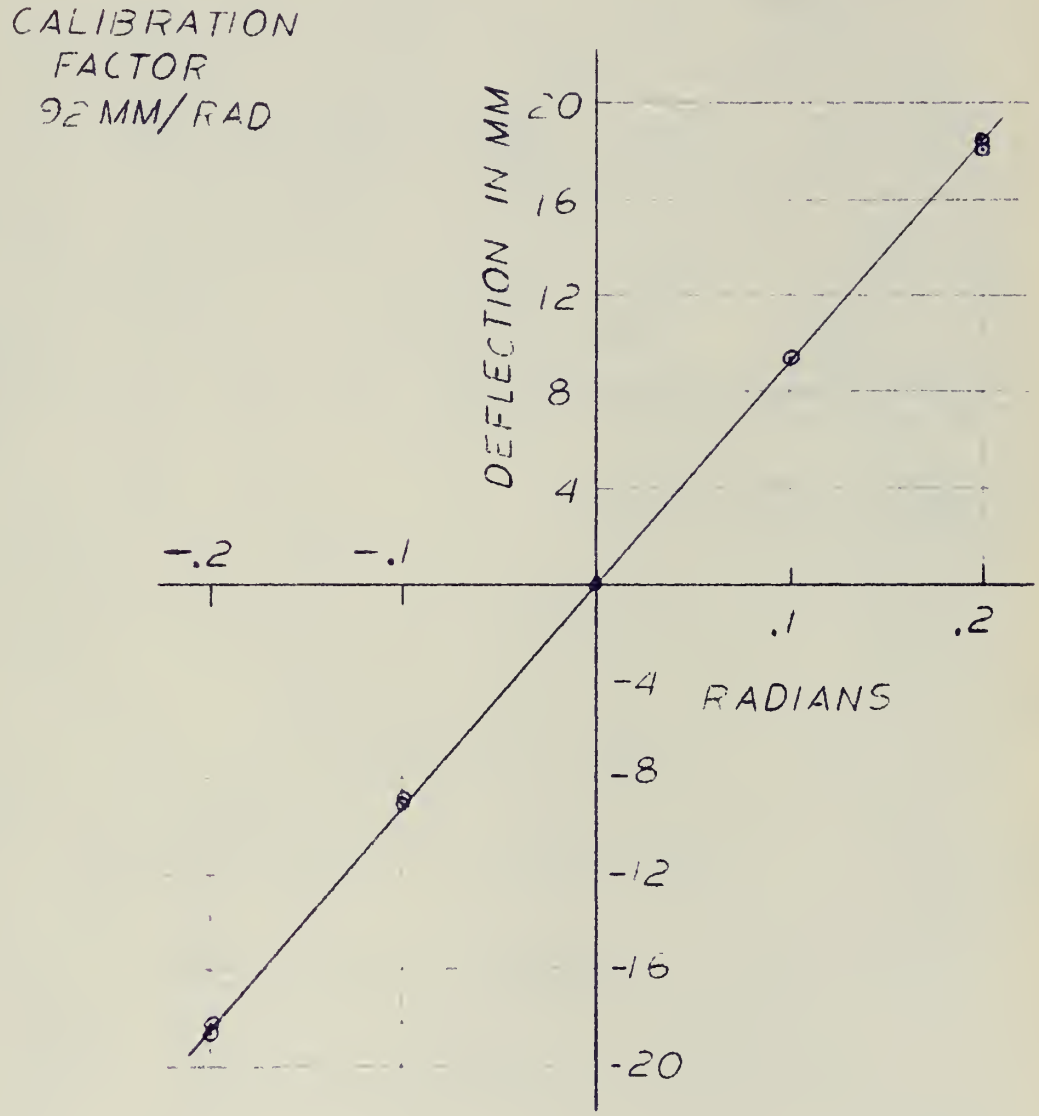

Overall Sensitivity of Method

If a sufficiently large sample of wave records were taken, the percent deviation of $\bar{C}_w$ at 90% confidence could readily be reduced to a few percent. Maximum combined calibration and reading errors constitute about $2\frac{1}{4} + 1\ 3/4$ or 4% error. Therefore, the longitudinal cut method, when conscientiously followed, with an adequate number of records, should provide wave resistance values accurate to within 6% or less. However, when only three samples are used, a 6% accuracy is available with only a 50% confidence level.


ACCORDION
BRAND
GENUINE PRESSB RD
B-2507
RED ROPE STATIONERY
INDUSTRIES INC
BROOKLYN 1, N. Y